

17167

C/

LEACHING OF METAL OXIDES

by

ERIC AUGUST PIERRE DEVUYST

Ing. Civ. Mines, U.L.B. Brussels, 1968
M.A.Sc., U.B.C., 1970

A THESIS SUBMITTED IN PARTIAL FULFILMENT OF
THE REQUIREMENTS FOR THE DEGREE OF

DOCTOR OF PHILOSOPHY

in the Department

of

METALLURGY

We accept this thesis as conforming to the
required standard

THE UNIVERSITY OF BRITISH COLUMBIA

September, 1973

In presenting this thesis in partial fulfilment of the requirements for an advanced degree at the University of British Columbia, I agree that the Library shall make it freely available for reference and study.

I further agree that permission for extensive copying of this thesis for scholarly purposes may be granted by the Head of my Department or by his representatives. It is understood that copying or publication of this thesis for financial gain shall not be allowed without my written permission.

Department of Metallurgy

The University of British Columbia
Vancouver 8, Canada

Date September 26, 1973

ABSTRACT

The leaching of metal oxides in acids has been investigated. The experiments were focussed on the leaching of ferric oxides in perchloric, hydrochloric, sulphuric, oxalic and malonic acids. Additional studies were made of the leaching of aluminum, cuprous, cupric and manganous oxides in the above acids.

In dilute solutions of the acids ($<0.2M$), the rates of leaching of the oxides showed a dependence on the mean activity of the acids (a_{\pm}), varying between first and second order. In acids which do not form strong complexes with the metal ions considered, e.g. $HClO_4$, the order was approximately one; in acids with strong complexing power the order was close to two. In more concentrated acids ($>0.2M$), the order decreased progressively by one unit (i.e. from 1 to 0 or 2 to 1), with increasing acidity. The addition of ferrous salts to oxalic and malonic acids greatly enhanced the rates of leaching of ferric oxides.

A general mechanism for the direct leaching of metal oxides in acids has been proposed. It is postulated that the oxide surface becomes rapidly hydroxylated, followed by the successive adsorptions of hydrogen ions, anions of the acid and again hydrogen ions at hydroxylated sites. With the exception of dehydrated aluminum oxides, the kinetics of the leaching of the oxides in acids were consistent with the assumption that the rate determining step was the desorption of

metal species which are formed at the oxide surface during the above adsorption reactions. For the dissolution of dehydrated aluminum oxides, it appeared that the rate of surface hydroxylation was rate-controlling under some conditions. The adsorption pre-equilibria could be correlated to the pH of zero-point of charge (Z.P.C.) of the oxide surface. Oxide surfaces exhibiting a high pH of Z.P.C., e.g. Cu_2O , CuO and MnO , are suggested to become more rapidly saturated by ionic species from solution with increasing acidity than oxide surfaces having a lower pH of Z.P.C., e.g. $\alpha\text{-Fe}_2\text{O}_3$. This saturation of the oxide surface is postulated to be the reason for the observed decreasing dependence of the rates of leaching on a_{\pm} with increasing acidity. It is also concluded that the complexing ability of the acids for metal ions is essentially correlated with the rates of desorption of the metal-anion species formed at the oxide surface.

The catalytic effect of ferrous ion additions to oxalic and malonic acids is explained by an electrochemical mechanism involving the formation and rapid desorption of ferrous and ferric species at the ferric oxide surface.

TABLE OF CONTENTS

	<u>Page</u>
1. REVIEW OF PREVIOUS INVESTIGATIONS	1
1.1 Introduction	1
1.2 The Chemistry of Oxide Surfaces	2
1.2.1 Hydration-Dehydration of Oxide Surfaces	2
1.2.2 Zero-Point of Charge	6
(a) Variables Affecting the Zero-Point of Charge.....	6
(b) Selectivity of Adsorption	10
1.3 The Direct Leaching of Metal Oxides	15
1.3.1 Kinetics of Leaching	15
1.3.2 Mechanisms of Leaching of Metal Oxides	21
1.4 The Leaching of Metal Oxides Involving Electron- Transfer	26
1.4.1 Kinetics of Electron-Transfer Reactions	26
1.4.2 Mechanism of the Leaching involving Charge Transfer at the Oxide-Electrolyte Interface ..	33
1.5 Critical Summary	37
2. SCOPE OF THE PRESENT INVESTIGATION	44
3. EXPERIMENTAL	45
3.1 Minerals and Reagents	45
3.1.1 Natural Minerals	45
3.1.2 Synthetic Minerals	45
(a) Hematite (α -Fe ₂ O ₃)	45

	<u>Page</u>
(b) Cuprous Oxide (Cu_2O)	47
(c) Cupric Oxide (CuO)	47
(d) Manganous Oxide (MnO)	47
(e) Aluminum Oxides	50
3.1.3 Reagents	50
3.2 Apparatus Design	50
3.3 Experimental Procedure	52
3.4 Analytical Methods	53
3.4.1 Iron	53
3.4.2 Aluminum	54
3.4.3 Copper	54
3.4.4 Manganese	54
3.4.5 Determination of the Ferrous Content of Hematite Specimens	54
4. RESULTS	55
4.1 The Leaching of Metal Oxides in Aqueous Perchloric Acid Solutions	55
4.2 The Leaching of Metal Oxides in Aqueous Hydrochloric Acid Solutions	59
4.3 The Leaching of Metal Oxides in Aqueous Sulphuric Acid Solutions	70
4.4 The Leaching of Ferric Oxide in Oxalic Acid in the Absence of Added Ferrous Salt in Solution	71
4.5 The Leaching of Ferric Oxide in Oxalic Acid in the Presence of Added Ferrous Oxalate in Solution..	76
4.5.1 Preliminary Experiments	76
4.5.2 The Effect of Sample Weight	79

	<u>Page</u>
4.5.3 The Effect of Added Ferrous Oxalate Concentration	79
4.5.4 The Effect of Adding Ferrous Ion Complexing Agents to the Oxalate Electrolyte	82
4.5.5 The Effect of Adding Various Cations in Solution	82
4.5.6 The Effect of the Concentration of Oxalic Acid..	83
4.5.7 The Effect of the Ti Content of Synthetic Ferric Oxide	83
4.5.8 The Effect of Temperature	85
4.5.9 The Effect of pH	88
4.5.10 Distribution of Ferrous Species in 0.2 M Oxalic Acid as a Function of pH	88
4.6 The Leaching of Ferric Oxide in Malonic Acid in the Presence of Added Ferrous Ion	91
4.7 The Leaching of Ferric Oxide in Various Other Acids ...	95
4.7.1 In the Absence of Added Ferrous Salts in Solution	95
4.7.2 In the Presence of Added Ferrous Salts in Solution	95
5. DISCUSSION	97
5.1 The Direct Leaching of Metal Oxides in Acids	97
5.1.1 Model for the Mechanism of Leaching	97
5.1.2 Leaching of Metal Oxides in HClO_4 Solutions	104
5.1.3 Leaching of Metal Oxides in HCl Solutions	108
5.1.4 Leaching of Metal Oxides in H_2SO_4 Solutions	116
5.1.5 The Leaching of Ferric Oxide in $\text{H}_2\text{C}_2\text{O}_4$ Solutions	119
5.1.6 The Leaching of Ferric Oxide in Various Other Acids	120

	<u>Page</u>
5.2 The Acid Leaching of Ferric Oxides in the Presence of Added Ferrous Salts in Solution	122
5.2.1 The Leaching of Ferric Oxide in $H_2C_2O_4$ Solutions	122
5.2.2 The Leaching of Ferric Oxide in Malonic Acid	129
5.2.3 The Leaching of Ferric Oxide in HCl	130
6. CONCLUSIONS	131
7. SUGGESTIONS FOR FUTURE WORK	133
8. APPENDIX A	135
9. APPENDIX B	140
10. REFERENCES	167

LIST OF FIGURES

<u>Figure</u>		<u>Page</u>
1	Rate of leaching of Cu_2O in H_2SO_4 and HClO_4 at various concentrations of H^+ ($T=31^\circ\text{C}$).....	24
2	Rate of leaching of goethite in HCl versus the mean activity of HCl ($T=85^\circ\text{C}$).....	24
3	Electron microprobe pictures for Ti or Mg of synthetic $\alpha\text{-Fe}_2\text{O}_3$ samples (Table 5) (x1,000).....	48
	(a) 0.1% Ti; (b) 0.2% Ti; (c) 0.5% Ti; (d) 1.3% Ti ...	48
	(e) 3.0% Ti; (f) 0.5% Mg	49
4	Apparatus design	51
5	Relative rates of leaching of Cu_2O and CuO in HClO_4 versus the concentration of HClO_4 at 12°C	56
6	Relative rate of leaching of goethite (Surana and Hay, $T=110^\circ\text{C}$) and hematite ($T=90^\circ\text{C}$) versus the concentration of HClO_4	57
7	Relative rate of leaching of ferric oxide in dilute HCl as a function of the mean activity of HCl	60
8	Relative rate of leaching of ferric oxide in HCl as a function of the mean activity of HCl	61
9	Ratio of the relative rate of leaching of ferric oxide and a_{\pm} as a function of a_{\pm}	62
10	Effect of adding LiCl on the relative rate of leaching of ferric oxide (Michigan) in 2.4 M HCl at 80°C	64
11	The effect of adding NaOH or HClO_4 on the relative rate of leaching of $\alpha\text{-Fe}_2\text{O}_3$ (Michigan) in 2.4 M HCl at 80°C	65
12	Relative rates of leaching of aluminum oxides in HCl versus the mean activity of HCl ($T=80^\circ\text{C}$)	67
13	Relative rates of leaching of Cu_2O and CuO in dilute HCl versus the mean activity of HCl ($T=12^\circ\text{C}$)	68
14	Relative rates of leaching of CuO in HCl versus the mean activity of HCl ($T=12^\circ\text{C}$).....	69

<u>Figure</u>		<u>Page</u>
15	Relative rate of leaching of ferric oxide in H_2SO_4 versus the concentration of H_2SO_4	72
16	Relative rate of leaching of Cu_2O , CuO and MnO in H_2SO_4 versus the concentration of H_2SO_4 ($T=12^\circ C$)	73
17	Distribution of species in oxalic acid at $80^\circ C$ versus pH	74
18	Rate of leaching of ferric oxide (Michigan) in 0.3 M oxalic acid versus pH ($T=80^\circ C$)	75
19	Leaching of goethite (Minnesota) in 0.2 M oxalic acid in the presence of air, O_2 and He versus time ($T=80^\circ C$, pH=2.8)	77
20	Rate of leaching of ferric oxide in 0.2 M oxalic acid versus the concentration of added ferrous ion ($T=80^\circ C$, pH=2.8)	80
21	Log-log plot of the rate of leaching of ferric oxide in 0.2 M oxalic acid versus the concentration of added ferrous ion ($T=80^\circ C$, pH=2.8)	81
22	Rate of leaching of ferric oxide in oxalic acid versus the concentration of oxalic acid ($T=80^\circ C$, pH=2.8, added ferrous=6 mg/liter)	84
23	Relative rate of leaching of ferric oxide in 0.2 M oxalic acid (pH=2.8, added ferrous=6 mg/liter) and 2.4 M HCl at $80^\circ C$ versus the titanium content of the oxide	86
24	Arrhenius plots for the leaching of ferric oxide in 0.2 M oxalic acid (pH=2.8)	87
25	Normalized rate of leaching of ferric oxide in 0.2 M oxalic acid versus pH ($T=80^\circ C$, Fe(II)=6 mg/liter)	89
26	Log-log plot of the total solubility of ferrous species in 0.2 M oxalic acid versus the concentration of oxalate ion at $80^\circ C$	92
27	Distribution of ferrous species in 0.2 M oxalic acid versus pH at $80^\circ C$	93

FigurePage

- 28 Rate of leaching of ferric oxide (Michigan) in
0.3 M malonic acid versus pH (T=80°C, Fe(II)=9 mg/liter) 94
- 29 Rate of leaching of ferric oxide (Michigan) in HCl
versus the concentration of added ferrous ion (T=80°C) 96
- 30 Morphology of the acid attack on the basal plane of a
 α -Fe₂O₃ single crystal 128
(a) 9 M HClO₄, 80°C, 10 days, x 2,000
(b) 6 M HCl, 60°C, 10 min, x 2,000
(c) 6 M H₂SO₄, 60°C, 20 min, x 2,000
(d) 0.2 M oxalic acid, 6 mg/liter Fe(II), 80°C, 20 min, x 1,000

LIST OF TABLES

<u>Table</u>		<u>Page</u>
1	Zero Points of Charge for Various Oxides	9
2	Experimental Values of n in Rate= k [Acid] ⁿ	18
3	Activation Energies (kcal/mole) for the Leaching of Various Oxides in Various Acids	22
4	Rate Constants and Enthalpies and Entropies of Activation for Various Homogeneous Ferrous-Ferric Electron Transfer Reactions	29
5	Synthetic Hematite Specimens	46
6	Leaching of Metal Oxides in HClO ₄ . Calculated Constants in Rate Expression (5.6)	106
7	Leaching of Metal Oxides in HCl Calculated Constants in Rate Expression (5.6)	110
8	Leaching of Cu ₂ O in HCl. Constants in Rate Expressions (5.14) and (5.15)	115
9	Leaching of Metal Oxides in H ₂ SO ₄ . Calculated Constants in Rate Expression (5.17)	118
10	Leaching of α -Fe ₂ O ₃ (Michigan) in Oxalic Acid. Calculated Constants in Rate Expressions (5.18) and (5.19)	121
A.1	Analysis of Goethite (Minnesota) and Hematite (Michigan)	135
A.2	X-Ray Diffraction Patterns of Synthetic Hematite (Table 5).	136
A.3	X-Ray Diffraction Patterns for Synthetic Cu ₂ O and CuO ..	137
A.4	Chemical Analysis of Pyrolusite	138
A.5	X-Ray Diffraction Patterns of Al(OH) ₃ , γ -Al ₂ O ₃ and α -Al ₂ O ₃	139
B.1	PH of a 0.2 M Oxalic Acid Aqueous Solution at 80°C as a Function of Added HClO ₄ and NaOH	140

<u>Table</u>	<u>Page</u>
B.2	Calculated Distribution of Oxalate Species in 0.2 M Oxalic Acid at 80°C 141
B.3	Total Solubility of Ferrous Species in 0.2 M Oxalic Acid as a Function of pH at 80°C (Figure 18) 142
B.4	Calculated Mean Activities of HClO ₄ Solutions at 25°C ... 143
B.5	Experimental and Calculated Rates of Leaching of Metal Oxides in HClO ₄ Solutions (Table 6, Figures 5 and 6) 144
B.6	Calculated Mean Activities of HCl Solutions 146
B.7	Experimental and Calculated Rates of Leaching of Metal Oxides in HCl Solutions (Table 7, Figures 7, 8, 9, 12, 13 and 14) 147
B.7.a	Calculated Relative Rates of Leaching of Ferric Oxide Using Simplified Rate Expressions 151
B.8	Ratios of the Relative Rates of Leaching of Ferric Oxides and a_{\pm} as a Function of a_{\pm} 152
B.9	Experimental and Calculated Rates of Leaching of Ferric Oxide (Michigan) in HCl-LiCl, HCl-NaOH and HCl-HClO ₄ Solutions (Table 7, Figures 10 and 11) 153
B.10	Calculated Mean Activities of H ₂ SO ₄ Solutions 154
B.11	Experimental and Calculated Rates of Leaching of Metal Oxides in H ₂ SO ₄ Solutions (Table 9, Figures 15 and 16) ... 155
B.12	Calculated and Experimental Rates of Leaching of α -Fe ₂ O ₃ (Michigan) in 0.3 M Oxalic Acid at 90°C versus pH (Figure 18) 157
B.13	Experimental Relative Rates of Leaching of α -Fe ₂ O ₃ in 0.2 M Oxalic Acid at 80°C versus the Ti Content (Figure 23) 158
B.14	The Effect of Added Ferrous Oxalate on the Leaching of α -Fe ₂ O ₃ in 0.2 M Oxalic Acid at 80°C and pH 2.8 (Figures 20 and 21)..... 159
B.15	Effect of Sample Weight (Sample Q, Table 5). Leaching of α -Fe ₂ O ₃ in 0.2 M Oxalic Acid at 80°C and pH 2.8, with 6 mg Fe(II)/liter 160

<u>Table</u>		<u>Page</u>
B.16	Effect of Temperature on the Rate of Leaching of α -Fe ₂ O ₃ in 0.2 M Oxalic Acid at pH 2.8 (Figure 24)	161
B.17	Calculated Distribution of Ferrous Oxalate Species in 0.2 M Oxalic Acid versus pH, at 80°C (Figure 27).....	162
B.18	Experimental and Calculated Rates of Leaching of α -Fe ₂ O ₃ (Sample O, Table 5) at 80°C versus pH (Figure 25)	163
B.19	Effect of Oxalic Acid Concentration on the Rate of Leaching of α -Fe ₂ O ₃ (Sample Q, Table 5) at 80°C and at pH 2.8 (Figure 22)	164
B.20	Rate of Leaching of α -Fe ₂ O ₃ (Sample H, Table 5) in 0.5 M Malonic Acid at 80°C versus pH in the Presence of 9 mg/liter of added Ferrous Ion (Figure 28).....	165
B.21	Effect of Adding Ferrous Ion on the Leaching of α -Fe ₂ O ₃ (Michigan) in HCl Solutions at 80°C (Figure 29).....	166

ACKNOWLEDGEMENT

The author wishes to express his gratitude for the advice and aid of Dr. I.H. Warren during the course of the work and desires to thank members of faculty, fellow graduate students and the technical staff for their helpful collaboration.

Financial support from the National Research Council of Canada in the form of a Research Assistantship is gratefully acknowledged.

1. REVIEW OF PREVIOUS INVESTIGATIONS

1.1 Introduction

Metals can be leached from their oxides by direct reaction with an aqueous solution of an acid or an alkali, or by reaction with either of these reagents in the presence of an oxidizing or reducing agent. Reactions of the first type are represented by the historic Bayer process for alumina production (1) and the recent Jarosite process for zinc recovery from zinc-ferrite (2), whilst the leaching of uranium oxide with sulphuric acid in the presence of oxygen (3) and the leaching of manganese dioxide with sulphurous acid (4) are examples of the second type. Although much has been published in recent years on the thermodynamics of metals in oxide-water systems (5), the kinetics and mechanisms of oxide leaching reactions have been only sparsely studied and this despite the potential significance of such studies in the field of corrosion in addition to extractive metallurgy.

Burkin (6), in a 1966 review of the chemistry of hydrometallurgical processes, commented briefly on the kinetics of dissolution of ferric oxide and cuprous oxide in acids and of uranium dioxide in oxygenated carbonate solutions. More recently Habashi (7) assembled an extensive bibliography on the leaching of oxides, but did not attempt a comprehensive discussion of the kinetics and mechanism of their dissolution.

The present study, whilst concerned principally with the leaching

of iron oxides, was undertaken with the ultimate objective of attempting to develop a general mechanism to explain the dissolution of oxides. Warren et al (8,9) have proposed a simple model for the dissolution of goethite and hematite in perchloric and hydrochloric acids which could account for the leaching of these oxides in dilute solutions of the acids. In this model it was postulated that the oxide surface immersed in the aqueous solution of the acid is subjected to rapid hydroxylation followed by rapid equilibration with the ionic species in solution. The much more rapid dissolution of ferric oxide in hydrochloric acid than in perchloric acid was explained in terms of the activation of positively charged surface sites by adsorbed chloride ions.

As a preliminary in attempting to expand this model to a variety of acids and oxides, a detailed review of the factors affecting the oxides surface hydroxylation, the charging of the oxides-electrolytes interfaces and the selectivity of anion and/or cation adsorption at these interfaces will be reviewed. Other mechanisms of oxides dissolution under a variety of conditions which have been proposed in earlier work will also be considered.

1.2 The Chemistry of Oxide Surfaces

1.2.1 Hydration-Dehydration of Oxide Surfaces

If the first step in the overall leaching mechanism of oxides is hydroxylation of the surfaces, as proposed by Mackay and Wadsworth (10) for leaching UO_2 in oxygenated dilute sulphuric acid and by Warren and Monhemius (8) and Warren and Surana (9) for leaching goethite, then

clearly the kinetics of hydration of oxides are of considerable interest. A very complete survey to 1967 of the studies of hydration and dehydration of oxide surfaces has been made by Hair (11).

For aluminum oxide Peri and Hannan (12) have concluded from infrared studies that the surfaces of the oxide produced by heating $\gamma\text{-Al}_2\text{O}_3$ above 800°C still retain some hydroxyl groups but that no increase in their number occurs on exposure of the surfaces to water vapour at room temperature and pressure. The surface of the oxide calcined at 800°C revealed the presence of at least five types of isolated hydroxyl groups. Peri (13) was able to propose a computer model for the dehydration process of the $\gamma\text{-Al}_2\text{O}_3$ surface in which the possible remaining isolated hydroxyl groups are indeed on five types of sites on which they have from zero to four nearest oxide neighbours. These hydroxyl groups apparently show a similar behaviour to those isolated hydroxyl groups produced on the surface of silica calcined above 400°C . It has been observed (14,15) that water molecules cluster around these isolated hydroxyls without reacting with adjacent oxide groups to rehydroxylate them. Bielanski and Sedzimir (16) in a study of the adsorption of water vapour on boehmite calcined at various temperatures between 500°C and 1300°C showed that the rate of water adsorption decreased with increasing calcination temperature until at between 1100°C and 1300°C oxide ($\alpha\text{-Al}_2\text{O}_3$) with an essentially hydrophobic surface was produced.

Unfortunately, conflicting views on the kinetics of hydration-dehydration have been advanced. Wade and Hackerman (17) and Hendriksen et al (18) concluded from studies of the heats of immersion of $\alpha\text{-Al}_2\text{O}_3$

in water that the rehydroxylation of $\alpha\text{-Al}_2\text{O}_3$ was rapid and independent of the temperature of dehydration, but Morimoto et al (19) had observed earlier that a maximum occurred in the heat of immersion of γ and α -aluminas with increasing temperature of dehydration pretreatment of the oxides, suggesting that irreversible dehydration of the oxide surface had taken place. Hendriksen et al (18) suggested that the aluminas used by Morimoto possibly had annealed upon heat-pretreatment resulting in a decreased surface area of the samples.

Very recently, Baker et al (20) identified six different mechanisms for the sorption of water by oxides, namely:

(a) Hydrogen bonding between adsorbed water molecules and surface hydroxyl groups.

(b) Hydrogen bonding between sorbed water molecules and hydroxyl groups in micropores.

(c) Hydration of exposed surface cations by adsorbed water molecules.

(d) Dissociative chemisorption of water with the formation of hydroxyl groups.

(e) Hydration in depth of poorly ordered cations.

(f) Hydroxide or oxide-hydroxide formation in depth.

According to Baker et al (20) the slowness of processes (c) and (d) are at the origin of the irreversible rehydration of dehydroxylated silica and chromia. Apparently process (c) contributed to a large extent to the rehydration of the dehydroxylated α -alumina surface; Baker also concludes that process (d) is rapid for $\alpha\text{-Al}_2\text{O}_3$, but he agrees however that slow adsorption of water vapour on $\alpha\text{-Al}_2\text{O}_3$ continued over a period of months. Moreover, their water vapour uptake measurements for

$\alpha\text{-Al}_2\text{O}_3$ were made after outgassing this oxide at 500°C, and thus it appears possible that many hydroxyl groups are still present on the alumina surface at this temperature.

Titanium dioxide is a typical tetravalent metal oxide. However, in contrast with silica, the surface of dehydrated TiO_2 is at least partly rapidly rehydroxylated upon rehydration (21,22). Primet et al (22) showed that dehydroxylation of crystallized TiO_2 is only partially reversible, as the decrease in surface area of TiO_2 during the dehydration-rehydration cycles was not sufficient to account for the observed decrease in rehydration. Primet et al (22) postulate the formation of three types of sites at the TiO_2 surface upon dehydration. The first type of sites are basic in character and appear by the condensation of adjacent hydroxyl groups. The second and third types of sites are acidic (Lewis); the strongest Lewis sites are created by the removal of isolated hydroxyl groups and the weakest Lewis sites are due to the removal of molecular water (around 150°C). Rehydration of dehydrated TiO_2 apparently proceeds by dissociative adsorption of water on Ti-O pairs (basic sites) until 50% of the surface is hydroxylated and by molecular adsorption on isolated Ti ions (strong) and on isolated oxygen ions (weak) (23).

In contrast with the behaviour of alumina, silica and titanium dioxide, ferric oxide which has been dehydrated by calcination appears to react readily with water in a process that has been suggested (24) as involving interaction of one surface Fe-O species with a H_2O mole-

cule to produce two surface OH groups. Recent observations by McCafferty and Zettlemyer (25) suggest that the first layer of physically adsorbed water on $\alpha\text{-Fe}_2\text{O}_3$ is immobile and doubly hydrogen bonded to the underlying hydroxyl layer, but that succeeding layers are mobile.

Infra-red studies on the surface hydration of divalent metal oxides are rendered difficult by the presence of a high background adsorption in the spectral regions of interest. Anderson et al (26) observed an irreversible modification of the surface of MgO crystals following complete dehydration. As with the silica surface, the species formed during the re-adsorption process are dependent upon the prior thermal history of the oxide sample, but contrary to silica, MgO rehydroxylates rapidly.

In contrast with the behaviour of the oxides mentioned above, isolated hydroxyl groups are apparently not formed at the surface of BeO upon dehydration (27). It also seems that the hydration-dehydration cycle of BeO is reversible on material heated to temperatures of at least 550°C.

1.2.2. Zero-Point of Charge

(a) Variables Affecting the Zero-Point of Charge

Oxides, especially the hydrous oxides, exhibit ion exchange properties (28). The ion exchange capacity of oxides arises from the existence of a pH-dependent surface charge. Charge can develop on a hydroxylated

surface through amphoteric dissociation of the surface hydroxide groups. Dissociation reactions can be written as follows,



($\left| \underset{s}{-}$ is a symbol referring to the surface of the oxide).

The Z.P.C. (zero-point of charge) of an oxide refers to the p_{H} in any system, however complex, at which there is no net charge on the surface of the oxide. If the charge is established by H^+ , OH^- , and species capable of interacting with H^+ , OH^- or H_2O to form species present in the solid lattice (called potential determining ions, P.D.I.), then the Z.P.C. may be given the special name I.E.P.(s) (29) (isoelectric point of the surface, as compared to the I.E.P. of species in solution). Adsorption of species (molecules or ions) under the combined influence of ionic and non-ionic bonding is called "specific adsorption". The following relationship among the I.E.P.(s) of an oxide or hydroxide, the charge or oxidation state of the cation and its radius was derived by Parks (29):

$$\text{I.E.P.}(s) = A - B \cdot \left[\left(\frac{Z}{R} \right) + 0.0029C + a \right] \quad (1.3)$$

where Z = cationic charge

$$R = r_+ + 2r_o$$

r_o = oxygen ion radius

A,B = constants for all oxides

C = correction for crystal field stabilization of M-OH bond

a = combined corrections for coordination number and state of hydration.

Table I shows the range of values of Z.P.C. extracted from a 1964 review by Parks (29).

The role of such variables as crystal structure and electrolyte composition in determining the solution pH at which there will be no net charge on the oxide surface have been the subject of extensive study. Increasing crystallinity as observed in aging precipitates, for example, shifts the Z.P.C. in the basic direction. Healy et al (30) have interpreted the wide range of Z.P.C.'s (pH 1.5 to 7.3) they observed for various polymorphs of MnO_2 in terms of variation in crystallinity. They conclude that as the atomic packing in the MnO_2 lattice increases, the electrostatic field within the lattice increases and the pH of the Z.P.C. increases; the pH of Z.P.C. can be approximated by the following relation, based on the Huckel equation for the electrostatic field strength of solids:

$$pH \text{ (Z.P.C.)} = \frac{A}{r_c^2} + B$$

where A and B are positive constants for an oxide series and r_c the shortest M-O interionic distance.

TABLE 1
Zero Points of Charge for Various Oxides

Oxide	Coordination M-O	Z.P.C. (pH)	Structure	Example with Z.P.C.* (at 25°C)
M_2O	2-4	>11.5	Octahedral	Cu_2O
MO	6-6	8.5-12.5	Cubic	MgO (12.4) CdO (10.4) NiO (10.3) CuO (9.5)
	4-4		Hexagonal	ZnO (9-10)
M_2O_3	6-4	6.5-10.4	Hexagonal Rhombohedral	$\alpha-Al_2O_3$ (6.5-9.5) $\alpha-Fe_2O_3$ (8.5) $\alpha-Cr_2O_3$ (7.0)
MO_2	8-4	0-7.5	Cubic	UO_2 (3.5-6.5) ThO_2 (8.5-11)
			Monoclinic	ZrO_2 (4-6.7)
	6-3		Tetragonal	TiO_2 (4.7) SnO_2 (5.5) $\beta-MnO_2$ (7.0)
			Hexagonal	$\alpha-SiO_2$ (2.2)
MO_3	6-2	<0.5	Rhombohedral	WO_3 (0.5)

*Selected values of Z.P.C. after Parks (29).

Partial oxidation or reduction leading to nonstoichiometry in solids such as TiO_2 , Fe_3O_4 or MnO_2 may be expected to shift the Z.P.C. toward that characteristic of the oxidation (or reduction) state produced (29).

The effect of temperature of the electrolyte in contact with an oxide can be roughly anticipated; the decrease of the dissociation constant of water, K_w , with increasing temperature, would result in a shift of the pH of Z.P.C.

Specific adsorption of ions other than OH^- and H^+ at the oxide surface will undoubtedly influence the Z.P.C. To achieve zero charge in the presence of a specifically adsorbed ionic species, the pH must be shifted away from the I.E.P.(s) to increase or decrease hydrogen ion adsorption, whichever is appropriate. In general, anionic impurities shift the Z.P.C. to a more acid value; cationic impurities shift it to more basic values (29).

(b) Selectivity of Adsorption

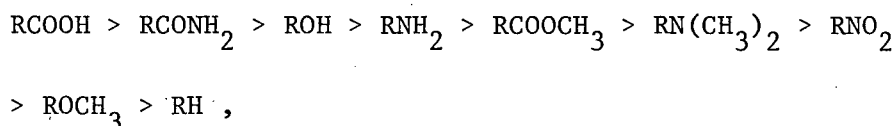
Selectivity of adsorption and the relative tendency toward adsorption are fundamental factors in discussing the kinetics of the leaching of oxides and may be inferred from ion exchange behaviour. O'Connor et al (31) investigated the behaviour of natural Al_2O_3 and $\text{AlO}\cdot\text{OH}$, and of the former after ignition to temperatures up to 1100°C in acid and alkaline solutions. On ignition to high temperatures, the original disordered surface of $\text{Al}(\text{OH})_3$ crystallized successively to a

layer of α -AlO·OH ($\approx 300^\circ\text{C}$), γ -Al₂O₃ (300°C-900°C) and α -Al₂O₃ (>900°C). According to O'Connor et al (31), α -Al₂O₃ only re-hydrates to a limited extent when exposed to a solution, to give a layer approximating to AlO·OH. O'Connor et al (31) pointed out that AlO·OH is likely to be weakly acidic in comparison to basic Al(OH)₃, resulting in a net negative charge on the surface of the solid in water. Indeed, Robinson et al (32) observed the Z.P.C. of α -Al₂O₃ having a fully hydroxylated surface to occur at pH = 9.0 - 9.4; the latter when calcined at temperatures above 1000°C exhibited its Z.P.C. at a pH 6.7. The effects of HCl and H₂SO₄ on the zeta-potential, ζ^* , of alumina samples was explained by O'Connor et al (31) in terms of physical adsorption of anions and anion exchange processes. In dilute HCl solutions, hydrated aluminas are subjected to increasing OH⁻ - Cl⁻ anion exchange with increasing HCl concentration, but heat-treated aluminas show preferential physical adsorption of Cl⁻ in very dilute HCl (0.001N) and anion exchange in more concentrated solutions. In dilute H₂SO₄ solutions, both hydrated and calcined alumina's showed preferential SO₄⁼ - OH⁻ anion exchange. Earlier, Graham and Crawford (33) had studied the adsorption of oxalate (C₂O₄⁼) by hydrous alumina. The adsorption of oxalate by hydrous alumina from either an acid solution or a neutral salt solution was greater than that of chloride; Graham and Crawford (33) suggested that the favourable C₂O₄⁼ - OH⁻ anion exchange can be related to the much greater tendency of oxalate anions to complex with aluminum cations than do chloride ions. It should be noted that firing the hydrous alumina to 1300°C for three

* ζ is the potential difference at the interface between the oxide and the electrolyte; ζ is chosen to be zero at the Z.P.C. of the oxide.

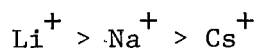
hours, producing Al_2O_3 at the surface, lowered the adsorption of oxalate by two orders of magnitude.

Ions which can form insoluble compounds or undissociated complexes with a component of the solid crystal lattice appear to adsorb more strongly than those which cannot (34). The observed order of adsorption of organic electrolytes onto $\alpha\text{-Al}_2\text{O}_3$ is (35):

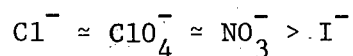


and the organic electrolytes with larger hydrocarbon chains form indeed less soluble compounds.

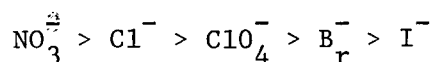
Selective ionic adsorption at oxide surfaces can also be interpreted by considering ion-ion interactions. Ions having a high electrostatic field are structure-promoters for surrounding water as opposed to large ions with a relatively weak field strength which are structure-breakers and are weakly hydrated. Berube and De Bruyn (36) based their model of the TiO_2 -water interface on ion-ion interactions. The OH superficial groups firmly anchor the neighbouring water molecules by hydrogen bonding, this phenomenon being strengthened by the large crystalline field of the small Ti^{4+} ion. This results in the presence of "frozen" water near the surface, the latter behaving as a structure-promotor macro-ion. Thus, strong specific adsorption is to be expected by those ions which also favour structure-promotion. The observed order of specific adsorption of alkali-cations,



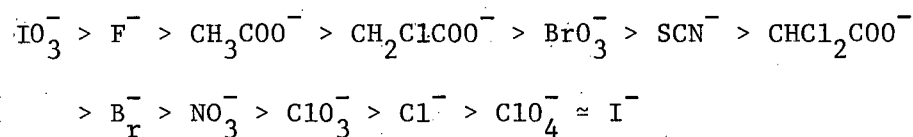
on a negatively charged TiO_2 surface is in accord with this prediction. This concept may also be applied to the anions of acids for their adsorption on a positively charged TiO_2 surface, but no clearly defined order of adsorption can be obtained as in the case of cations. Specific adsorption of some inorganic anions is in the order:



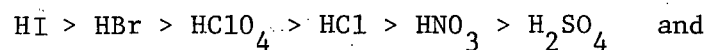
compared to the order of structure-promoting effect

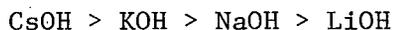


For $\alpha\text{-Fe}_2\text{O}_3$, the field strength exerted by the surface upon the electrolyte is somewhat weaker than that of TiO_2 . Dumont and Watillon (37) developed the following series of adsorption selectivity in acidic media,

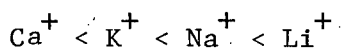
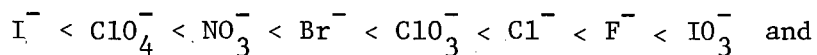


The observed adsorption sequence on $\alpha\text{-Fe}_2\text{O}_3$ can also be compared to the order of decreasing mean activity coefficients of the corresponding acids and bases which reflect ion-ion interaction properties; these are (38),





Finally, the increasing order of Baumé coefficients of viscosity (39) also appear to reflect a similar sequence, namely,



A reasonable parallelism between the various sequences is observed. Nevertheless, some discrepancies arise; e.g., SCN^- , which can undergo chemical binding with the Fe^{3+} ion, is more strongly adsorbed on ferric oxide. Moreover, $\text{CH}_2\text{ClCOO}^-$ and $\text{CHCl}_2\text{COO}^-$ which are structure-breakers as a whole, are specifically adsorbed on $\alpha\text{-Fe}_2\text{O}_3$ in acid media; the COO^- group which can organize water around itself is therefore probably turned toward the surface.

The problem of competitive adsorption at oxide surfaces will arise in solutions which contain more than one type of ionic species, and this is almost always the case when an oxide is dissolving in an electrolyte. Recently, Hingston et al (40) investigated the competitive adsorption of phosphate + arsenate and phosphate + selenite ions on goethite and gibbsite. It appears from their results that the oxide surfaces contain sites common to both anions on which adsorption takes place and sites on which only one or the other anion is able to adsorb. The maximum amount of anions adsorbing from a mixture is approximately equal to the sum of the maximum adsorption for each anion in the absence

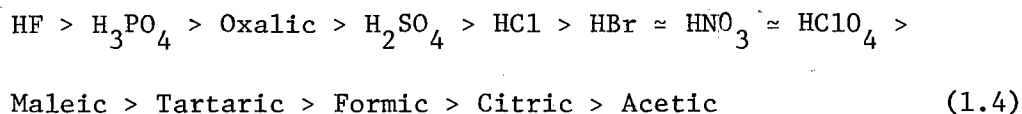
of a competitor. In mixed systems it is thus possible to occupy more sites with anions than when either ion is present alone. Hingston et al (40) suggest that possibly one type of anion is shared between two Fe atoms on the crystal surface through a bridging link, whereas the other type of ion has two bridging ligand links to each Fe atom.

1.3 The Direct Leaching of Metal Oxides

1.3.1 Kinetics of Leaching

In studies of the leaching of goethite ($\text{FeO}\cdot\text{OH}$) and hematite (Fe_2O_3) in perchloric, sulphuric and hydrochloric acids various workers (9,41,42,43,44) have shown rates of attack which increase for both oxides in the order HClO_4 , H_2SO_4 , HCl of equal normality ($>1\text{N}$). Because of the drastic change in surface area which occurs with HCl attack, due to pitting, it is impossible to quote rates for the different acids on an equivalent surface area basis.

For the leaching of hydrated aluminum oxide ($\text{Al}_2\text{O}_3 \cdot 2.7 - 2.9 \text{H}_2\text{O}$), Clay and Thomas (45) and Graham and Thomas (46) have observed in their studies that the rates of leaching of the oxide in several organic and inorganic acids (0.2N) are in the following sequence:



Parts of these results were recently confirmed for the dissolution of gibbsite ($\text{Al}(\text{OH})_3$) in HClO_4 , HCl and H_2SO_4 solutions by Packter and

and Dhillon (47). Gibbsite dissolves about five times more rapidly in HCl solutions than in HClO_4 solutions of equal strength, and H_2SO_4 solutions react about five times faster than HCl solutions of equal mean activity.

Azuma and Kametani (41,48) correlated the increasing absolute rates of leaching in the different acids with the increasing complexity constants of the anions of the various acids for ferric iron. A similar correlation appears to be applicable to the leaching of the alumina hydrates because the order (1.4) is in the order of complexing power of the anions for the aluminum ion, provided corrections are made for the differences in dissociation constants of the acids. In addition, Wadsworth and Wadia (49) observed a more rapid rate for the leaching of cuprite in sulphuric than perchloric acid, consistent with the sulphate complex for cupric ion being relatively strong, whilst the perchlorate ion is a non complexer (50). Finally, the observations by Koch (51) on the leaching of beryllia (BeO) are also consistent with the above pattern since the order of complexing powers for the beryllium ion by the anions (50), namely $\text{C}_2\text{O}_4^{=}$ > $\text{SO}_4^{=}$ > Cl^- , is in the order of absolute leaching rates. Whilst apparent uniformity exists in the properties required of an anion of an acid to achieve rapid leaching, there appears at present to be none in the observed effects of the variation of concentration of acids on the rates of leaching of the different oxides.

The rate dependence on the acid concentration in dilute solutions (<IM) can be qualitatively expressed by the following relation:

$$\text{Rate} = k \cdot [\text{Acid}]^n \quad (1.5)$$

A plot of $\log (\text{Rate})$ versus $\log [\text{Acid}]$ should give a slope of n ; the values of n obtained by various workers for several metal oxides are listed in Table 2. It can be concluded that in dilute solutions:

(a) monobasic acids: - if the anion of the acid is a strong complexer for the metal, $n \approx 2$

- if the anion of the acid is a weak complexer for the metal, $n \approx 1$ or smaller.

(b) dibasic acids: n is always smaller than 1, and close to 0.5.

The value of $n = 1$ obtained for HF does not contradict the observed sequence as twice the amount of acid is needed to obtain an equivalent concentration of HF_2^- ions in solution as in the case of the other monobasic acids.

The values of n reported in Table 2 only hold for dilute solutions. In more concentrated solutions n becomes equal to 1 for sulphuric acid and increases (sometimes up to 2.5) for strong monobasic acids. This apparent complex behaviour of the acids has not been explained.

Very recently Kabai (53) showed that the rate of leaching of any oxide could be described by an 'empirical' differential equation of the form:

$$\frac{dC}{dt} = K \cdot \frac{\alpha}{1-\alpha} (1-C) \quad (1.6)$$

where K is a constant depending on the nature and temperature of the electrolyte and type of oxide, C is the weight fraction of the total mineral which has dissolved (total weight is equal to one), t is the

TABLE 2

Experimental Values of n in Rate = k · [Acid]ⁿ

Oxide	Acid (<IM)	Ions in Solution	Complexing Ability	Slope n	Reference
Fe ₂ O ₃ · xH ₂ O (0 ≤ x ≤ 3)	HF	H ⁺ , HF ₂ ⁻	Strong	1.06	41,48
	HCl	H ⁺ , Cl ⁻	Strong	1.92-2.2	41,42,48
	HBr	H ⁺ , Br ⁻	Strong	1.94	41,48
	HNO ₃	H ⁺ , NO ₃ ⁻	Weak	0.93	41,48
	HClO ₄	H ⁺ , ClO ₄ ⁻	Weak	0.93-1.0	41,42,48
	H ₂ SO ₄	H ⁺ , HSO ₄ ⁻	Weak	0.56	41,48
			, SO ₄ ⁼	Strong	
H ₃ PO ₄		H ⁺ , H ₂ PO ₄ ⁻	Weak	0.59	41,48
		HPO ₄ ⁼ , PO ₄ ⁼	Strong		
Al ₂ O ₃ · 3H ₂ O	HCl	H ⁺ , Cl ⁻	Weak	≈ 1	47
	H ₂ SO ₄	H ⁺ , HSO ₄ ⁻ , SO ₄ ⁼	Weak	< 1	47
	HClO ₄	H ⁺ , ClO ₄ ⁻	Weak	< 1	47
Cu ₂ O	H ₂ SO ₄	H ⁺ , HSO ₄ ⁻ , SO ₄ ⁼	Strong	< 1	49
	HClO ₄	H ⁺ , ClO ₄ ⁻	Weak	< 1	49
BeO	HCl	H ⁺ , Cl ⁻	Weak	0.53	51
	H ₂ SO ₄	H ⁺ , HSO ₄ ⁻ , SO ₄ ⁼	Strong	0.70	51
	H ₂ C ₂ O ₄	H ⁺ , HC ₂ O ₄ ⁻ , C ₂ O ₄ ⁼	Strong	0.42	51
ZnO	H ₂ SO ₄	H ⁺ , HSO ₄ ⁻ , SO ₄ ⁼	Strong	< 1	52

time and α is a dimensionless number depending on the chemical composition and structure of the oxide. Expression (1.6) differs from the Nernst equation (54) essentially in the constant α and is identical to the Nernst equation when $\alpha = 1$. Kabai obtained the values of constants α and K from plots of the $\log \left[\log \left(\frac{1}{1-C} \right) \right]$ versus $\log t$ which were linear according to equation (1.7)

$$\log \left[\log \left(\frac{1}{1-C} \right) \right] = \log K + \alpha \cdot \log t \quad (1.7)$$

This equation has no meaning when $t = 0$ or when $C = 1$. Changes in the nature and concentration of the electrolyte only influenced K according to the 'empirical' equation (1.8), namely

$$K = B \cdot e^{n \cdot \gamma \cdot \alpha} \quad (1.8)$$

where B is a constant [$t^{-\alpha}$], n is the concentration of the acid [gm.eq/liter] and γ is a constant for a given acid [liter/gm.eq]. Kabai obtained the activation energies for the dissolution of the various oxides in acids from Arrhenius plots of $\log K$ versus $\frac{1}{T}$ and was able to derive equation (1.9).

$$\Delta H^\ddagger = \delta \cdot \alpha \quad (1.9)$$

where α is the structure factor as defined in rate equation (1.6) and $\delta = 21.2$ kcal/mole is the energy required for the dissolution of any oxide independent of its composition and structure and of the properties of the electrolyte. It can be shown however that expression (1.9) for

the activation energy obtained by Kabai depends on the mathematical form of his rate expression (1.6) and that (1.9) does not give the true activation energy. Indeed, the true activation energies should take into account the variation of rate of leaching of the oxides with increasing temperature for a constant amount of dissolved mineral, C, i.e. constant surface area, and this condition leads to equation (1.10)

$$\frac{K_1}{K_2} = \left[\frac{t_2}{t_1} \right]^\alpha \quad (1.10)$$

where the subscripts 1 and 2 refer to the absolute temperatures T_1 and T_2 . The corresponding ratio of the rates of leaching at the two temperatures is then given by

$$\frac{\text{Rate}_1}{\text{Rate}_2} = \frac{K_1}{K_2} \cdot \left[\frac{t_2}{t_1} \right]^{1-\alpha} = \left[\frac{K_1}{K_2} \right]^{\frac{1}{\alpha}} \quad (1.11)$$

and hence relation (1.11) yields

$$K^{\frac{1}{\alpha}} = k \cdot e^{-\frac{E}{RT}} \quad (1.12)$$

where k is a rate constant independent of temperature and E is the true activation energy for the dissolution of the oxide. Kabai, however, postulated that

$$K = A \cdot e^{-\frac{\Delta H^\ddagger}{RT}} \quad (1.13)$$

From the comparison of (1.12) and (1.13) the following relation is derived:

$$E = \frac{\Delta H^\ddagger}{\alpha} = \delta \quad (1.14)$$

It follows that the true activation energies E for the dissolution of the oxides in acids are equal to the δ defined by Kabai. This leads to a remarkable suggestion, namely that the activation energy for the dissolution of any oxide in whatever acid does not vary by much more than 6 kcal/mole, i.e.

$$E = 20.00 \text{ kcal/mole} \pm 3 \text{ kcal/mole} \quad (1.15)$$

and this can be seen in Table 3.

Cuprous oxide seems to dissolve with a much lower activation energy but this oxide also shows some particular behaviour during dissolution as will be discussed in the present investigations.

1.3.2 Mechanisms of Leaching of Metal Oxides

The hypotheses developed to explain the observed kinetics of leaching individual oxides are basically of two types. In the first, developed by Wadsworth and Wadia (49) for the leaching of Cu_2O no hydroxylation or charging of the oxide surface is assumed and the following sequence of steps is envisaged:

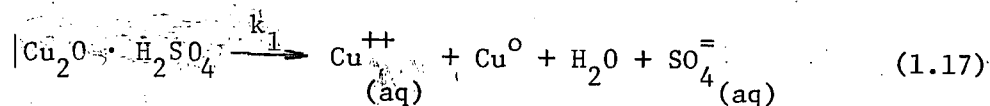
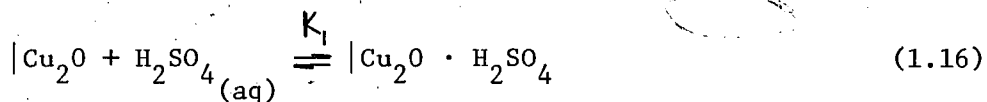
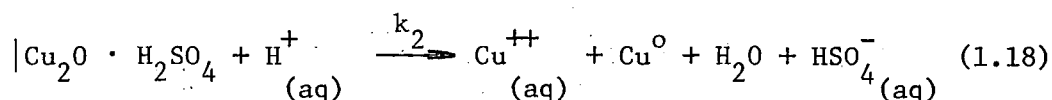


TABLE 3

Activation Energies (kcal/mole) for the Leaching
of Various Oxides in Various Acids

Oxide	Acid	E* (kcal/mole)	References
Fe(OH) ₃	1N HCl	20.17-22.18	(53)
α-FeO·OH	HCl, H ₂ SO ₄ , HClO ₄	17.8-22.5	(9,42)
α-Fe ₂ O ₃	HCl, H ₂ SO ₄ , HClO ₄	19.2-22.9	(41,42,43,53)
Al(OH) ₃	HCl, H ₂ SO ₄ , HClO ₄	14.7-22.18	(47,53)
Cu ₂ O	H ₂ SO ₄	10.5	(49)
Cu(OH) ₂	0.5N C ₂ H ₅ COOH	18.1	(53)
Mg(OH) ₂	0.75N H ₃ BO ₃	17.28	(53)
Cr(OH) ₃	0.7N H ₂ SO ₄	21.3-23.12	(53)
Mn(OH) ₂	0.5N HCl	22.86	(53)

*E = $\frac{\Delta H^\ddagger}{\alpha}$ for the results reported by Kabai (53).



Equation (1.16) represents the hydrolytic adsorption of H_2SO_4 on the Cu_2O surface and the first leaching reaction (1.17) the thermal decomposition of occupied surface sites. The second leaching reaction (1.18) indicates the influence of H_3O^+ ion and its ability to react with sites on which H_2SO_4 is adsorbed. A rate equation (1.20) can be developed which includes a Langmuir type equation (1.19) for the fraction of sites, θ_x , covered by H_2SO_4 :

$$\theta_x = \frac{K_1 \cdot [\text{H}_2\text{SO}_4]}{1 + K_1 \cdot [\text{H}_2\text{SO}_4]} \quad (1.19)$$

and
$$R_T = \theta_x \cdot [k_o \cdot k_2 \cdot (\text{H}^+) + k_o \cdot k_1] \quad (1.20)$$

(k_o includes the surface roughness factor).

When $K_1 \cdot [\text{H}_2\text{SO}_4]$ is much greater than one the value of θ_x approaches one and equation (1.20) becomes the linear portion of the rate versus $[\text{H}^+]$ plot as shown in Figure 1. Note that Wadsworth calculated K_1 to be equal to 1.59×10^6 liter/M, and thus, the active surface of Cu_2O would be saturated by H_2SO_4 at $\theta_x = 0.9$ for $[\text{H}_2\text{SO}_4]_{\text{(aq)}} = 5 \times 10^{-6}$ M/liter.

Other workers who have used the above hypothesis of an uncharged surface (or have not taken into account the variation of charge at the oxide surface) are Koch (51) for the dissolution of BeO in HCl , $\text{H}_2\text{C}_2\text{O}_4$ and H_2SO_4 , Pearson and Wadsworth (55) for the dissolution of UO_2 in

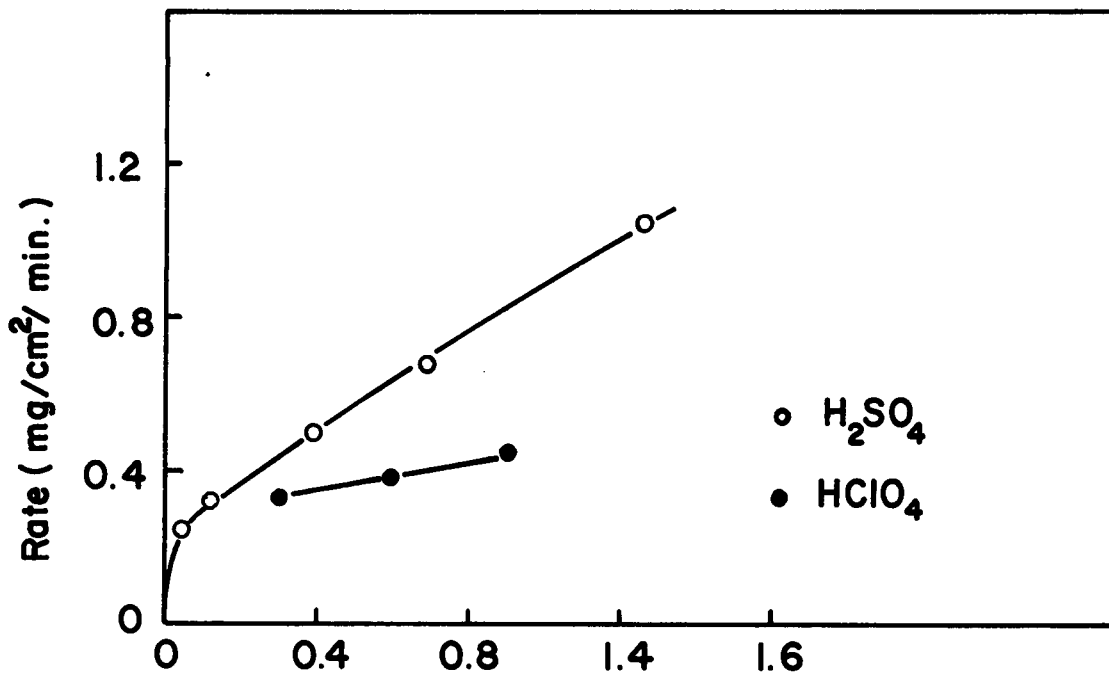


Figure 1. (H⁺) (M/liter)

Rate of leaching of Cu₂O in H₂SO₄ and HClO₄ at various concentrations of H⁺ (T= 31°C) (After Wadsworth (49).)

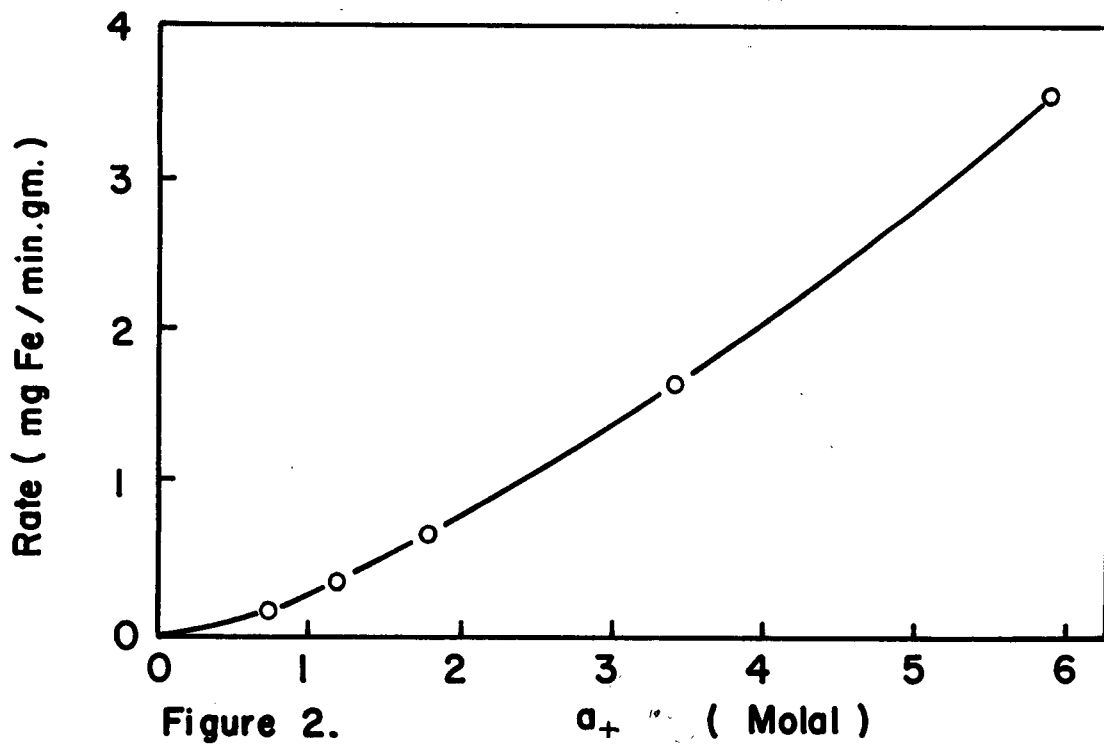
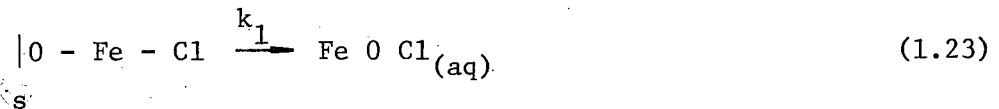
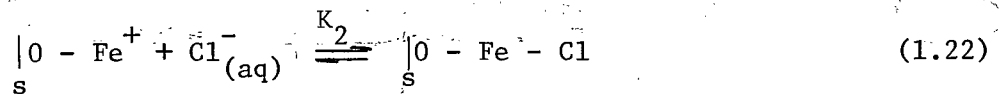
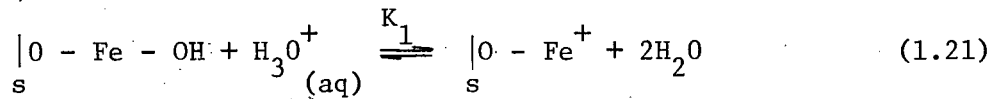


Figure 2. a_± (Molal)

Rate of leaching of goethite in HCl versus the mean activity of HCl (T= 85 °C) (After Surana (9).)

carbonate solution, Takeuchi et al (56) for the dissolution of ThO_2 in hydrofluoric acid and nitric acid mixtures, and Judge (57) for the leaching of SiO_2 in hydrofluoric acid solutions.

The second hypothesis assumes that the surface of the oxide becomes hydroxylated and then charged by protonation or ionization according to equations (1.21) and (1.22) for goethite in dilute HCl (9):



(Rate determining step)

This leads to a simple rate equation of the form:

$$R = K \cdot \left[\left| \underset{\text{s}}{\text{O}} - \text{Fe} - \text{OH} \right] \cdot a_{\text{H}^+} \cdot a_{\text{Cl}^-} \quad (1.24)$$

$$(K = k_1 \cdot K_1 \cdot K_2)$$

In equation (1.24) $\left[\left| \underset{\text{s}}{\text{O}} - \text{Fe} - \text{OH} \right] \right.$ is assumed to be large in comparison with $\left[\left| \underset{\text{s}}{\text{O}} - \text{Fe}^+ \right] \right.$. For perchloric acid no specific adsorption of the anion is expected (58) and the rate determining step then becomes desorption from a simple protonated site. Equation (1.24) however, cannot describe the reactions of solutions containing high concentrations of HCl with goethite (Figure 2), nor can it account for the 'two

part' type leaching curves observed in the sulphuric acid leaching of cuprite (Figure 1).

Several workers have included the charging of the oxide surface in acids into their studies of the kinetics of leaching of the oxides. Biermann and Heinrichs (59) proposed a qualitative mechanism for the dissolution of chromite in sulphuric acid based on an initial protonic attack, followed by formation of various sulphate complexes of chromium. A mechanism for the dissolution of gibbsite in perchloric, hydrochloric and sulphuric acids based on the protonation of the hydrated gibbsite surface has been advanced by Packter and Dhillon (47). They proposed a common rate expression (1.25) for the three acids.

$$R = k \cdot a_{\pm} \cdot a_w^2 \quad (1.25)$$

with k a rate constant typical for each acid, a_{\pm} the mean activity of the acids and a_w the activity of water in the corresponding acids.

1.4 The Leaching of Metal Oxides Involving Electron-Transfer

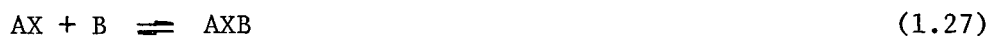
1.4.1 Kinetics of Electron Transfer Reactions

Heterogeneous electron transfer reactions at the oxide-electrolyte interface are similar to homogeneous electron transfer reactions in solution for which there is ample information in literature. Major theoretical treatments of electron transfer have been given by Libby (60), Weiss (61), Halpern and Orgel (62), Hush (63), Sacher and Laidler (64), Marcus (65) and Ruff (66). The brilliant experimental work of Henry Taube and his associates (67, 68) forms a most important chapter

in the recent studies of electron transfer reactions. Electron-transfer is restricted by the "Franck-Condon" principle, i.e. the "electron-jump" process involving a net transfer of an electron from an orbital belonging essentially to one metal to an orbital belonging essentially to the other metal occurs in a time short ($\sim 10^{-15}$ sec) compared to that required for nuclear position change ($\sim 10^{-13}$ sec). There are two major consequences of the Franck-Condon principle for electron transfer reactions. The first is that the total energy of the reactants' activated complex must be identical with the energy of the products' activated complex. That is, the energy of the activated complex as described by nuclear coordinates must be two fold degenerate, and degenerate in a special way that places the migrating electron on one reactant before transfer and on the other after transfer.

When two complex ion reactants share one or more ligands of their first coordination spheres in the activated complex, it is termed an inner-sphere activated complex and the mechanism an inner-sphere mechanism. Outer-sphere activated complexes are formed when the inner coordination shells of the reactant complex ions are left intact as to the number and kind of ligands present.

A generalized pathway for inner-sphere electron transfer has been given by Sutin (69) which is represented by the following scheme;



This is an example of the oxidation of cation B by cation A in the presence of anion X. Possible rate determining steps are the formation of a reactant complex (1.26) or a precursor complex (1.27), the electron transfer step (1.28) or the dissociation of the successor complex (1.29).

The bridging group X in an inner-sphere activated complex can perform several functions. Libby (60) stressed the importance of reducing coulombic repulsions between two cations with an intervening negative ion. But, additionally, the negative ion might complex the reducing agent as it is oxidized, generally stabilizing it in the higher valence state. However, in general the available data on redox reactions do not show that coulombic attractions and repulsions play a dominant role. Perhaps the most important factor in bridging is that an easier pathway for an electron transfer is made.

The electron-transfer reactions between Fe(II) - Fe(III) complexes may be of special interest in the present work. Many anions catalyze the Fe(II) + Fe(III) electron exchange. Exchange paths involving F^- , Cl^- , $C_2O_4^{2-}$, SO_4^{2-} , EDTA, phenanthroline, and CN^- are known. Rate constants and enthalpies and entropies of activation, when known, are listed in Table 4.

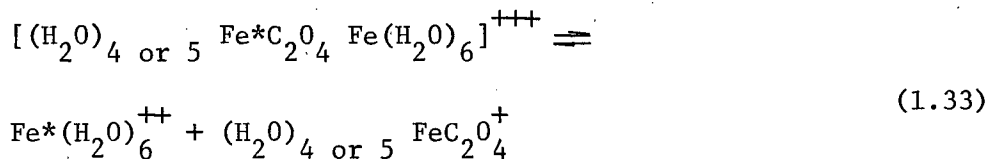
Attempts to interpret the kinetics and establish the mechanism of the Fe(II) - Fe(III) exchange have tended to fall into two principal categories - anion bridging theories (67, 68) and water bridging theories (79). If the electron is transferred across an anion bridge, one might reasonably expect that the activation energy of the exchange process

TABLE 4

Rate Constants and Enthalpies and Entropies of Activation for Various
Homogeneous Ferrous-Ferric Electron Transfer Reactions

Reaction	μ (g. eq/l)	T° (°C)	k $\left(\frac{1}{\text{mole sec}}\right)$	ΔH^\ddagger $\left(\frac{\text{kcal}}{\text{mole}}\right)$	ΔS^\ddagger (e. v.)	References
$\text{Fe}^{2+} + \text{Fe}^{3+}$	0.55	0	0.87	9.3	-25	(70)
$\text{Fe}^{2+} + \text{FeOH}^{2+}$	0.55	0	10^3	6.9	-18	(70)
$\text{Fe}^{2+} + \text{FeF}^{2+}$	0.50	0	9.7	8.6	-21	(72)
$\text{Fe}^{2+} + \text{FeF}_2^+$	0.50	0	2.5	9.0	-22	(72)
$\text{Fe}^{2+} + \text{FeF}_3^{2+}$	0.50	0	0.5	-	-	(72)
$\text{Fe}^{2+} + \text{FeCl}_2^+$	0.55	20	29.0	8.3	-24	(70)
$\text{Fe}^{2+} + \text{FeCl}_2^+$	0.55	20	53.0	9.5	-20	(70)
$\text{Fe}^{2+} + \text{FeC}_2\text{O}_4^+$	0.55	0	7×10^2	9.2	-14	(73)
$\text{Fe}^{2+} + \text{Fe}(\text{C}_2\text{O}_4)_2^-$	0.55	0	3.6×10^3	-	-	(73)
$\text{Fe}^{2+} + \text{FeSO}_4^+$	0.25	25	692	-	-	(74)
$\text{Fe}^{2+} + \text{Fe}(\text{SO}_4)_2^-$	0.25	25	1.94×10^4	-	-	(74)
$\text{Fe}^{2+} + \text{Fe}(\text{EDTA})^-$	-	25	$< 4 \times 10^{-4}$	-	-	(75)
$\text{Fe}^{2+} + \text{Fe}(\text{ph})_3^{3+}$	-	25	3.7×10^4	0.2	-37	(76)
$\text{Fe}(\text{ph})_3^{2+} + \text{Fe}(\text{ph})_3^{3+}$	-	0	$> 10^5$	-	-	(71)
$\text{Fe}(\text{CN})_6^{4-} + \text{Fe}(\text{ph})_3^{3+}$	-	25	$> 10^8$	-	-	(77)
$\text{Fe}(\text{CN})_6^{4-} + \text{Fe}(\text{CN})_3^3$	-	0.1	355	4.1	-32	(78)

and the final step is the dissolution of the activated complex and any rearrangements of the waters of solvation:



Conflicting evidence was brought up later by Sheppard and Brown (82) in their study of the catalyzed electron-transfer reactions of Fe(II) - Fe(III) by acid phosphate, oxalate and sulphate anions. The large energies of activation, 15, 13.5 and 21.0 kcal/mole for H_2PO_4^- , $\text{C}_2\text{O}_4^{=}$ and $\text{SO}_4^{=}$ respectively, suggest that the process of electron transfer for these oxyanions may be different from that for the halide paths.

The transfer of electrons between a metal or semiconductor and a dissolved or surface-bound reactant is not different in kind from homogeneous solution processes described above. Laxen (83) has compared the rate of dissolution of UO_2 in the presence of Fe^{+++} with the rates of electron transfer between Fe(II) - Fe(III) complexes in solution.

In a perchlorate medium both the Fe(II) - Fe(III) exchange and the dissolution of UO_2 by Fe^{3+} were strongly catalyzed by the presence of small concentrations of sulphate, while both reactions are also affected in a similar manner by the concentration of H^+ in solution. Of the anions tested, NO_3^- did not improve the dissolution rate and Cl^- had only a slight effect. In perchlorate solutions, when the H^+ addition was increased the dissolution rate increased up to a pH value of 2 and decreased at lower pH values. The increase in dissolution rate

was ascribed by Laxen to the increase in concentration of Fe(OH)^{2+} , the most effective electron-transfer species. It should be noted that the maximum of Fe(OH)^{2+} concentration does not occur at pH 2 according to Needes and Finkelstein (84) and this particular aspect suggests that other factors may be involved in the leach. In sulphuric acid solutions, the rate of leaching of UO_2 by Fe^{3+} with pH also reached a maximum at $\text{pH} \approx 2$ and could be attributed to the combined effect of Fe(OH)^{++} , FeSO_4^+ and $\text{Fe(SO}_4)_2^-$ species in solution. At constant pH, however, the rate of dissolution of UO_2 showed a square root dependence on the concentration of ferric ion in solution.

The very high rates of dissolution of UO_2 reported by Hunt and Taube (85) with Fe(dipy)_3^{3+} and Fe(O-phen)_3^{3+} in 1M HCl serve to confirm the correlation between rate of dissolution of UO_2 and the very fast homogeneous electron transfer of these two complexes with Fe^{3+} in solution.

Recent work published by Needes and Nicol (86) on the oxidative dissolution of UO_2 in dilute perchloric acid showed that the order of leaching rates of UO_2 with various oxidants was $\text{Tl(III)} > \text{VO}_2^+ > \text{Fe(III)} \approx \text{Hg(II)}$, whereas the equivalent order of electron-exchange rates was $\text{VO}_2^+ > \text{Hg(II)} > \text{Fe(III)} > \text{Tl(III)}$. The conclusion to be drawn from this information is that the rate of dissolution of UO_2 is a function of both the potential and the electron-exchange rate of the redox couple used.

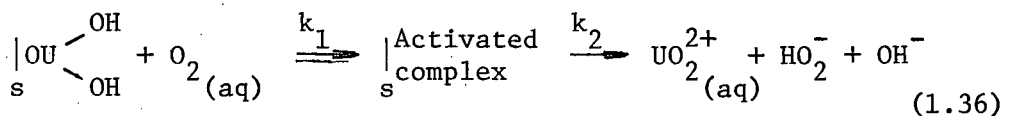
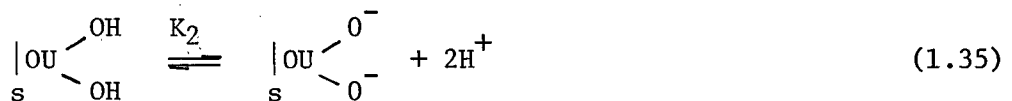
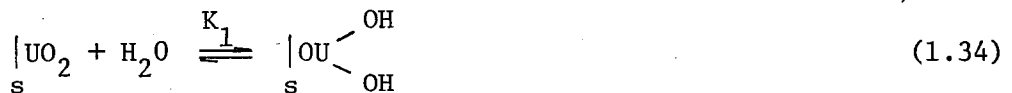
The reductive dissolution of MnO_2 in Fe^{2+} containing acid solutions has been investigated by Koch (87). The rate of leaching of MnO_2 in

Fe^{2+} containing sulphuric acid solutions was two orders of magnitude larger than in perchloric acid solutions of equal strength. Koch (87), however, excluded the possibility of an electron-transfer rate-controlling step because the rate of dissolution of MnO_2 by Fe^{2+} was independent of the concentration of Fe^{2+} , H^+ and H_2SO_4 . It should be emphasized here that Koch used large concentrations of Fe^{2+} (0.05-0.075 M/liter) and that the possibility of surface saturation by the active ferrous species should be considered.

1.4.2 Mechanisms of the Leaching involving Charge Transfer at the Oxide-Electrolyte Interface

To date, essentially two types of mechanisms have been developed to explain the observed kinetics of leaching individual oxides involving an oxidation - reduction step.

In the first, developed by Mackay and Wadsworth (10) for the oxidative leaching of UO_2 in dilute acid, the formation of an activated complex of uranium at oxide active surface sites is postulated, followed by charge transfer through the activated state to form a U(VI) intermediate and desorption of UO_2^{2+} in solution; the following sequence of steps is envisaged:



Equations (1.34) represents the formation of a hydroxylated surface and equation (1.36) the reaction of these hydroxylated sites with dissolved oxygen producing a surface activated complex of U(VI) which is then readily soluble in the electrolyte. The surface hydroxylated sites are in equilibrium with the solution according to the deprotonation equilibrium equation (1.35). A rate equation (1.38) can be developed which includes a Langmuir type equation (1.37) for the fraction of sites, θ , covered by hydroxyl ions:

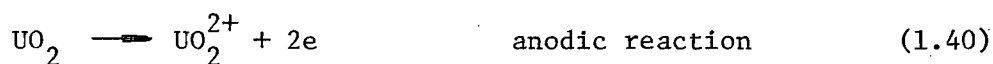
$$\theta = \frac{[H^+]^2}{K_2 + [H^+]^2} \quad (1.37)$$

and $R_T = \theta \cdot k_1 \cdot pO_2 \quad (1.38)$

The important feature of the first type of mechanism is that no attempt is made to subdivide the overall reaction into anodic and cathodic reactions. A mechanism involving the formation of a surface activated complex has also been considered by Warren and Devuyt (88) in an attempt to explain the kinetics of the reductive dissolution of pyrolusite by hydrazine in ammonium carbamate solutions, and the reductive dissolution of manganese dioxide in the presence of SO_2 was approached in a similar manner by Herring and Ravitz (89).

The second hypothesis which was proposed by Habashi and Thurston (90) for the mechanism of the oxidative dissolution UO_2 assumes that the dissolution of this oxide proceeds by an electrochemical mechanism in a similar way to the corrosion of metals. Habashi and Thurston

propose that the following two electrochemical reactions proceed simultaneously:



In general, the rate of the cathodic reaction can be given by:

$$V_c = k_c \cdot A_c \cdot [\text{D}]^n \quad (1.41)$$

where k_c is a rate constant, A_c the cathodic surface, $[\text{D}]$ the concentration of the depolarizer, i.e. O_2 , and n is the order of the reaction with respect to the depolarizer. The rate of the anodic reaction can similarly be given by the equation:

$$V_a = k_a \cdot A_a \cdot [\text{C}]^m \quad (1.42)$$

where k_a is a rate constant, A_a the anodic surface fraction, $[\text{C}]$ the concentration of a complexing agent, i.e. H^+ , and m the order of the reaction with respect to the complexing agent. At the steady state, $V_a = V_c$, but, since $A_a + A_c = A$, total surface area of the oxide, substituting the value of A_c in the rate equation giving V_c ,

$$V_c = V_a = \frac{k_a \cdot k_c \cdot A [\text{D}]^n [\text{C}]^m}{k_c [\text{D}]^n + k_a [\text{C}]^m} \quad (1.43)$$

At high concentration of C, or if k_a is large, the velocity equation (1.43) simplifies to :

$$V_c = V_a = k_c \cdot A \cdot [\text{D}]^n \quad (1.44)$$

and at high concentration of [D], or if k_c is large, the rate equation (1.43) becomes:

$$V_a = V_c = k_a \cdot A \cdot [C]^m \quad (1.45)$$

An alternative model for the electrochemical dissolution of oxides was recently proposed by Neeedes and Nicol (86). In this model it is assumed, in agreement with Habashi and Thurston (90), that the overall reaction corresponding to the dissolution of an oxide can be subdivided into an anodic and a cathodic part. A fundamental mathematical expression for the relation between the current density and the overpotential η is given by the Butler-Volmer equation:

$$i = i_o \cdot \left[\exp \left((1-\alpha) \frac{nF}{RT} \eta \right) - \exp \left(-\alpha \frac{nF}{RT} \eta \right) \right] \quad (1.46)$$

where i_o , the exchange-current density, represents the speed of the forward and backward reactions at equilibrium, η represents the difference between the applied potential and the equilibrium potential of the reaction, and F is the Faraday constant. The transfer coefficient α is defined as the fraction of the overpotential contributing to the increase in the rate of the reaction. Experimental values of α are often found to be close to 0.5. The exchange - current density, i_o , is directly proportional to k_o , the potential independent rate-constant of the reaction at the surface. Thus, the larger the value of k_o , the faster will be the rate of electron transfer at the oxide surface.

The potential, E_M , at which the anodic and cathodic currents are equal is termed the "mixed" or "open circuit" potential, i.e. the

potential at which no external current is flowing. In the case of an oxide dissolving by an electrochemical mechanism in which there is no barrier to the dissolution or complexing of the species at the surface of the oxide once charge transfer occurs, the dissolution current density is a direct measure of the rate of dissolution of the oxide. Under these conditions, it can be seen from equation (1.45) that the rate of leaching of an oxide will also depend on the equilibrium potentials of the oxide and the redox couple, since

$$|\eta_a| = E_a^\circ - E_M \quad (1.47)$$

$$|\eta_c| = E_c^\circ - E_M \quad (1.48)$$

where η_a and η_c are the anodic and cathodic overpotentials, E_a° and E_c° are the anodic and cathodic equilibrium potentials, and E_M is the mixed potential defined above.

1.5 Critical Summary

A major difficulty of considering previous studies of the leaching of oxides is that few extensive studies of single oxides have been made. Additionally, the range of conditions used by various workers to study individual oxides varies from one to the other. Although the effect of acid anions upon the rate of leaching of several metal oxides in different acids can be correlated with the complexing affinity of the anions for oxide cations, there appears to be no explanation of the observed effects of the variation of concentration of acids on

the rates of leaching of metal oxides.

A satisfactory general hypothesis of the mechanism of the direct dissolution of oxides must be able to explain in addition to the effects of anions on the relative rates, at least the following observations:

(a) An apparent dependency of the rates of leaching of $\alpha\text{-Fe}_2\text{O}_3$ and $\alpha\text{-FeO}\cdot\text{OH}$ in perchloric acid over the range of acid concentration studied (0-1.5N) on either $[\text{H}^+]$ or $[\text{HClO}_4]$ added, whilst the rate of leaching of Cu_2O in the same acid appears to show some type of 'saturation' dependence followed by a rate which appears to be proportional to $([\text{H}^+] + C)$ or $([\text{HClO}_4] + C)$ (where C is some constant) (Figure 1).

(b) A dependency of the rates of leaching of $\alpha\text{-Fe}_2\text{O}_3$ and $\alpha\text{-FeO}\cdot\text{OH}$ in low concentrations of hydrochloric acid ($<2.5\text{M}$) on either $a_{\text{H}^+}^2$, $a_{\text{Cl}^-}^2$ or $a_{\text{H}^+} \cdot a_{\text{Cl}^-}$, and at high concentrations an apparent dependency on a_{H^+} or a_{Cl^-} (where a = activity of various ionic species) (Figure 2).

(c) An apparent 'saturation dependency' of leaching rate of Cu_2O in dilute sulphuric acid and a possible similar behaviour by goethite, which causes both oxides to leach by a rate law in stronger sulphuric acid which shows an apparent dependency on $([\text{H}^+] + C)$, $([\text{HSO}_4^-] + C)$ or even possibly $([\text{SO}_4^{2-}] + C)$.

(d) The widely differing rates of leaching observed for Cu_2O and for BeO in sulphuric acid under the same conditions (Cu_2O leaching about 10^6 x faster than BeO).

For the leaching of metal oxides involving a change in oxidation state during dissolution, a mechanistic model must be able to explain at least the following observations:

- (a) A maximum of the rate of leaching of UO_2 , in the presence of Fe^{+++} , occurring at a pH value of approximately 2, in both HClO_4 and H_2SO_4 solutions.
- (b) The large differences in rates of leaching of MnO_2 with Fe^{++} in HClO_4 and H_2SO_4 solutions of equal normality and indeed the same for the leaching of UO_2 in the presence of Fe^{+++} .
- (c) The square root dependency of the rate of leaching of UO_2 with Fe^{+++} on the concentration of Fe^{+++} , whilst the rate of leaching of this oxide with O_2 shows a first order dependency on $p\text{O}_2$.

Whether or not hydroxylation of the oxide surface has to be considered in a general mechanism for the leaching of oxides is open to question. If oxides adsorb water dissociatively very rapidly to the extent of one hydroxyl group per metal atom, no distinct behaviour difference might be observed between a totally hydroxylated or bare oxide surface. This may justify Wadsworth's and Wadia's (49) choice of a bare cuprous oxide surface if this surface becomes rapidly hydroxylated in comparison to the overall rate of dissolution of this oxide. However, Peri (12) has shown that γ - and α - Al_2O_3 heat-treated at temperatures above 800°C do not rehydroxylate rapidly. If hydroxylation of the oxide surfaces is indeed a prerequisite for dissolution, and if this under some conditions, in the case of α - Al_2O_3 is the slow step in the overall leaching of this oxide, the rate of leaching of α - Al_2O_3

would be expected to depend only on the activity of water.

As already discussed, a net positive charge develops on the hydroxylated oxide surface in solutions of pH below the pH of Z.P.C of the oxide. This charge is established by H^+ , OH^- and anions of the acid present in solution and may arise in one of the following ways:

(a) Simultaneous or consecutive adsorption of H^+ , OH^- and anions of the acid at the oxide-electrolyte interface.

(b) Adsorption of undissociated acid at neutral oxide surface sites and of H^+ at the same oxide surface sites.

Warren et al(8,9) suggest that process (a) occurs during the leaching of ferric oxide in perchloric and hydrochloric acids, whereas Wadsworth and Wadia(49) postulated process (b) to explain the leaching of cuprous oxide in sulphuric acid. It thus appears important to study the leaching kinetics of cuprous oxide in both perchloric and hydrochloric acids, as neither process (a) nor process (b) seem to be sufficient to describe the kinetics of the leaching of oxides in general.

Leaching studies in which the concentration of anionic species are varied independently or in a controlled manner should be able to indicate whether anions or undissociated acids of the anions are taking part in the leaching of oxides. Although it is observed that the complexing power of anions in solution for the oxide cation has a large effect on the leaching of metal oxides, it is not clear if this effect is due either to the preferential adsorption of the anion or to the enhanced desorption rate of metal-anion complexes from the oxide surface. Indeed, Berube and De Bruyn(36) and Dumont and Watillon(37) have corre-

lated the driving force for adsorption of anions to their action upon surrounding water molecules, and thus of water adjacent to the oxide surface, and found little correlation between the adsorption sequence and the complexing affinity of the anions for the oxide cation.

Kabai (53) proposed an empirical equation correlating the rate of leaching of oxides to the concentration of the acid as exponent of an exponential, but little fundamental information is obtained from this relation. Finally, several workers (8,9,41,45,46) have suggested that the adsorption affinity of an anion may be associated with the complexing power of the anion for the oxide cation. Clearly, study of a selection of various acids which produce anions having different complexing power for an oxide cation might provide more insight into the role of anions in the leaching of metal oxides.

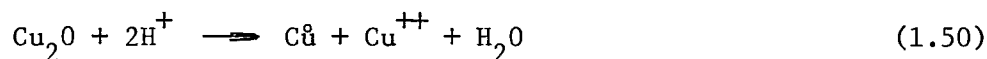
The pH of Z.P.C. of an oxide may be a very important characteristic for the leaching of oxides in acids, mainly for two reasons:

- (a) It gives an indication of how favourable production of a net positive charge at the oxide surface is with decreasing pH.
- (b) It may be related to the anion-exchange capacity of the oxide surface.

The concept of Z.P.C. has been intuitively used by various investigators, (8,9,47,59). Warren et al (8,9) for example represented the rapid formation of an excess positive charge by an equilibrium equation involving the adsorption of H^+ ions at the oxide surface. This equation of course, would only be acceptable if the pH of the solution is far enough away from the pH of Z.P.C. of the oxide. The equilibrium

constant for H^+ adsorption is then a measure of the relative tendency of oxides to adsorb H^+ ions and thus might also be associated with the pH of Z.P.C. of the oxide. The question may now arise regarding the possibility of saturating the oxide surface in H^+ and eventually in the anion(s) of the acid. According to Wadsworth and Wadia (49) the cuprous oxide surface is suggested to already become saturated by undissociated sulphuric acid in dilute solutions, but as mentioned earlier, by a process which involves the direct adsorption of the acid at neutral oxide sites. One could equally suggest that the oxide surface becomes saturated in hydrogen ions from solution, followed by increasing adsorption of HSO_4^- ions at these sites. Studies using oxides of different pH's of Z.P.C. might bring a solution to the problem of the species involved in the leaching of oxides and to the significance of the Z.P.C. of oxides.

So far, no explanation has been given for the large differences observed between the absolute rates of leaching of some oxides, i.e. Cu_2O leaching 10^6 x faster than BeO . Thermodynamically the leaching of BeO in water at a given pH is more favourable than the leaching of Cu_2O as the change in standard free energies for the reactions:



are respectively -10.7 and -6.17 kcal/mole (91). This clearly shows that kinetic factors can overrule drastically the expected driving forces from equilibrium considerations. The observed energies of acti-

vation for the leaching of most metal oxides are nearly constant from one oxide to the other, irrespective of the acid, as they vary between 17 and 23 kcal/mole (Table 3); this may suggest that a similar rate-determining step is operative during the leaching of metal oxides in acids, possibly the desorption of metal species into solution.

The acid leaching of metal oxides involving an oxidation-reduction step in the presence of a redox couple in solution has been studied, for the most part, under relatively restricted conditions. It is logical to expect that surface hydroxylation and charging may also be involved in the overall kinetics of the oxidative or reductive leaching of the oxides. Mackay and Wadsworth (10) have proposed that oxygen adsorbs at uncharged hydroxylated uranium dioxide surface sites and that the concentration of these neutral sites is increased by the reaction of hydrogen ions and the negatively charged portion of the UO_2 surface. This approach is consistent with the hydration-charging properties of UO_2 in acids. Laxen (83) and Needes and Nicol (86) however, did not consider the UO_2 surface properties in their model of the oxidative dissolution of this oxide and were indeed unable to explain the variation of leaching rate of UO_2 with pH in the presence of Fe(III). It appears likely from their studies that both the oxide-electrolyte double layer properties and the type of ferric species present in solution at each pH have to be considered in order to explain the observed kinetics of dissolution of UO_2 .

2. SCOPE OF THE PRESENT INVESTIGATION

The present work had as one objective the resolution of the differences which are apparent in the proposed mechanisms of leaching of metal oxides.

Ferric, aluminum, cuprous, cupric and manganous oxides were selected for the present investigations. Extensive studies on the leaching of ferric oxides were planned in the hope that they might provide a basis for comparing the behaviour of oxides in general. Leaching experiments on aluminum oxides were undertaken to attempt to provide some understanding of the role of surface hydroxylation in the kinetics of the leaching of oxides.

Studies on the leaching behaviour of cuprous oxide were included in the present investigations because the kinetics of leaching of this oxide in sulphuric acid have been explained in terms of a unique mechanism, involving as a first step the adsorption of undissociated acid at the oxide surface. Cupric and manganous oxides were chosen, in addition to the other oxides, in an attempt to correlate the pH of the zero point of charge (Z.P.C.) of an oxide to its leaching characteristics in acids.

Perchloric, hydrochloric, sulphuric and oxalic acids were selected as reagents in order to study the effect of anions on the rate of leaching of the oxides. Amongst other properties, these acids differ in the complexing power of their anions for metal ions in solution.

3. EXPERIMENTAL

3.1 Minerals and Reagents

3.1.1 Natural Minerals

Massive specimens of Micaceous hematite and goethite were obtained from Ward's Natural Science Establishment Inc., New York. The hematite originated from Ishpeming, Michigan and the goethite came from Minnesota. The quantitative chemical analyses and semi-quantitative spectrographic analyses for both minerals are given in Table A.1, Appendix A. For all the experiments the specimens were ground in a porcelain mortar and then wet screened to the 65-150 mesh Tyler sizes.

3.1.2 Synthetic Minerals

(a) Hematite

Synthetic $\alpha\text{-Fe}_2\text{O}_3$ was prepared from pigment grade goethite powder obtained from Harrison and Grosfield Ltd., Canada; its purity was 99.95% $\alpha\text{-FeO}\cdot\text{OH}$ with 0.05 of insoluble matter and traces of copper. The goethite powder was calcined at 800°C for 10 minutes producing pure hematite powder. This powder was cold pressed in discs (1 cm in diameter) followed by sintering at elevated temperature for various times and under various conditions as given in Table 5.

Titanium doped specimens were obtained by the method used by Morin (92). Reagent grade. TiO_2 pigment powder from Matheson Co., U.S.A., was wet mixed with the hematite powder, followed by the sintering

TABLE 5

Synthetic Hematite Specimens

Sample No	Pressure (psi)	Atmosphere	Sintering		Ti (%wt)	Fe ²⁺ (%wt)	Remarks
			T° (F)	Time/days			
A	15,000	air	2,100	4	0	0.12	
B	15,000	O ₂	1,650	3	0	0.24	
C	15,000	air	2,100	2	1.3	1.52	
D	15,000	air	2,100	2	0	0.24	
E	15,000	air	2,100	2	3.0	2.94	
F	15,000	air	2,100	2	0.5	0.65	
G	15,000	air	2,100	1	0	0.14	
H	15,000	air	2,100	8	0	0.10	
I	15,000	air	2,100	1	0.1	0.16	
J	15,000	air	2,100	1	0.2	0.24	
K	15,000	air	2,400	1	0.8	1.03	
L	15,000	air	2,400	1	0.4	0.77	
P	20,000	air	2,400	2	0	0.2	99.999 Fe
N	20,000	air	2,400	2	0		0.5% Ca
Q=A+D+G+H					0		
O=A+D+G+H					0		Mixtures
X	15,000	air	2,400	1	0		0.5% Mg

operations under the conditions indicated in Table 5. Calcium doped specimens were prepared by a method described by Geiger and Wagner (93) and magnesium doped samples were obtained in the fashion proposed by Gardner et al (94).

X-ray diffraction patterns of the samples were consistent with the ASTM card for hematite and are reported in Table A.2, Appendix A. Electron-Microprobe pictures of the Ti and Ca doped $\alpha\text{-Fe}_2\text{O}_3$ surfaces are shown in Figure 3a to 3f. Clustering of Ti is observed for Ti contents of 1.5 and 3.0%. No homogeneous Ca doping could be obtained.

(b) Cuprous Oxide (Cu_2O)

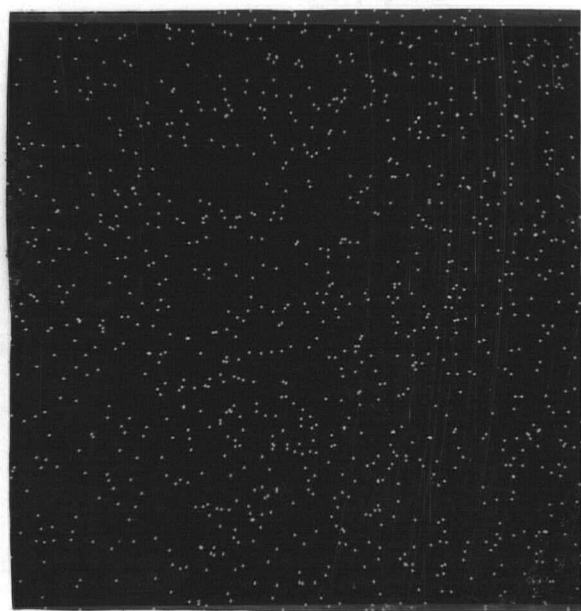
Cuprite was obtained by the thermal oxidation of pure copper wire, at 900°C under air for 24 hours. The Cu_2O powders obtained after crushing the samples in a porcelain mortar presented the X-ray diffraction pattern characteristics of Cu_2O as given by the ASTM card (Table A.3, Appendix A).

(c) Cupric Oxide (CuO)

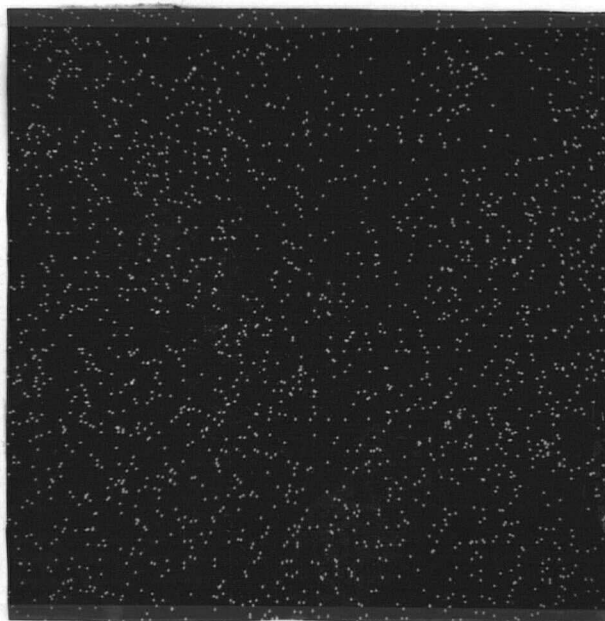
Cupric oxide was obtained by the further oxidation of Cu_2O at 700°C , under air, for 48 hours. The CuO powder obtained after crushing the sample presented all the X-ray diffraction pattern characteristics of CuO as given by the ASTM card (Table A.3, Appendix A). Traces of Cu_2O probably contaminated these samples, approximately 1% by wet analysis.

(d) Manganous Oxide

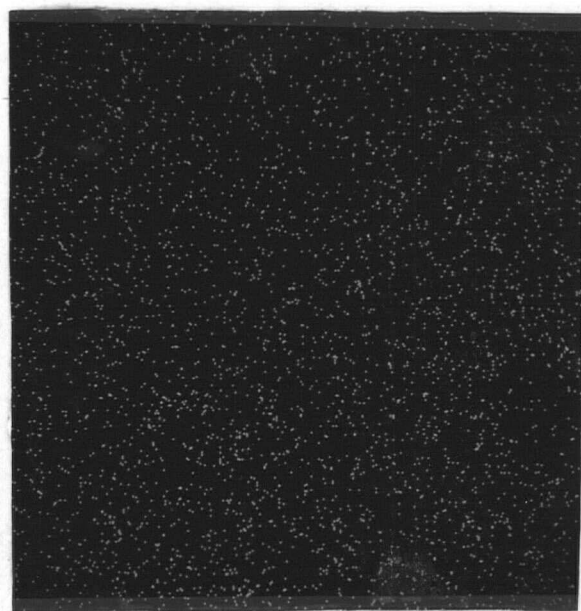
Manganous oxide was obtained by the reductive roasting of natural pyrolusite (analysis given in Table A.4, Appendix A) at 900°C under



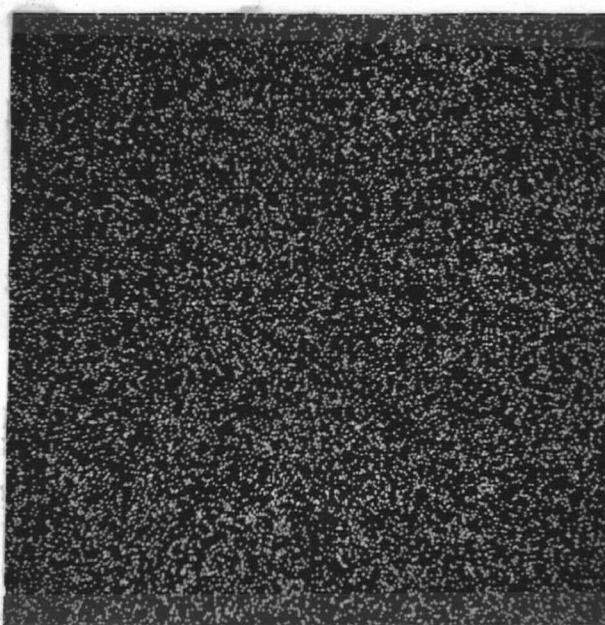
(a)



(b)



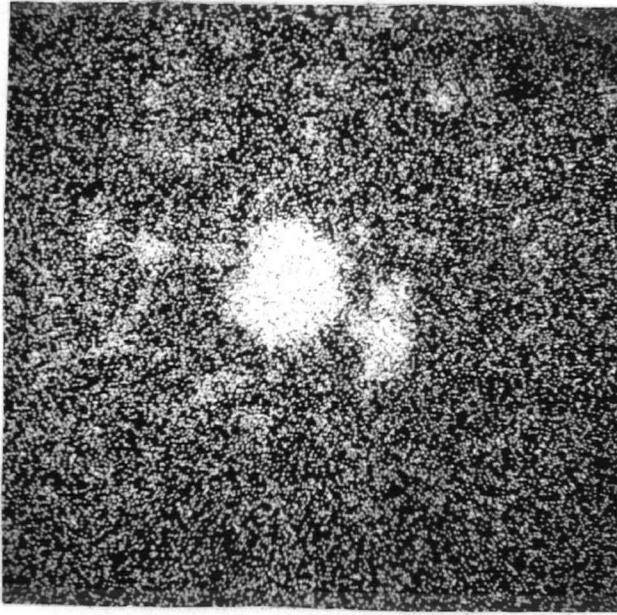
(c)



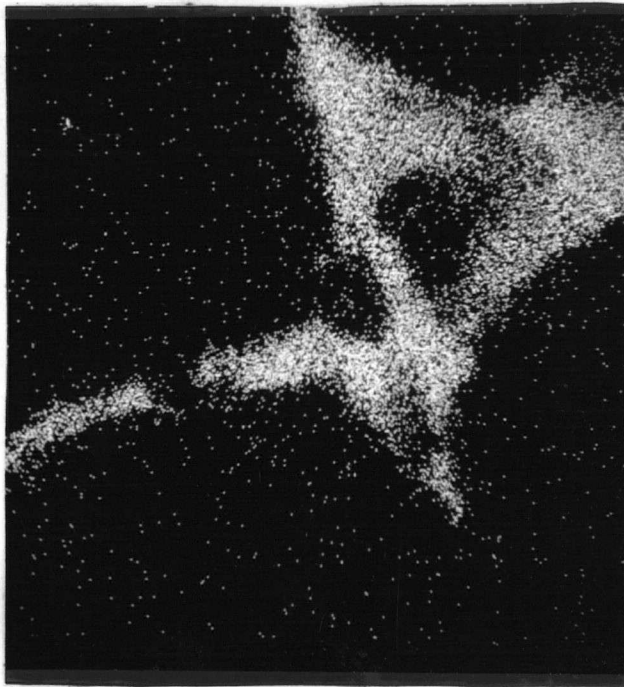
(d)

Figure 3. Electron microprobe pictures for Ti or Mg of synthetic $\alpha\text{-Fe}_2\text{O}_3$ samples (Table 5) (x 1,000)

(a) 0.1% Ti; (b) 0.2% Ti; (c) 0.5% Ti; (d) 1.3% Ti.



(e)



(f)

Figure 3. (e) 3.0% Ti
(f) 0.5% Mg

cracked ammonia for 24 hours. The weight loss indicated that all MnO_2 present in the ore had been converted to MnO .

(e) Aluminum Oxides

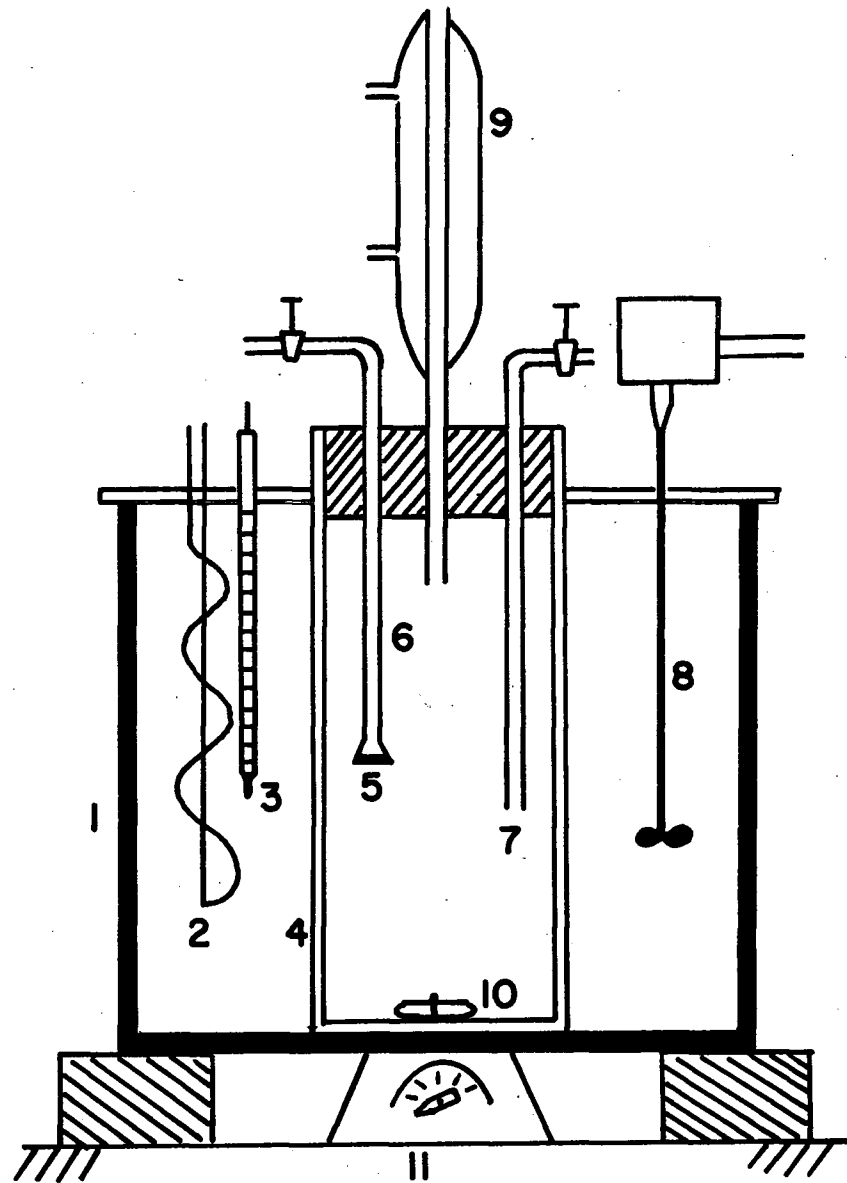
Pure gibbsite ($\alpha\text{-Al}_2\text{O}_3 \cdot 3\text{H}_2\text{O}$) was obtained from Alcan, Canada. Calcination of the gibbsite powder at 300°C for 24 hours under air produced boehmite ($\alpha\text{-Al}_2\text{O}_3 \cdot \text{H}_2\text{O}$), and calcination at 600°C for 24 hours under air transformed the gibbsite into $\gamma\text{-Al}_2\text{O}_3$. Calcination of the gibbsite powder at 1400°C for 24 hours under air resulted in the formation of pure $\alpha\text{-Al}_2\text{O}_3$. The X-ray diffraction patterns of the synthetic aluminum oxides mentioned above were consistent with the data given by the ASTM cards and are reported in Table A.5, Appendix A.

3.1.3 Reagents

Perchloric, hydrochloric and sulphuric acids were obtained from Allied Chemical, Canada. Oxalic acid was provided by J.T. Baker Chem. Co., U.S.A. Ferrous oxalate was from Griffin and George, England. All other chemicals which were used were reagent grade. Helium and oxygen came from Canadian Liquid Air Ltd.

3.2 Apparatus Design

Leaching experiments were carried out in a glass reaction vessel maintained at constant temperature in a heat controlled water bath and open to the atmosphere through a reflux condenser. The main features of the apparatus are schematized on Figure 4. The 1500 mls capacity cylindrical glass reaction flask was fitted with a gas inlet



- 1. Water Bath
- 2. Immersion Heater
- 3. Contact Thermometer
- 4. Reaction Flask
- 5. Fritted Glass Filter
- 6. Sampling Tube
- 7. Gas Inlet Tube
- 8. Stirrer Motor
- 9. Reflux Condenser
- 10. Spin Bar
- 11. Magnetic Stirrer

Figure 4. Apparatus Design.

tube and a sample tube terminating with a fritted glass filter. The solution in the flask was stirred by means of a Teflon-covered magnet rotated by a magnetic stirrer unit below the water bath vessel. Heat was supplied by a 100 watt immersion heater, which controlled the temperature within 0.2°C . through connection with a mercury relay which was itself connected to the contact thermometer. The water bath was stirred continuously by a variable speed stirrer.

3.3 Experimental Procedure

The experimental procedure consisted of the following steps:

- (a) The temperature controller was set at the required temperature.
- (b) The reaction flask, containing 1000 mls of solution of the required concentration, was immersed in the water bath, and the various connections made.
- (c) The system was allowed to come to thermal equilibrium. Flushing with He or O_2 , if desired, was carried out simultaneously.
- (d) The powder specimen (usually 1 gm) was added to the solution, and the flask was closed.
- (e) Stirring of the solution was started and a first sample taken (usually 5 mls) by applying an O_2 , air or He overpressure above the solution. The analysis of this first sample was considered as a blank for the successive samplings at regular intervals. The first 10 mls of solution removed in all samplings were immediately returned to the flask via the reflux condenser.
- (f) The samples were analysed for the desired metal content.

In the leaching experiments of ferric oxides with oxalic acid it was necessary to prevent the photo-catalyzed reduction of ferric ion in solution. The reaction flask used in these experiments was covered by black masking tape which prevented light from reaching the solution.

The pH's of the 0.2M oxalic acid solutions which were used were adjusted with NaOH and HClO₄ additions and were measured at 80°C against standard buffer solutions of pH 2 and 4 using an expanded pH meter. The measured and calculated pH's are reported in Table B.1, Appendix B.

3.4 Analytical Methods

3.4.1 Iron

The iron content of the solutions was determined by measuring the absorbance at 510 μ of the orthophenanthroline complex of ferrous ions after reduction with excess hydroxylamine hydrochloride (95).

In the presence of oxalic acid the solutions had to be heated up to 60°C in order to ensure complete conversion of ferric to ferrous ions. However, when the samples contained over 0.2M/liter of oxalic acid, ferrous oxalate precipitated upon adding the o-phenanthroline reagent buffer solution. It was then necessary to destroy the oxalic acid before analysis. This was accomplished by adding an excess of sodium persulfate (Na₂S₂O₈) to the sample and boiling it to eliminate the excess of oxidizing agent.

3.4.2 Aluminum

The aluminum contents of the solutions were determined by measuring the absorbance at 580 μ of the pyrocatechol violet complex of aluminum ions in an ammonium acetate buffer solution (pH 6.1-6.2)(96).

3.4.3 Copper

The copper contents of the solutions were obtained by measuring the absorbance at 640 μ of the tetraethylene pentamine complex of copper(II) (97).

3.4.4 Manganese

The manganese contents of the solutions were obtained by measuring the absorbance at 524 μ of the permanganate ion obtained by heating the sample in the presence of excess potassium periodate (98).

3.4.5 Determination of the Ferrous Content of Hematite Specimens

A five gram powder sample of the hematite was dissolved in 200 mls of 20% sulphuric acid at 80°C, under an He atmosphere. The solution was then cooled and an excess of phosphoric acid was added to eliminate the colour of ferric sulphate. This solution was titrated with a standardized 0.1N ceric sulphate solution in the presence of indicator. The red colour of the o-phenanthroline ferrous complex changed to the green colour of the ferric complex upon completion of the reaction $Ce^{4+} + Fe^{2+} \rightarrow Ce^{3+} + Fe^{3+}$. This method was found to be sensitive to as little 0.05% ferrous ion content in the five gram hematite sample (absolute error of $\pm 0.02\%$).

4. RESULTS

All the rates of leaching were obtained from measurement of the initial slopes of the plots representing the amount of metal dissolved versus time. It was usually observed that the rate of leaching of an oxide did not vary with time up to 10% dissolution of the contained metal. If the rate of leaching of the oxide was indeed varying steadily with time in the early stages of the leach, the experiment was repeated in order to obtain the best approximation of the initial rate.

4.1 The Leaching of Metal Oxides in Aqueous Perchloric Acid Solutions

The rates of leaching of cuprous oxide (Cu_2O), cupric oxide (CuO) and ferric oxide ($\alpha\text{-Fe}_2\text{O}_3$, Michigan) were measured at constant temperature as a function of the concentration of the acid (Figures 5 and 6). Hay's (99) and Surana's (100) results on the rates of dissolution of goethite ($\alpha\text{-FeO}\cdot\text{OH}$) are also included on Figure 6. The absolute rates of leaching of the oxides vary widely from one to the other and do not serve as a convenient basis for comparison. Hence only relative rates of leaching, that is the ratios of the actual rates of dissolution of the oxides over their rates of leaching in 0.9M HClO_4 , were plotted against the concentration of HClO_4 (Figures 5 and 6).

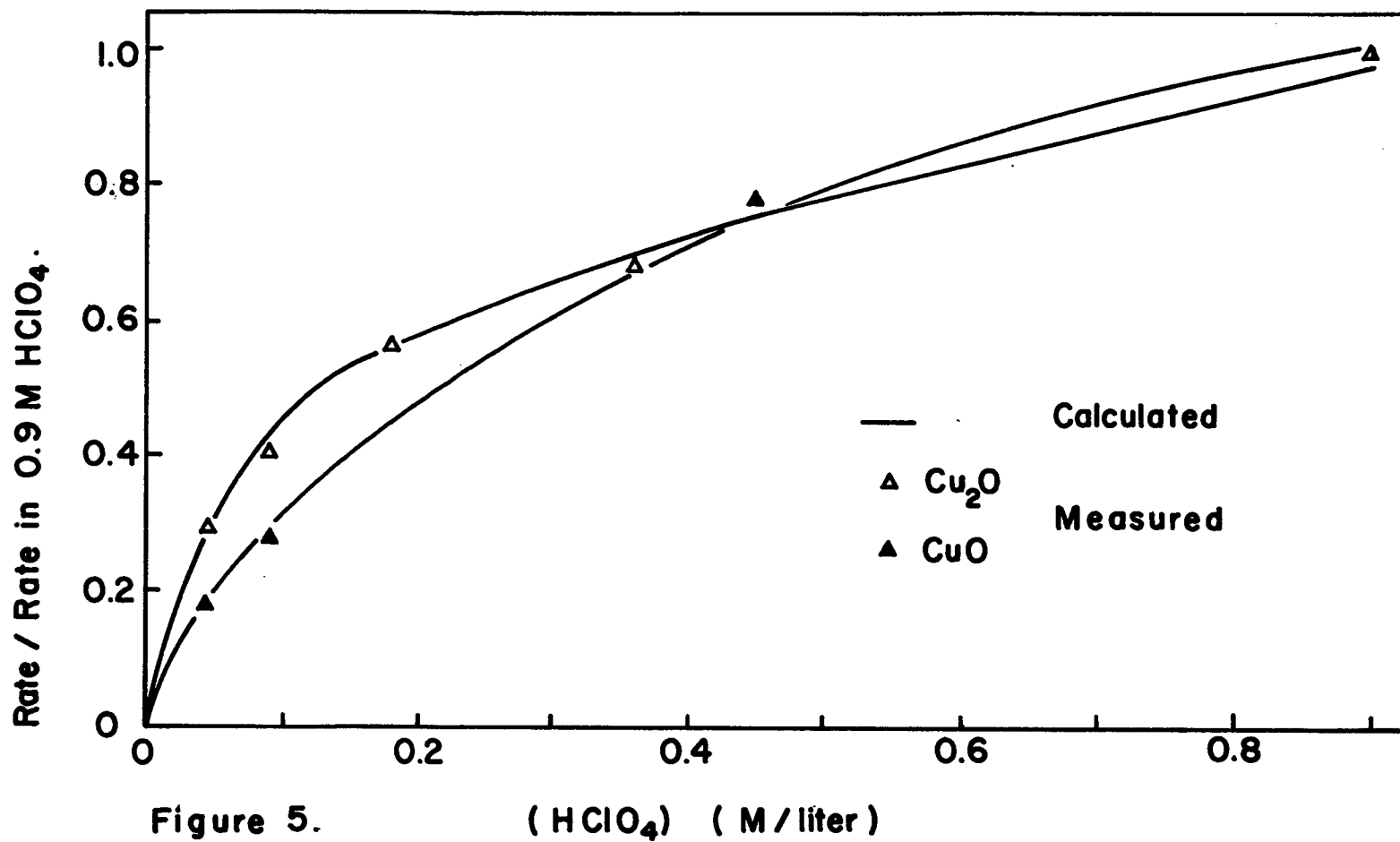
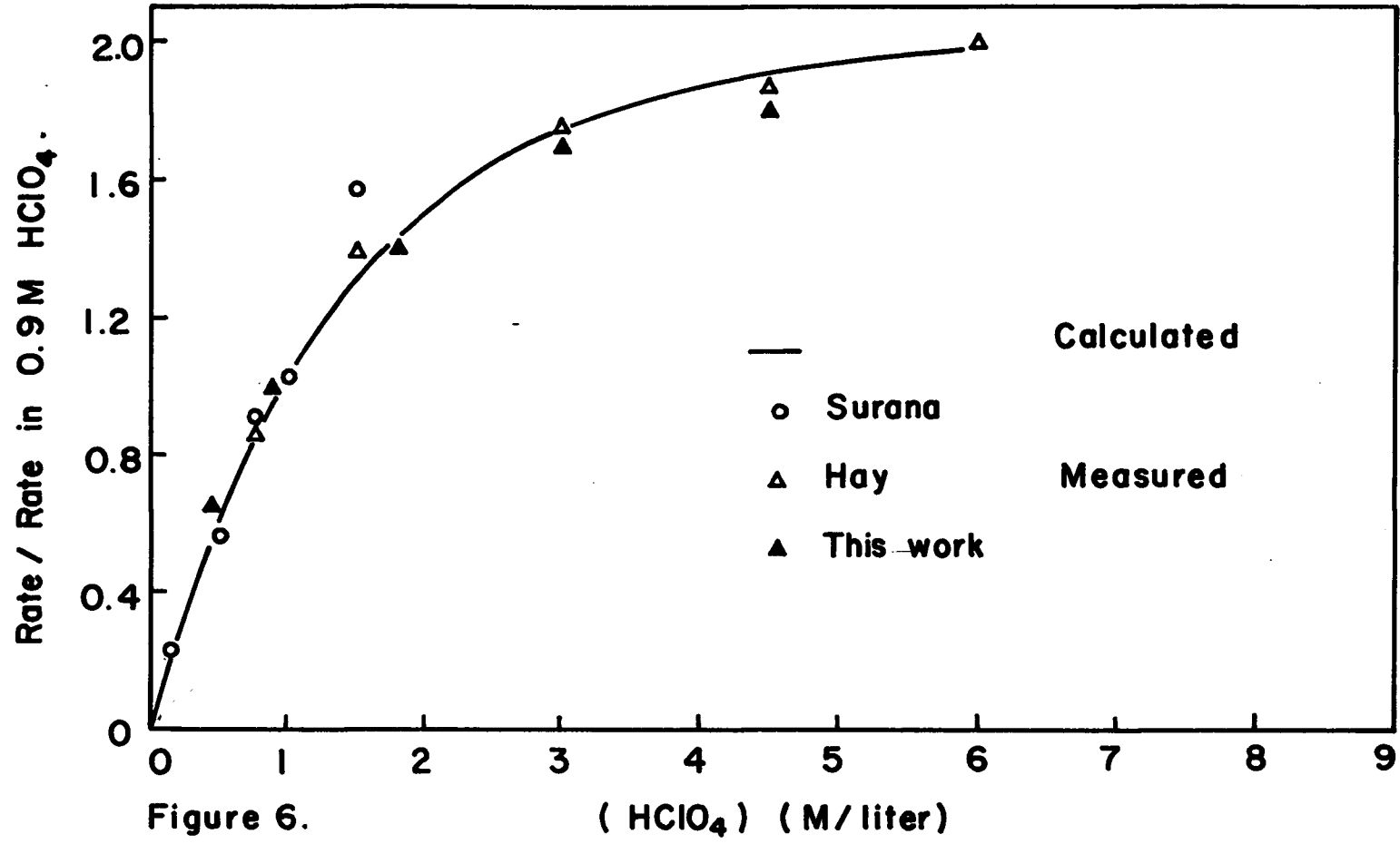


Figure 5. Relative rates of leaching of Cu₂O and CuO in HClO₄ versus the concentration of HClO₄ at 12 °C. (Table B.5 , Appendix B)



The rates of leaching of the oxides show a first order dependence on the concentration of added perchloric acid in dilute solutions, but a lower order in more concentrated solutions; this divergence of the rates to a lower order dependence on the concentration of HClO_4 begins at different acid concentrations for the various oxides, approximately in the order

$$0.1\text{M } (\text{Cu}_2\text{O}) < 0.3\text{M } (\text{CuO}) < 1.5\text{M } (\alpha\text{-Fe}_2\text{O}_3 \text{ and } \alpha\text{-FeO}\cdot\text{OH})$$

Very large differences are observed between the absolute rates of leaching of the oxides at a given concentration; in 0.9M HClO_4 at 12°C , for example, the absolute rates of leaching are approximately correlated in the following way:

$$\begin{aligned} \text{rate } (\text{Cu}_2\text{O}) &\approx 9 \times \text{rate } (\text{CuO}) \approx 8 \times 10^7 \times \text{rate } (\alpha\text{-FeO}\cdot\text{OH}) \\ &\approx 2.7 \times 10^8 \times \text{rate } (\alpha\text{-Fe}_2\text{O}_3) \end{aligned}$$

The relatively high energies of activation obtained for the leaching of the oxides (42,100) suggests that the dissolution was not controlled by diffusion under the conditions of the experiments. The rates of leaching of the oxides were not dependent on solution agitation and this is in support of the statement above. Finally, experiments with varying amounts of ore samples showed that the slow step in the leaching reactions for all the oxides was heterogeneous in nature.

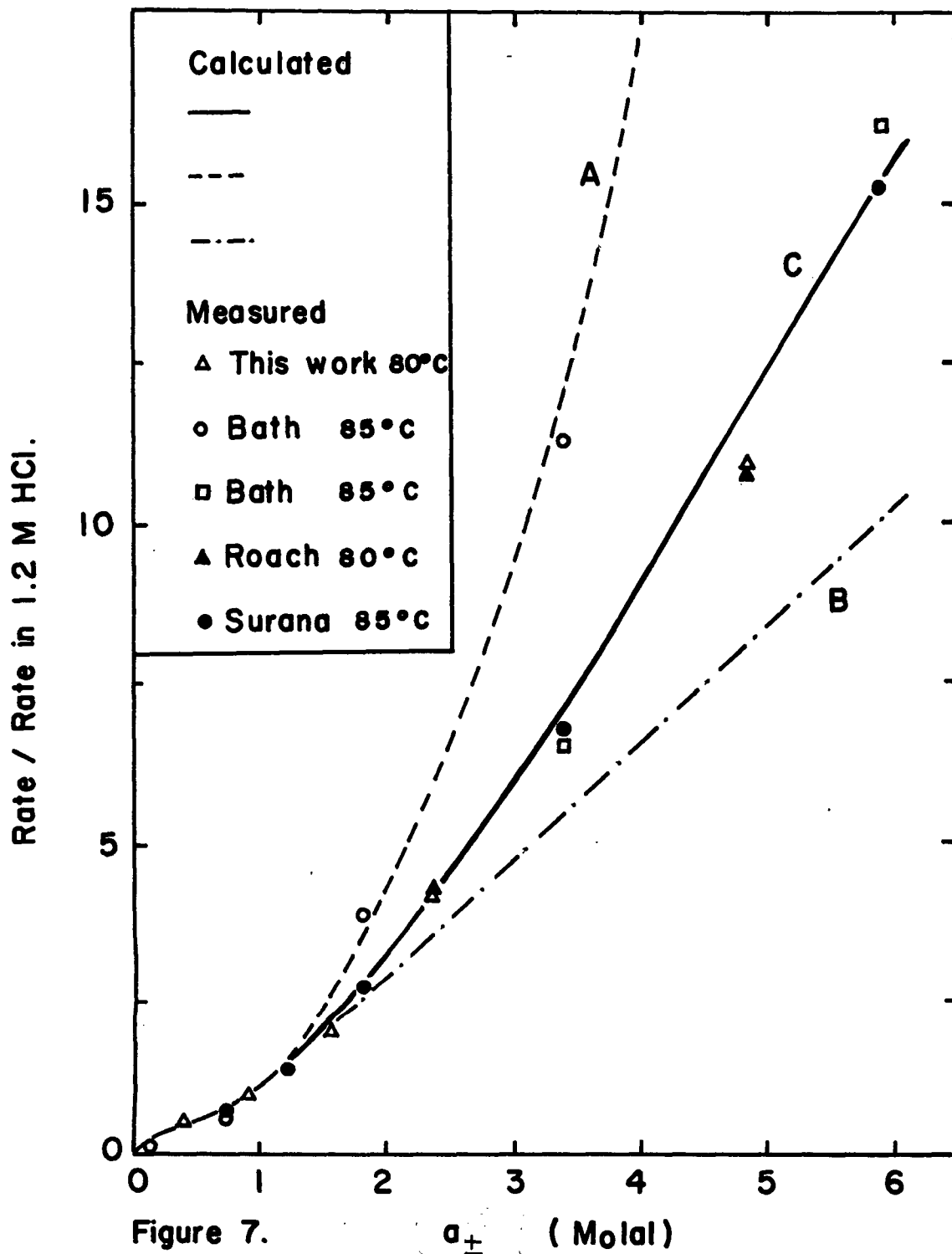
In the present investigations, the maximum concentration of HClO_4 had to be limited to 1M HClO_4 for the leaching of Cu_2O and CuO powders, and 6M HClO_4 for the dissolution of $\alpha\text{-FeO}\cdot\text{OH}$ and $\alpha\text{-Fe}_2\text{O}_3$, because in the

former case the rates of leaching became too large to measure accurately and in the latter diffusion control of the dissolution appeared to be unavoidable due to the increase of solution viscosity.

4.2 The Leaching of Metal Oxides in Aqueous Hydrochloric Acid Solutions

The rates of leaching of ferric oxides (goethite, hematite), cuprous and cupric oxides (Cu_2O and CuO) and aluminum oxides (gibbsite, $\gamma\text{-Al}_2\text{O}_3$ and $\alpha\text{-Al}_2\text{O}_3$) were investigated at constant temperature as a function of the concentration of the acid and were plotted against the calculated mean activities of HCl (Table B.6, Appendix B). The absolute rates of leaching vary greatly from one oxide to the other and only relative rates were plotted, every observed rate being divided by the rate of leaching of the oxide in 1.2N HCl.

The rates of dissolution of ferric oxides show a second order dependence on the mean activity of HCl (a_{\pm}) in dilute solutions ($a_{\pm} < 1$) (Figures 7 and 9), slowly decreasing to an apparent first order dependence on a_{\pm} in concentrated solutions ($a_{\pm} > 1.0$) (Figures 8 and 9). Earlier results on the rates of leaching of various natural ferric oxide powders obtained by Bath (101), Surana (100) and Roach (42) are included in Figures 7, 8 and 9. The transition from the second order to an apparent first order dependence of the rate on a_{\pm} is shown on Figure 9 in a plot of the ratios of the relative rates of leaching and the mean activity of HCl versus the mean activity of HCl. Such a plot yields a first order relation of the ratios with a_{\pm} for rates which show a second order dependence on a_{\pm} and a zero order



Relative rate of leaching of ferric oxide in dilute HCl as a function of the mean activity of HCl. (Tables B.7 and B.7a, Appendix B).

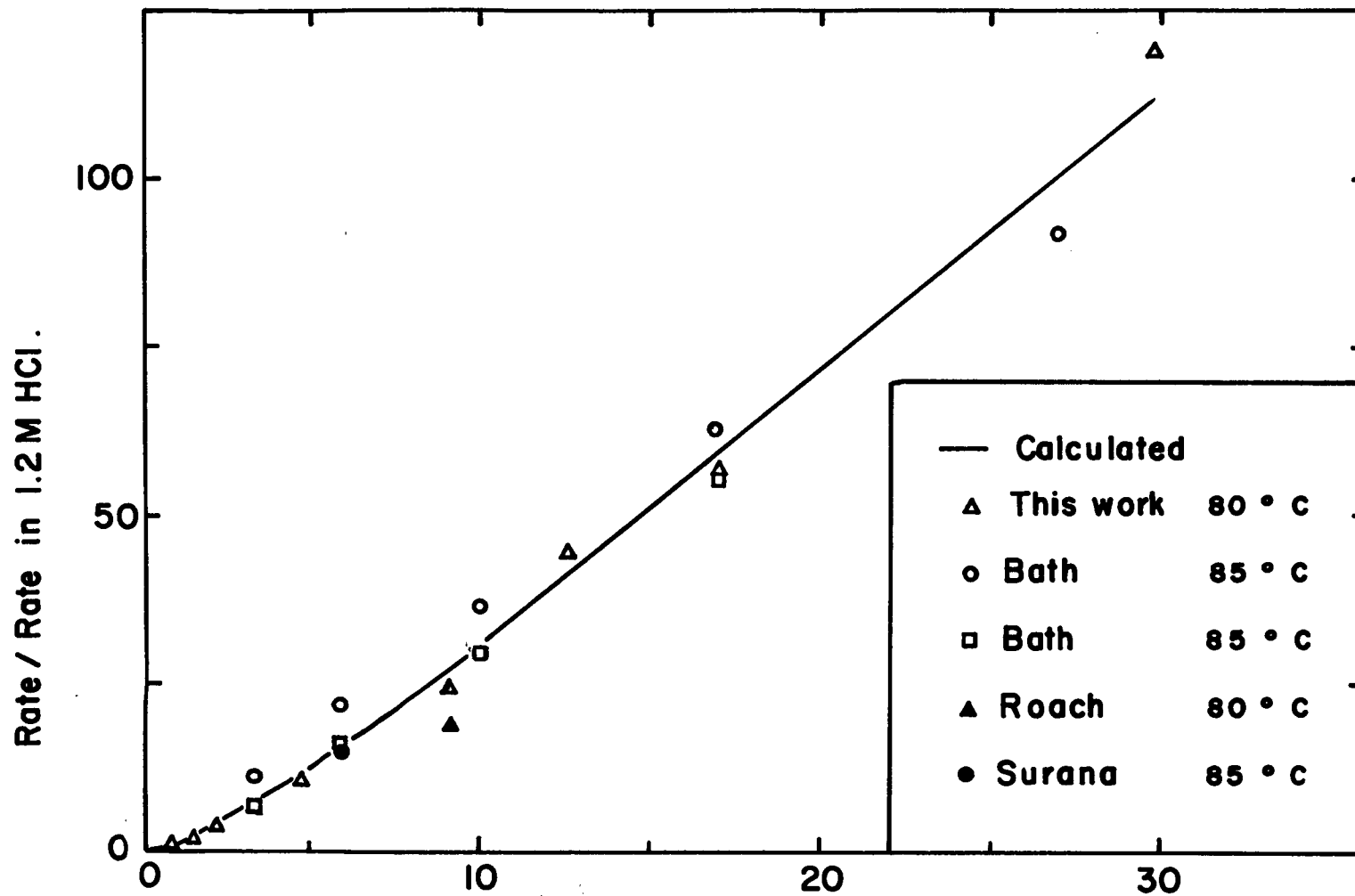
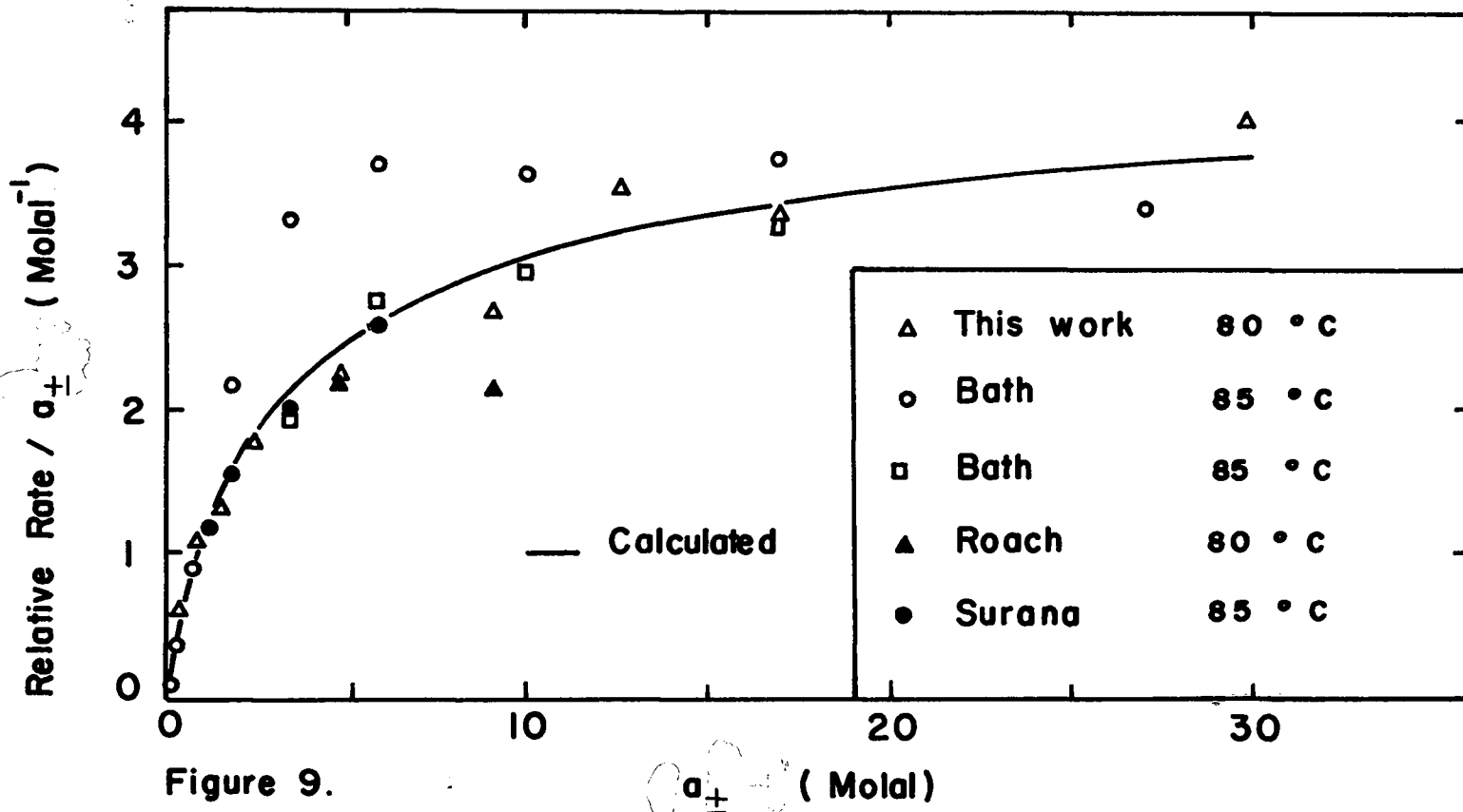


Figure 8.

a_{\pm} (Molal)

Relative rate of leaching of ferric oxide in HCl as a function of the mean activity of HCl (Table B.7, Appendix B).



Ratio of the relative rate of leaching of ferric oxide and a_{+} as a function of a_{+} (Table B.8, Appendix B)

dependence on a_{\pm} for rates which exhibit a first order dependence on a_{\pm} . Figure 9 clearly shows that the rates do not become proportional to a_{\pm} up to $a_{\pm}=30$. Most of the earlier studies on the leaching of ferric oxides are in good agreement with the present work, with the exception of some of Bath's results (Figures 7, 8 and 9). Bath obtained rates of leaching of synthetic $\alpha\text{-Fe}_2\text{O}_3$ powders which appear to yield much higher relative rates of dissolution in dilute HCl solutions when his results are compared with the present work in concentrated solutions. Moreover, his results suggest that the relative rates of leaching of ferric oxide are truly second order with respect to a_{\pm} up to $a_{\pm}=1.8$ and then become rapidly proportional to a_{\pm} at higher activities (Figure 9). It should be mentioned however, that Bath used 0.1 gm/liter powder samples in his experiments whilst all other workers used at least 1 gm/liter powder specimens. Additionally, Bath himself obtained contradictory results for his experimental rates of leaching of the basal plane of a $\alpha\text{-Fe}_2\text{O}_3$ single crystal. It transpires that these latter results are in agreement with the present work (Figures 7, 8 and 9).

The rates of leaching of ferric oxide appears to depend on both the activities of the hydrogen and the chloride ions as can be seen in Figures 10 and 11. Figure 10 shows the effect of adding 0.6, 1.2 and 2.4M of LiCl to a 2.4N HCl solution on the relative rates of dissolution of $\alpha\text{-Fe}_2\text{O}_3$ and Figure 11 shows the effects of adding 0.9, 1.2 and 1.8M HClO_4 and 1.2 and 1.8M NaOH to the same HCl solution on the relative rate of leaching of $\alpha\text{-Fe}_2\text{O}_3$ at 80°C.

The effect of HCl concentration on the relative rates of leaching

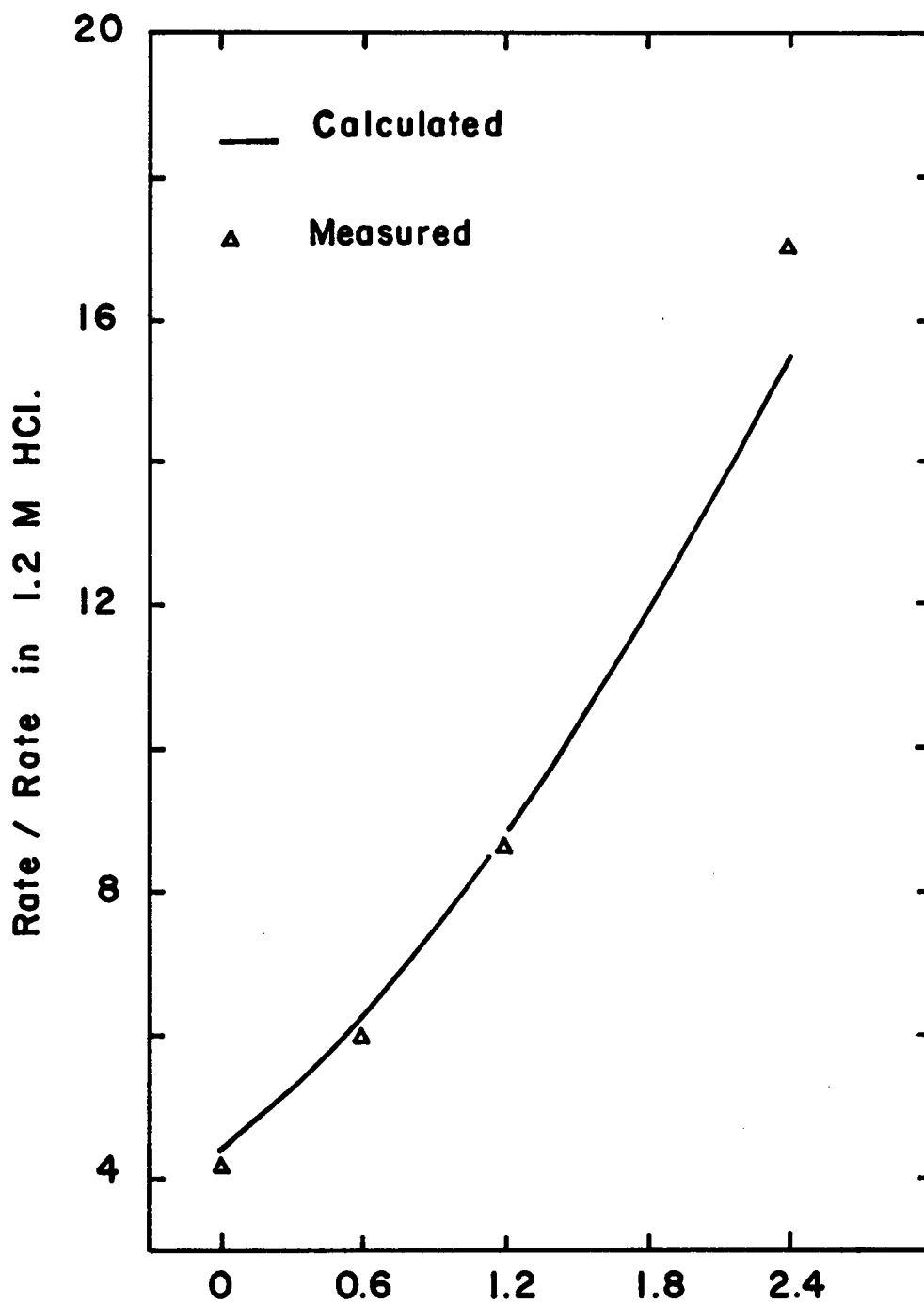


Figure 10. (LiCl) (M/liter) .

Effect of adding LiCl on the relative rate of leaching of ferric oxide (Michigan) in 2.4 M HCl at 80 ° C . (Table B.9 , Appendix B) .

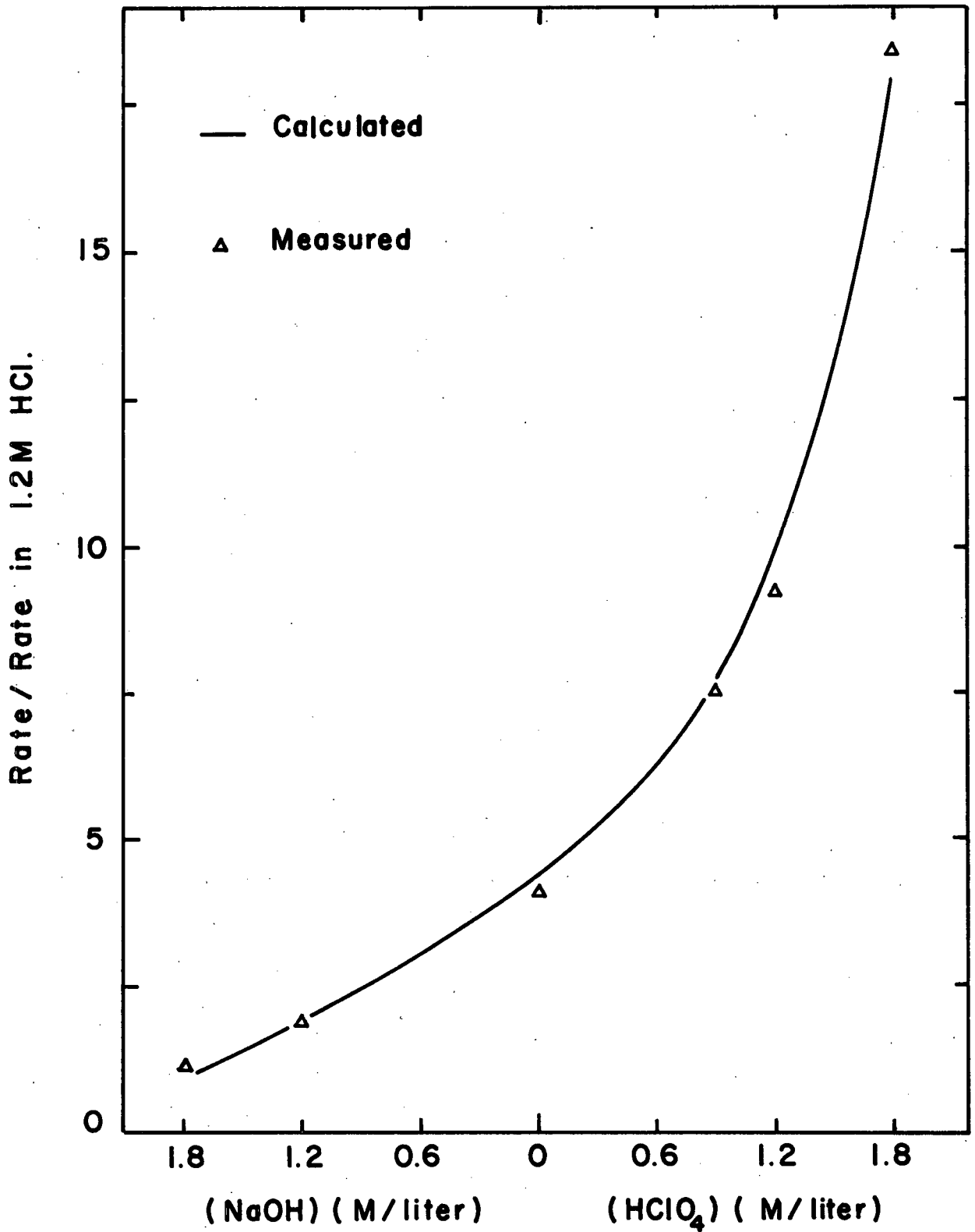


Figure II.

The effect of adding NaOH or HClO₄ on the relative rate of leaching of α -Fe₂O₃ (Michigan) in 2.4 M HCl at 80°C. (Table B.9, Appendix B).

of various aluminum oxides at constant temperature is shown in Figure 12. Gibbsite ($\text{Al}(\text{OH})_3$) dissolves in HCl solutions with a rate which shows approximately a first order dependence on a_{\pm} in dilute solutions, slowly becoming zero order with respect to a_{\pm} in concentrated HCl solutions. The γ -form of Al_2O_3 also appears to leach with a rate which exhibits a first order correlation with a_{\pm} in dilute solutions, but a sudden switch to a zero order function of a_{\pm} can be observed for $a_{\pm} > 2$. Finally, α - Al_2O_3 does not leach to any measurable extent in HCl even after 4 hours in 7.2N HCl at 80°C .

The kinetics of the constant temperature leaching of cuprous and cupric oxides in HCl are represented in Figure 13. The oxides both appear to dissolve with a first order dependence on a_{\pm} in dilute solutions, slowly varying towards a zero order dependence on a_{\pm} in concentrated solutions (Figure 14).

It is concluded from the above experimental results that all the oxides show a decreasing dependence of their rates of leaching on a_{\pm} with increasing acid concentration. Additionally, all the oxides leach more quickly in HCl than in HClO_4 at equal acidity and temperature, but not by the same magnitude. Ferric oxide, for example, leaches about 10 times more quickly in 1.2N HCl than in 1.2N HClO_4 , whilst cuprous oxide dissolves around 5 times more rapidly and gibbsite about 2.5 times faster. This enhancement effect exhibited by HCl over HClO_4 increases with increasing acidity; ferric oxide, for example, dissolves about 20 times more quickly in 2.4N HCl than in 2.4N HClO_4 .

As is the case with the leaching of the oxides in HClO_4 solutions,

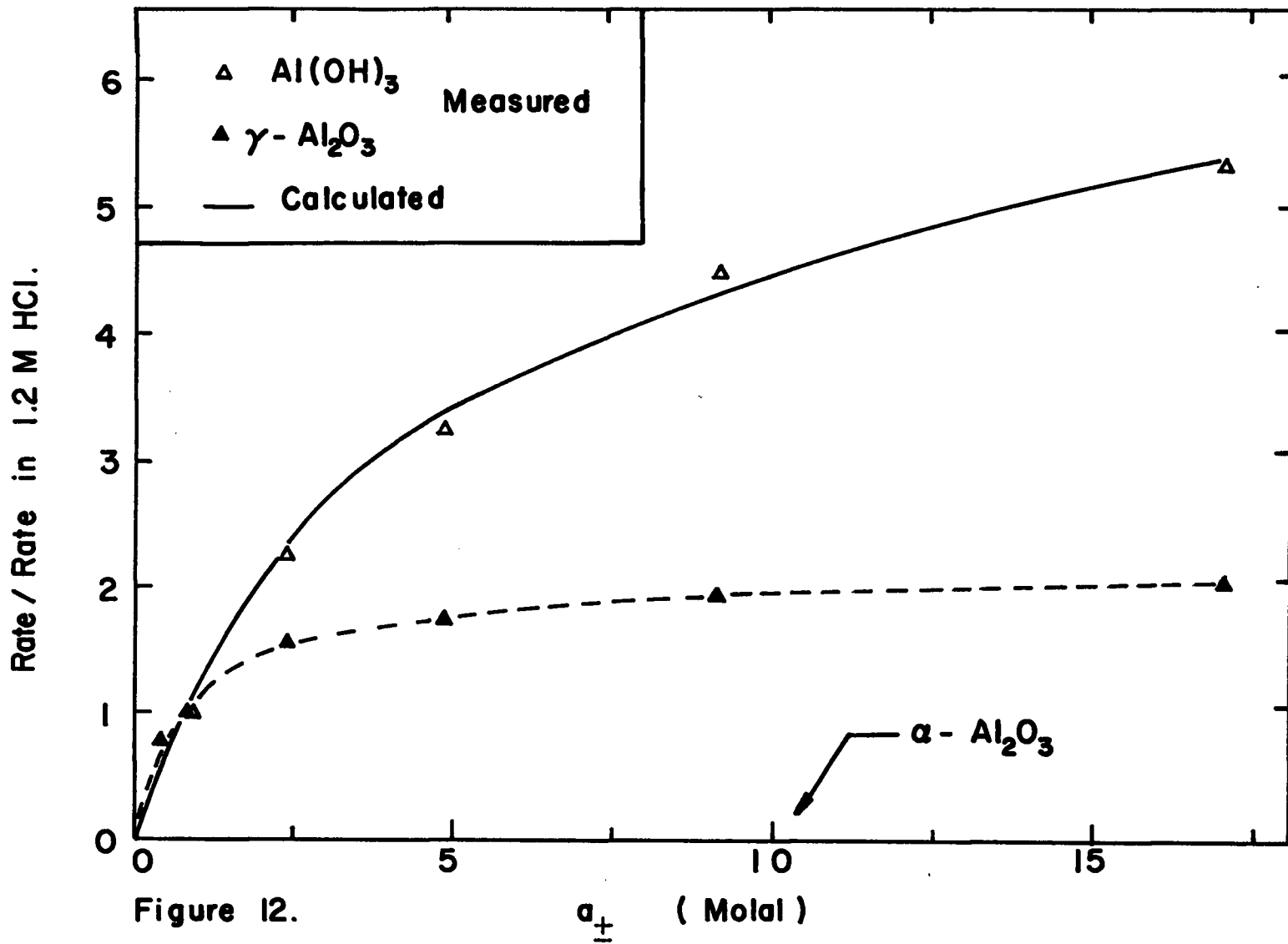
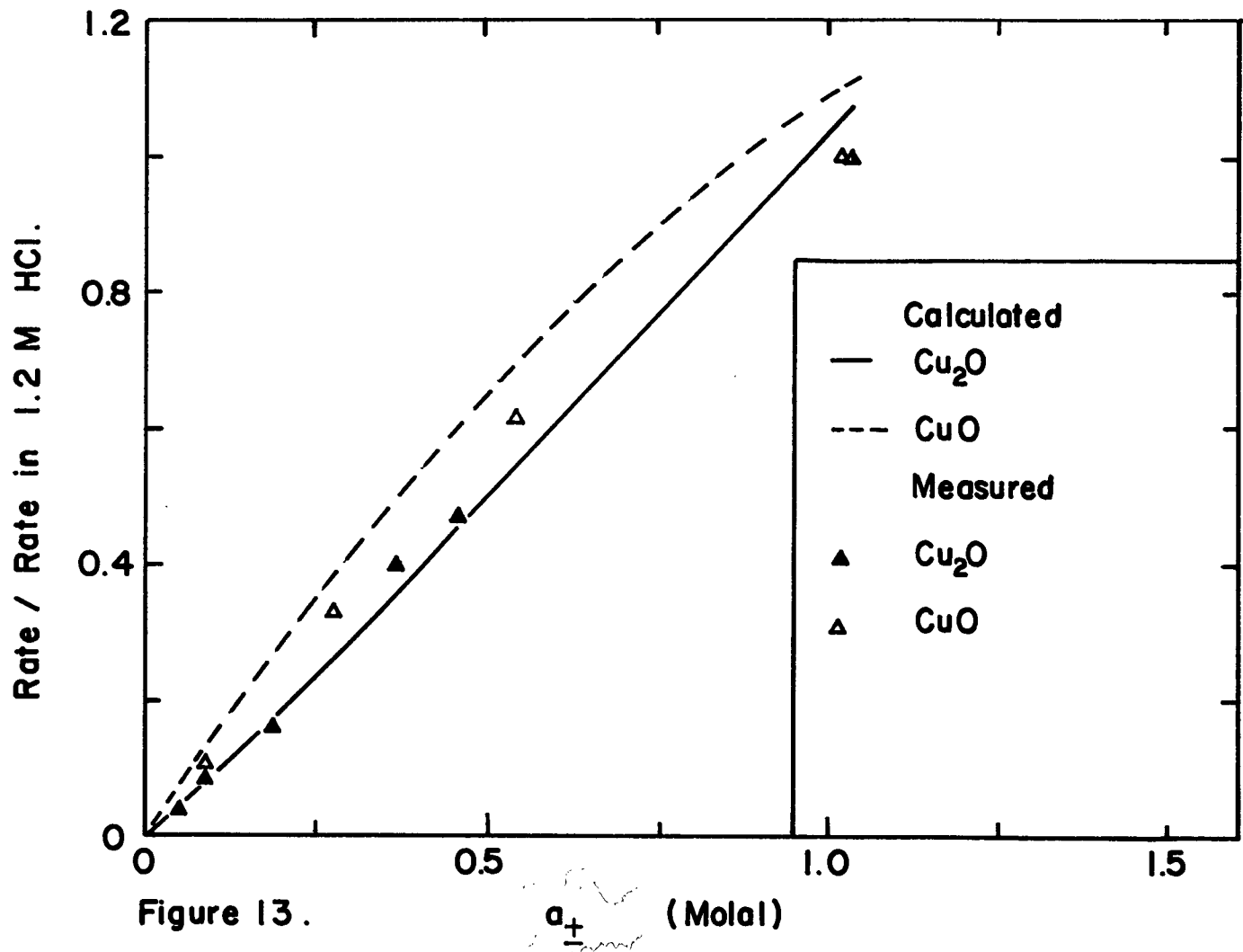
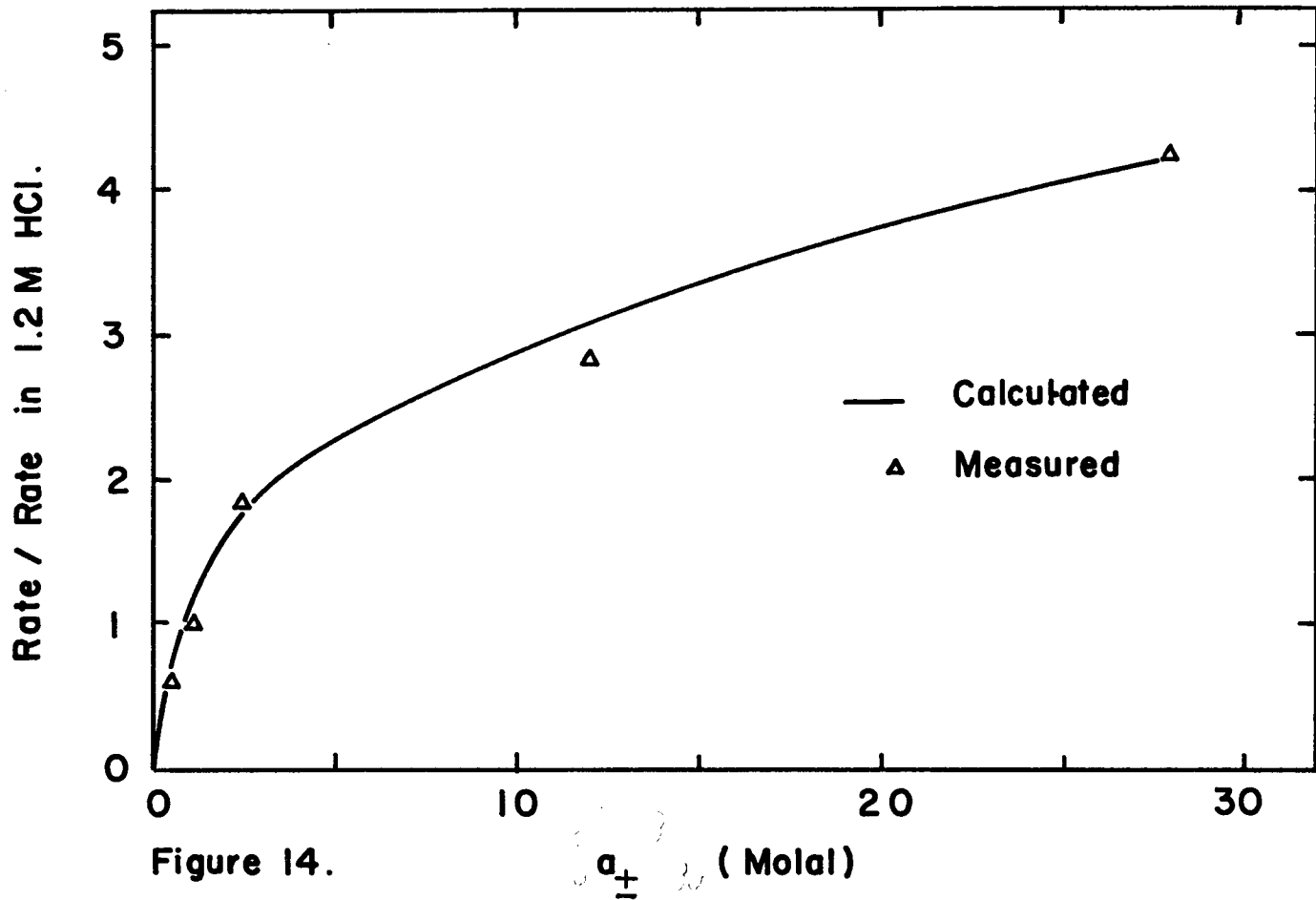


Figure 12. Relative rates of leaching of aluminum oxides in HCl versus the mean activity of HCl. (T = 80 °C) (Table B.7 , Appendix B) .



Relative rates of leaching of Cu₂O and CuO in dilute HCl versus the mean activity of HCl. (T = 12 ° C) (Table B.7 , Appendix B) .



the magnitude of the absolute rates of leaching of the oxides in HCl solutions varies widely from one oxide to the other, approximately in the sequence:

$$\text{Rate (Cu}_2\text{O)} \approx 6 \times \text{Rate (CuO)} \approx 10^5 \times \text{Rate Al(OH)}_3 \approx 10^5 - 10^7 \\ \times \text{Rate } (\alpha\text{-Fe}_2\text{O}_3)$$

The energies of activation for the dissolution of the oxides in HCl are 21-23 kcal/mole for $\alpha\text{-Fe}_2\text{O}_3$ (42,101), 17-18 kcal/mole for $\alpha\text{-FeO}\cdot\text{OH}$ (42,100), 13 ± 0.2 kcal/mole for $\gamma\text{-Al}_2\text{O}_3$ (this work), and 14.7-22.2 kcal/mole for Al(OH)_3 (47,53). It is to be noted that the activation energy for the leaching of $\gamma\text{-Al}_2\text{O}_3$ falls out of the range of activation energies which are generally observed for the dissolution of oxides in acids (Table 3).

4.3 The Leaching of Metal Oxides in Aqueous Sulphuric Acid Solutions

The rates of leaching of ferric, cuprous, cupric and manganous oxides were investigated at constant temperature as a function of the concentration of the acid (Figures 15 and 16). The average results obtained earlier by Surana (100) and Roach (42) on the leaching of various natural goethite and hematite minerals are included on Figure 15. The absolute rates of dissolution of the various oxides cannot be compared conveniently and only relative rates of leaching were considered; that is the ratios of the observed rates over the corresponding rates in 0.9M H_2SO_4 for each oxide.

The rate of leaching of ferric oxide shows a decreasing dependence on the concentration of H_2SO_4 in dilute solutions (0-1M), becoming proportional to the concentration of H_2SO_4 in stronger solutions (1-7.2M) (Figure 15). The present work also appears to correlate very well with earlier work.

Cuprous, cupric and manganous oxides all dissolve with a rate versus H_2SO_4 concentration which shows a similar dependence on the concentration of H_2SO_4 as does ferric oxide (Figure 16). A priori, no fundamental difference between the behaviour of the oxides can be detected from the results.

Again, as is observed for the leaching of the oxides in $HClO_4$ and HCl solutions, the absolute rates of leaching of the various oxides in H_2SO_4 solutions are quite different; in 1N H_2SO_4 at 12°C, for example, the rates are approximately in the sequence:

$$\text{Rate (MnO)} \approx 3.5 \times \text{Rate (Cu}_2\text{O)} \approx 20 \times \text{Rate (CuO)} \approx 2.5 \times 10^6 - 10^8 \\ \times \text{Rate } (\alpha\text{-Fe}_2\text{O}_3)$$

The energies of activation for the leaching of the oxides in H_2SO_4 are respectively, 10.5 kcal/mole for Cu_2O (49), and 21 ± 1 kcal/mole for $\alpha\text{-Fe}_2O_3$ (42).

4.4 The Leaching of Ferric Oxide in Oxalic Acid in the Absence of Added Ferrous Salt in Solution

The rate of leaching of $\alpha\text{-Fe}_2O_3$ (Michigan) was investigated as a function of pH in 0.3M oxalic acid at 85°C (Figure 18). Three distinct

Rate / Rate in 0.9 M H₂SO₄

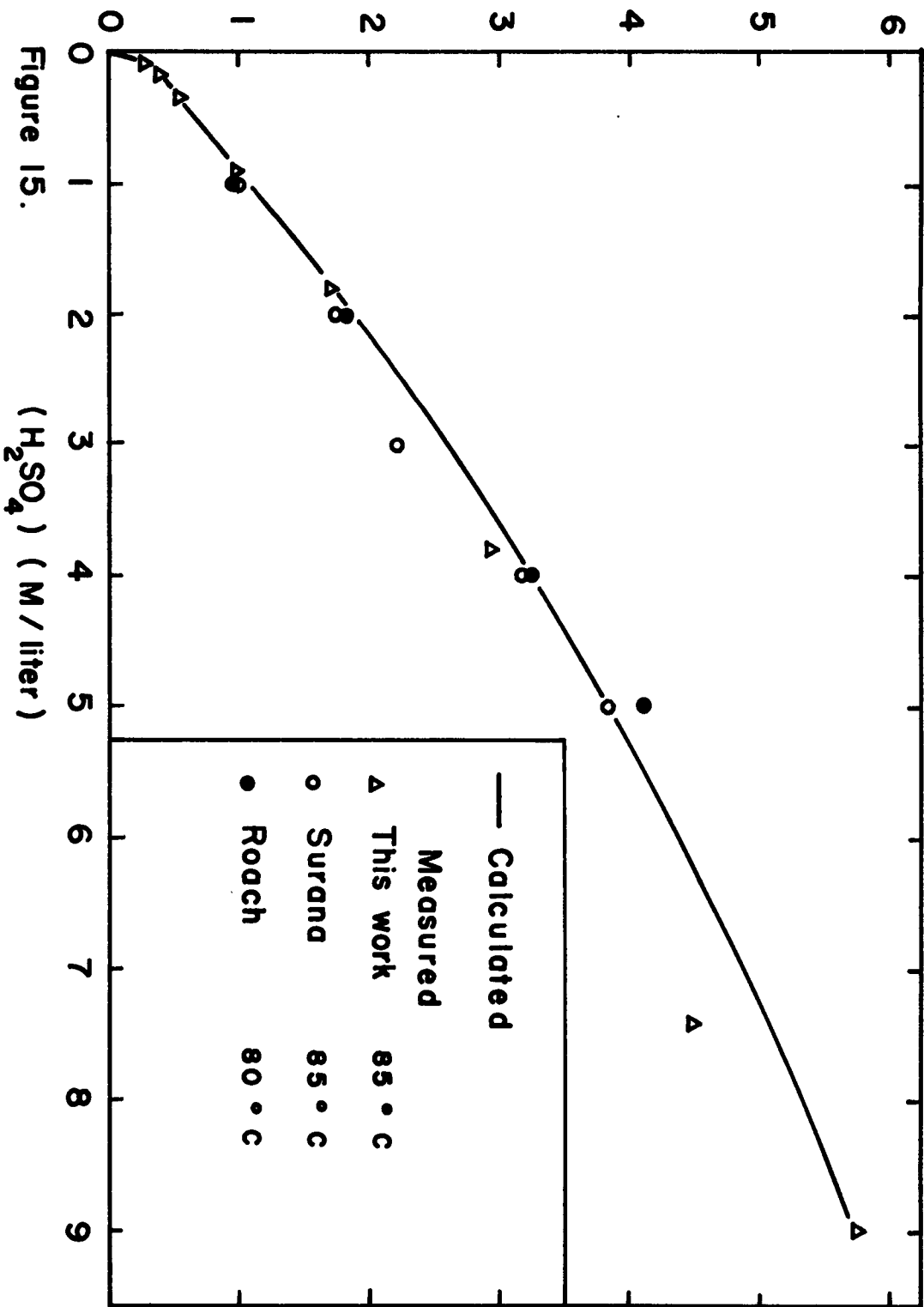


Figure 15. Relative rate of leaching of ferric oxide in H₂SO₄ versus the concentration of H₂SO₄. (Table B.11, Appendix B)

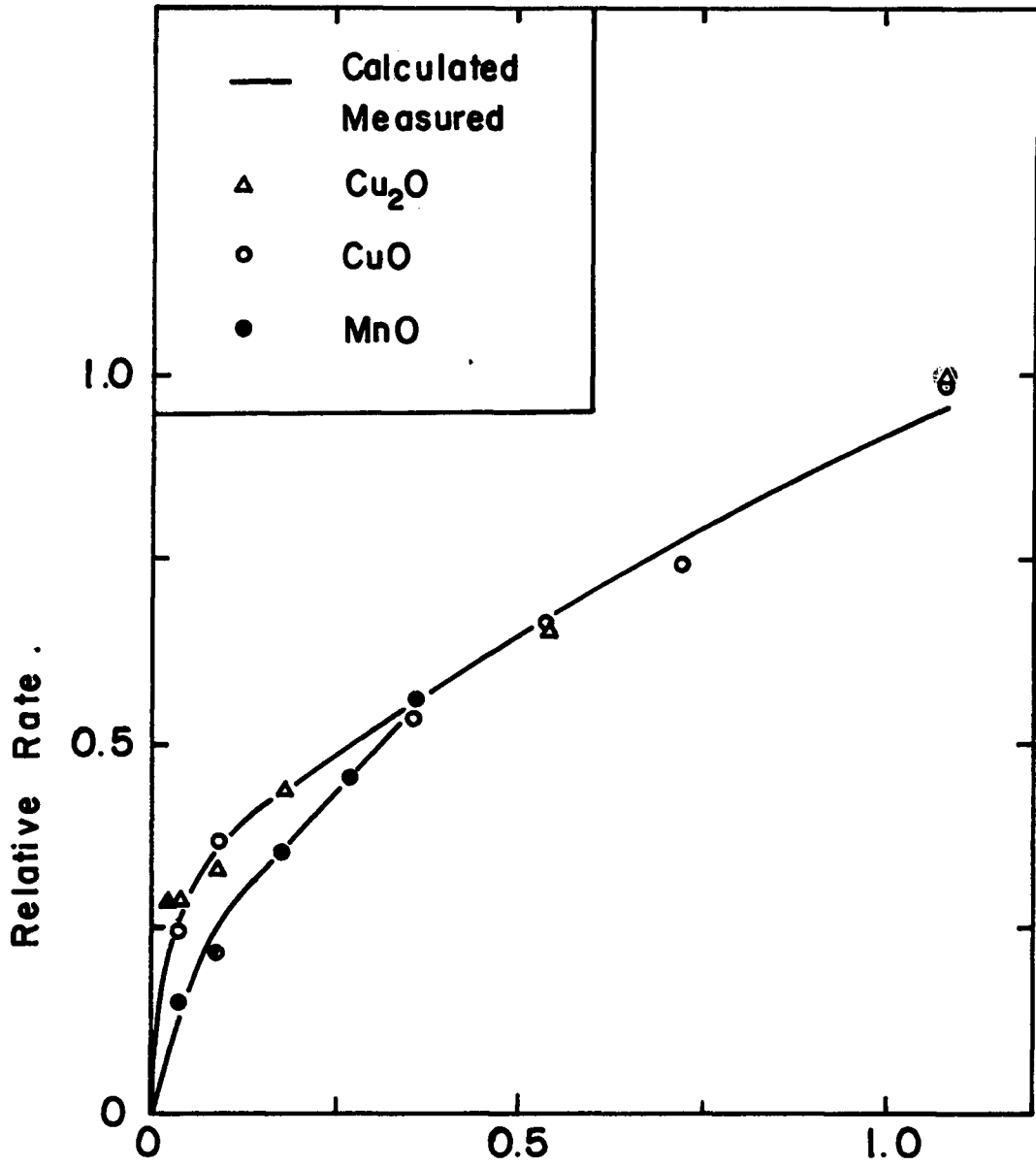
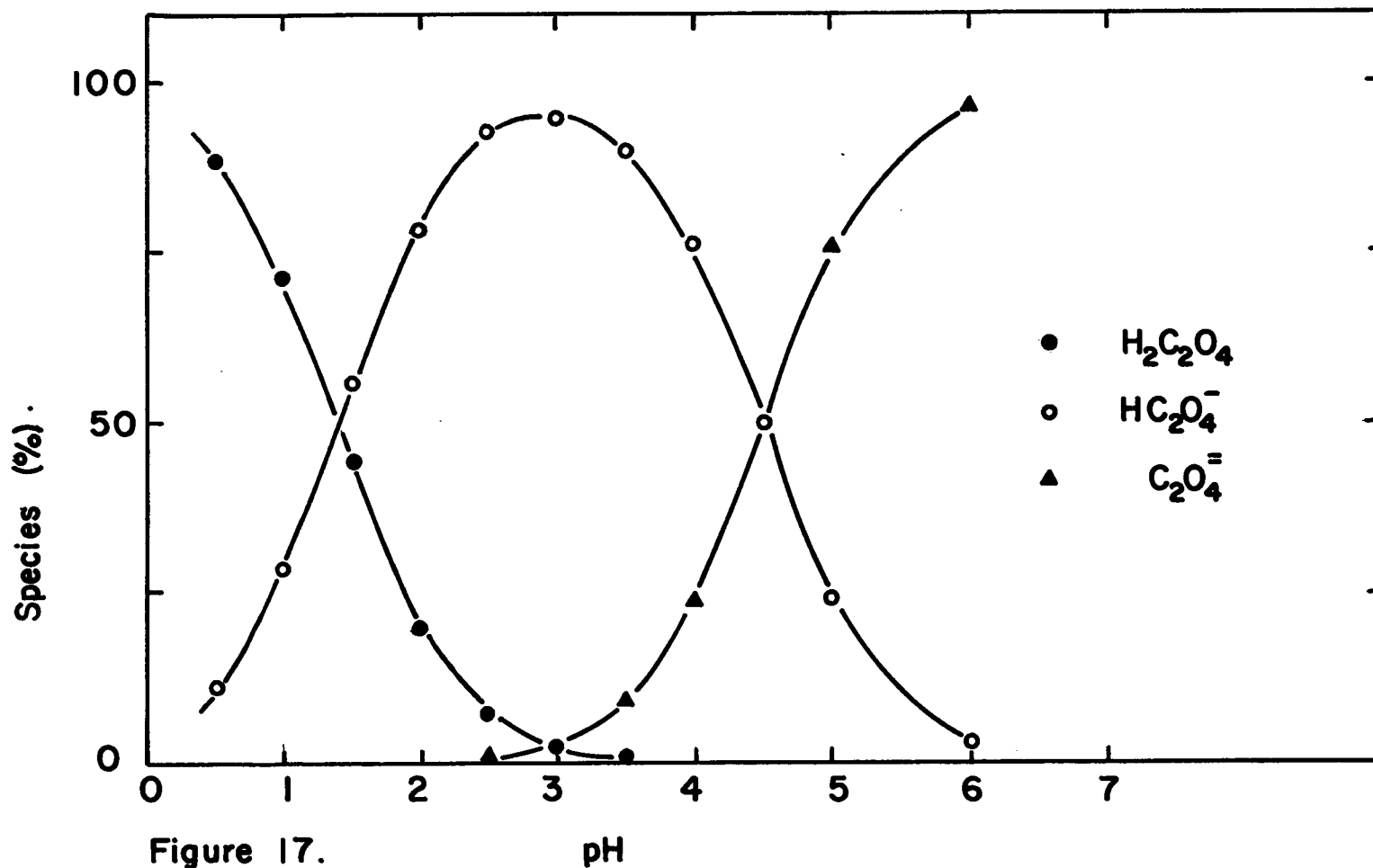
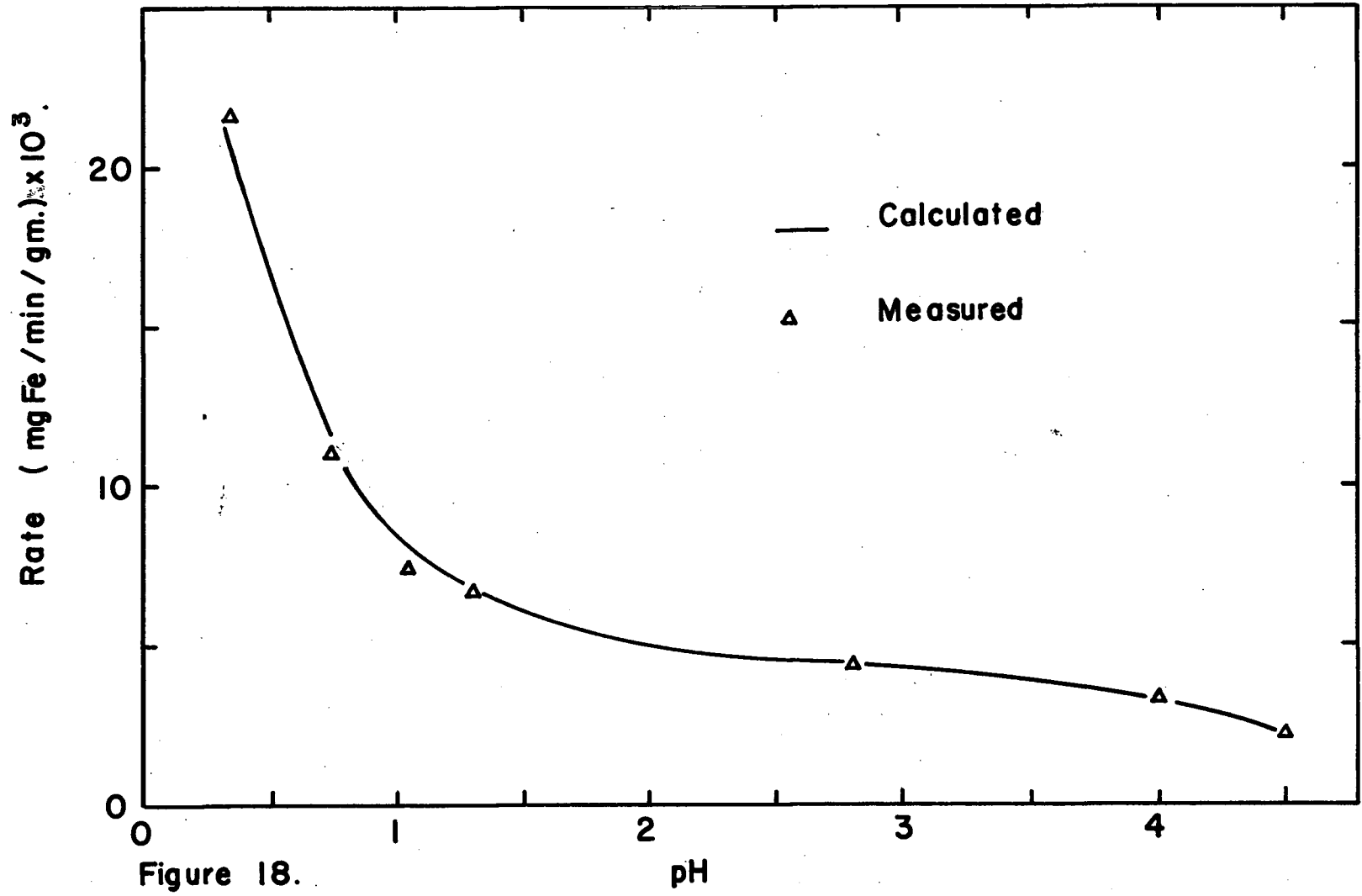


Figure 16. (H₂SO₄) (M / liter)

Relative rate of leaching of Cu₂O, CuO and MnO in H₂SO₄ versus the concentration of H₂SO₄ (T = 12 ° C).
 (Table B.11 , Appendix B)





pH regions can be observed in Figure 18; between pH 0.3 and 1 an exponential decrease in rate of leaching of $\alpha\text{-Fe}_2\text{O}_3$ was observed; from pH 1 to 3.5 a fairly constant rate of dissolution was obtained, and finally above pH 3.5 a steady decrease of the rate towards zero was measured. No ferrous ion was detected in solution during the leaching, which was performed in the absence of light. The distribution of $\text{H}_2\text{C}_2\text{O}_4$, HC_2O_4^- and $\text{C}_2\text{O}_4^{2-}$ present in oxalic acid versus pH at 80°C has been calculated using the dissociation constants of $\text{H}_2\text{C}_2\text{O}_4$ which were extrapolated from the data of Kurz and Farran (102) and Pinching and Bates (103) between 25°C and 55°C and is represented in Figure 17 (Table B.2, Appendix B).

4.5 The Leaching of Ferric Oxide in Oxalic Acid in the Presence of Added Ferrous Oxalate in Solution

4.5.1 Preliminary Experiments

During preliminary experiments on the leaching of various natural hematite and goethite specimens in a 0.2M oxalic acid solution at 80°C , it was observed that the rate of leaching of the oxides was small in the first hour of the run, but then began to increase exponentially with time up to complete dissolution of the contained iron (Figure 19). This leaching behaviour suggested that a time dependent change occurred either at the oxide-electrolyte interface or in the electrolyte. It was further observed that the exponential increase in rate of leaching did not appear when oxygen or air was bubbled through the electrolyte. In contrast, the initial period of slow dissolution disappeared when helium was introduced in solution prior to and during a run (Figure 19).

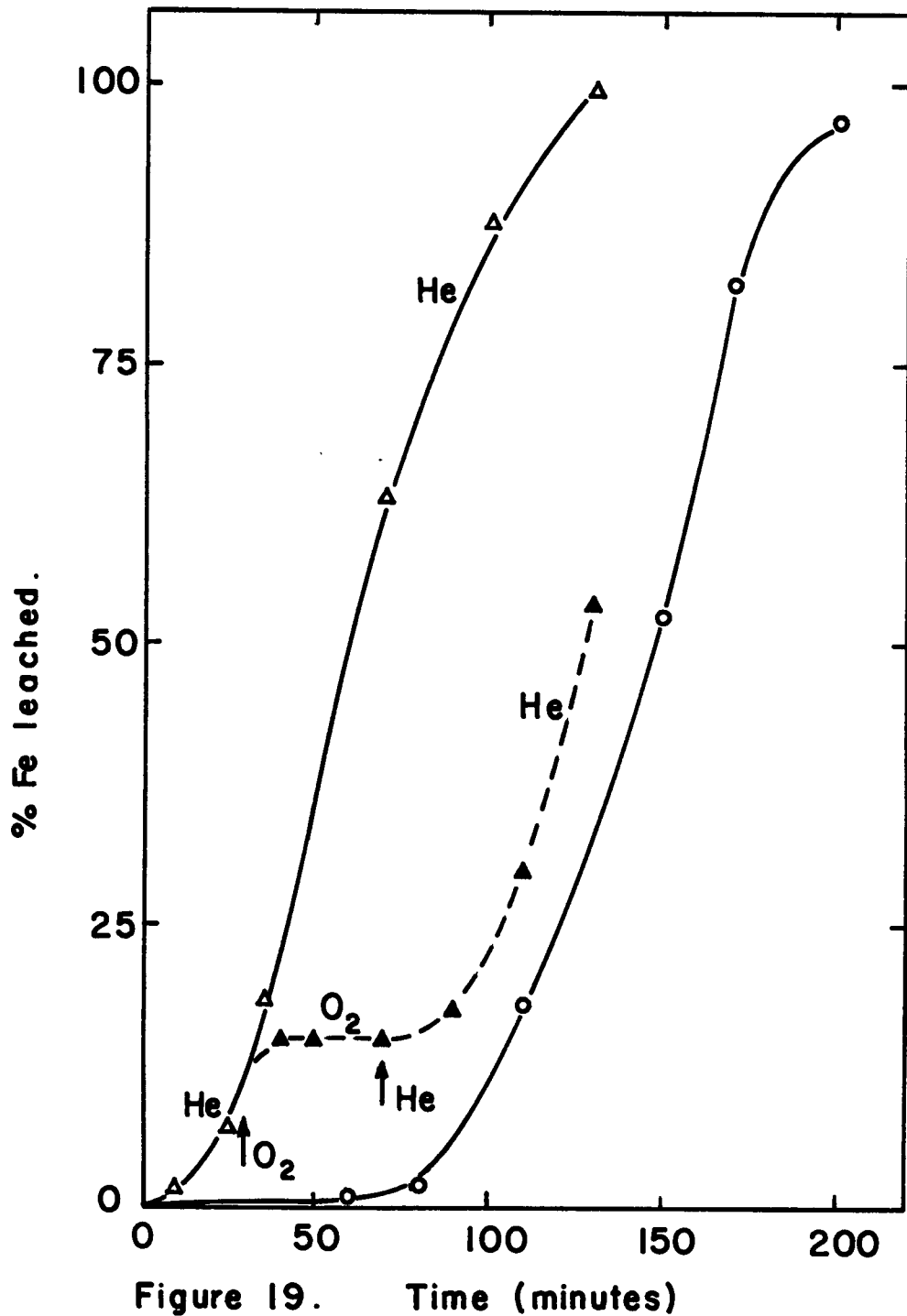


Figure 19. Time (minutes)

Leaching of goethite (Minnesota) in 0.2 M oxalic acid in the presence of air, O₂ and He versus time. (T = 80°C , pH = 2.8).

As any impurity appearing in solution could be responsible for the observed catalytic effect upon the rate of dissolution of the oxides, it was necessary to prepare pure synthetic ferric oxide (Table 5). Indeed, synthetic ferric oxides leached slowly independently of time and of the presence of either O_2 or He in solution. However, upon adding as little as $10^{-4}M$ of ferrous oxalate to the electrolyte, a high but constant rate of leaching of synthetic ferric oxide with time was obtained, provided O_2 was eliminated from the system. It was deduced that in the preliminary experiments on natural impure ferric oxide samples, ferrous species (or possibly other cations) appeared in solution. These were thought to be due to the presence of ferrous in the ores and possibly to the small iron contamination of these samples which were uniquely ground in an iron mortar. At the start of these runs any leached ferrous was probably oxidized to ferric by oxygen present in solution, but since the oxygen was not renewed in solution during the run, some ferrous would finally persist in solution and cause the exponential increase in the rate of leaching with time. This also explains the absence of the region of slow dissolution when O_2 was eliminated by He prior to and during a run (Figure 19), because any ferrous appearing in solution would then remain unoxidized.

4.5.2 The Effect of Sample Weight

The rates of leaching of 1 gm and 2 gm portions of ferric oxide (sample Q, Table 5) in 0.2M oxalic acid at pH 2.80 and at 80°C and in the presence of 6 mg/liter of ferrous species are given in Table B.15, Appendix B. It is observed that approximately twice the amount of iron is leached from the 2 gm ore sample than from the 1 gm sample in a given time, suggesting that the leaching of ferric oxide under these conditions is controlled by a reaction at the oxide-electrolyte interface, i.e. by a heterogeneous reaction.

4.5.3 The Effect of Added Ferrous Oxalate Concentration

The effect of adding ferrous oxalate to a 0.2M oxalic acid solution at pH 2.80 and at 80°C upon the rate of leaching of $\alpha\text{-Fe}_2\text{O}_3$ (sample Q, Table 5) and $\alpha\text{-Fe}_2\text{O}_3$ (sample C, Table 5) is represented in Figure 20. The rates of leaching of both hematites show only an approximately first order dependence on the ferrous species concentration in solution up to the solubility of ferrous oxalate in 0.2M oxalic acid, at which a constant rate of leaching is observed. Plots of log Rate versus $\log[\text{Fe}^{++}]_{\text{Total}}$ given in Figure 21 are straight lines. The slopes of these lines indicate that the rate of leaching of $\alpha\text{-Fe}_2\text{O}_3$ free of Ti varies with the 0.66 power of the ferrous concentration in solution whereas the rate of leaching of $\alpha\text{-Fe}_2\text{O}_3$ containing 1.3% Ti apparently only varies with the 0.60 power of the ferrous concentration.

No change in the concentration of ferrous species in solution was detected during the leach.

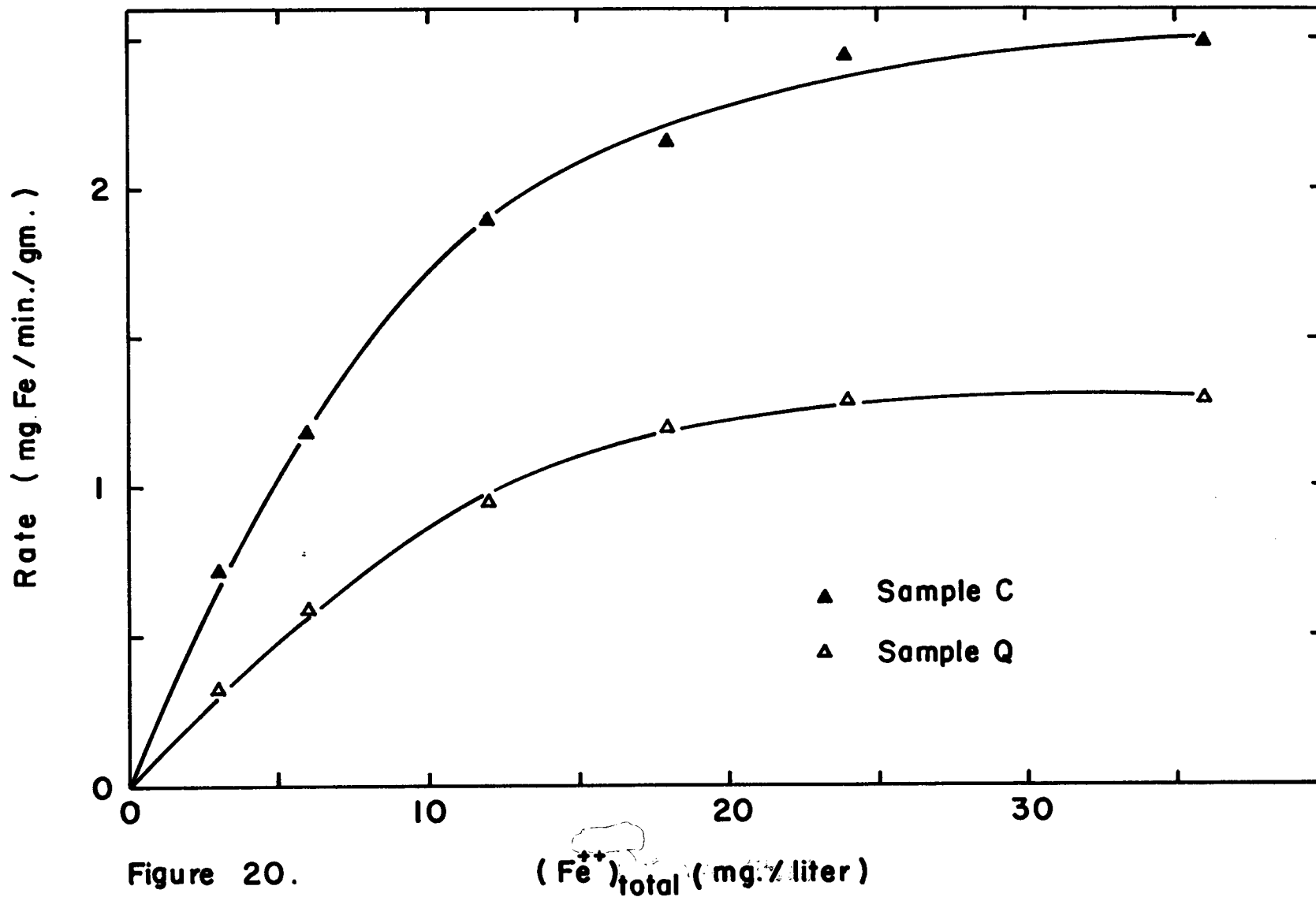


Figure 20.

Rate of leaching of ferric oxide in 0.2 M oxalic acid versus the concentration of added ferrous ion. (T=80°C, pH=2.8) (Table B.14, Appendix B)

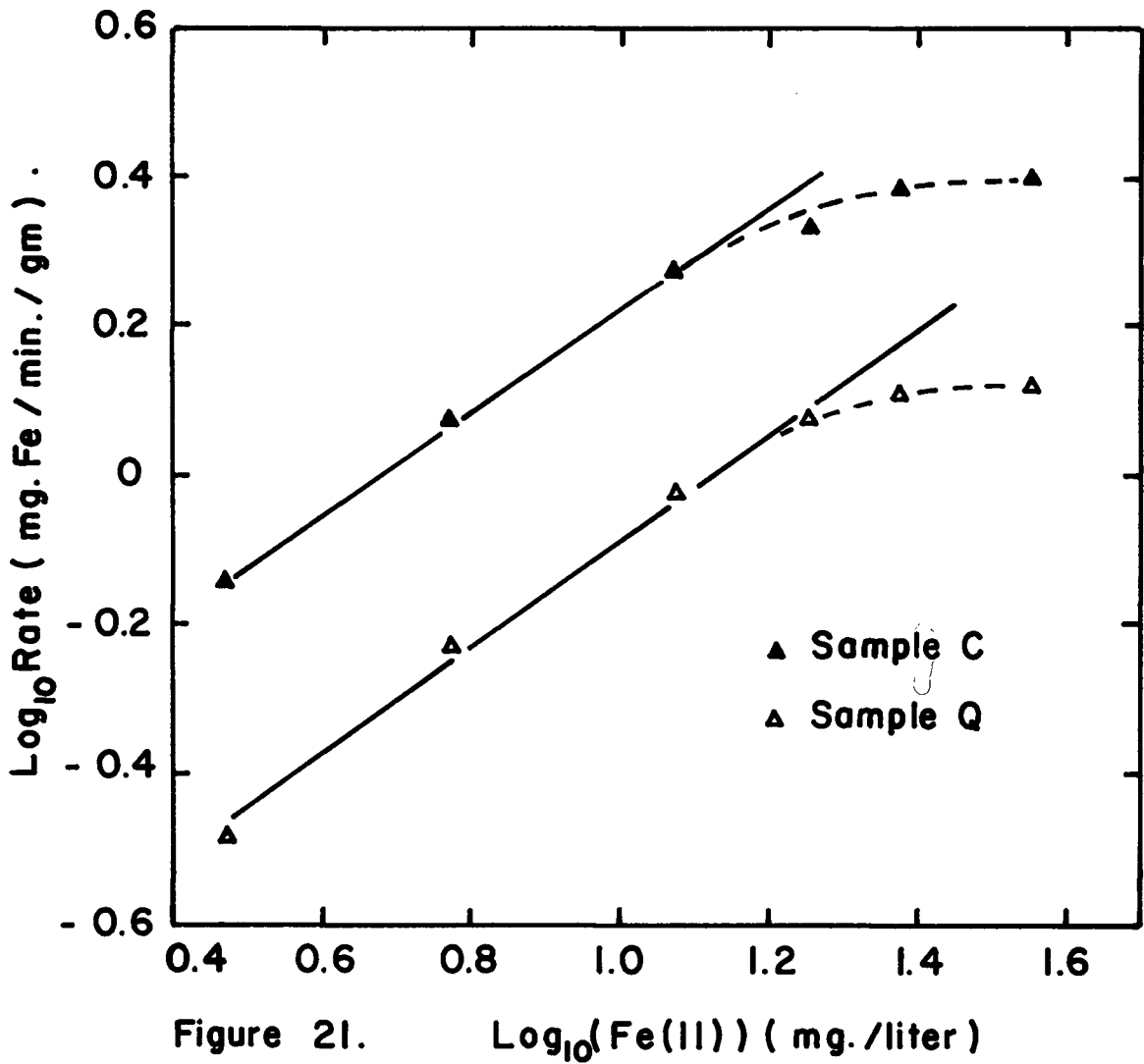


Figure 21. $\text{Log}_{10}(\text{Fe(II)})$ (mg./liter)

Log-log plot of the rate of leaching of ferric oxide in 0.2 M oxalic acid versus the concentration of added ferrous ion. ($T = 80^\circ\text{C}$, $\text{pH} = 2.8$) (Table B.14, Appendix B).

4.5.4 The Effect of Adding Ferrous Ion Complexing Agents to the Oxalate Electrolyte

The addition of an excess of o-phenanthroline or ferrozine, which are known ferrous ion complexing agents, to a 0.2M oxalate solution at pH 2.80 results in the reduction of the rate of leaching of ferric oxide (sample 0, Table 5) to the rate obtained in the absence of added ferrous salts in solution, suggesting that the active ferrous species in solution during the enhanced dissolution of $\alpha\text{-Fe}_2\text{O}_3$ are oxalato-ferrous complexes.

4.5.5 The Effect of Adding Various Cations in Solution

The observed catalyzed rate of dissolution of natural ferric oxides may not be due solely to the appearance of ferrous species in solution but also to such cations as Cr^{2+} , Mn^{2+} , Ni^{2+} , Cu^+ , Cu^{++} , Co^{2+} and Zn^{2+} . Experiments were performed separately in the presence of 10^{-4}M of each of these cations, and no effect on the rate of leaching of $\alpha\text{-Fe}_2\text{O}_3$ at pH 2.80 in 0.2M oxalic acid was detectable, except in the presence of 10^{-4}M of Cu^+ ion. In this case, an exponential increase in the rate of dissolution of synthetic $\alpha\text{-Fe}_2\text{O}_3$ was observed, but indeed the ferrous content in solution was also observed to increase steadily. This is attributed to the possible homogeneous reduction of Fe^{+++} in solution by Cu^+ (99), producing Fe^{++} species which then in the presence of oxalate can catalyze the rate of leaching of $\alpha\text{-Fe}_2\text{O}_3$.

4.5.6 The Effect of the Concentration of Oxalic Acid

The effect of 0.05, 0.10, 0.15, 0.20, 0.30, 0.40 and 0.60 M/liter oxalic acid on the rate of leaching of $\alpha\text{-Fe}_2\text{O}_3$ (sample Q, Table 5) at pH 2.80 and at 80°C, in the presence of 6 mg/liter of added ferrous is represented in Figure 22. The maximum concentration of oxalic acid which could be used was limited to 0.7M/liter by the solubility of the acid at 80°C. The results could suggest a Langmuir type adsorption isotherm dependence of the rate of leaching of $\alpha\text{-Fe}_2\text{O}_3$ on the concentration of oxalic acid.

4.5.7 The Effect of the Ti Content of Synthetic Ferric Oxide

Synthetic $\alpha\text{-Fe}_2\text{O}_3$ samples were prepared under various sintering conditions and with or without additions of Ti (Table 5). Undoped $\alpha\text{-Fe}_2\text{O}_3$ samples usually contained between 0.1 and 0.2 wt % of ferrous ion and additions of Ti to the oxide resulted in an increase of ferrous content of $\alpha\text{-Fe}_2\text{O}_3$ due to the replacement of Fe^{+++} atoms by Ti^{4+} atoms. The effect of sintering conditions and Ti doping upon the absolute rates of leaching of $\alpha\text{-Fe}_2\text{O}_3$ in ferrous species containing oxalic acid solutions can only be estimated if the total surface areas of the samples are known. However, surface area measurements are more convenient when fine powders can be used and such powders are unsuitable for this study because they produce filtering problems and possibly diffusion control of the leaching reactions. Also, surface area measurements do not give information on the number, size and crystallographic orientation of the grains in each particle and these factors

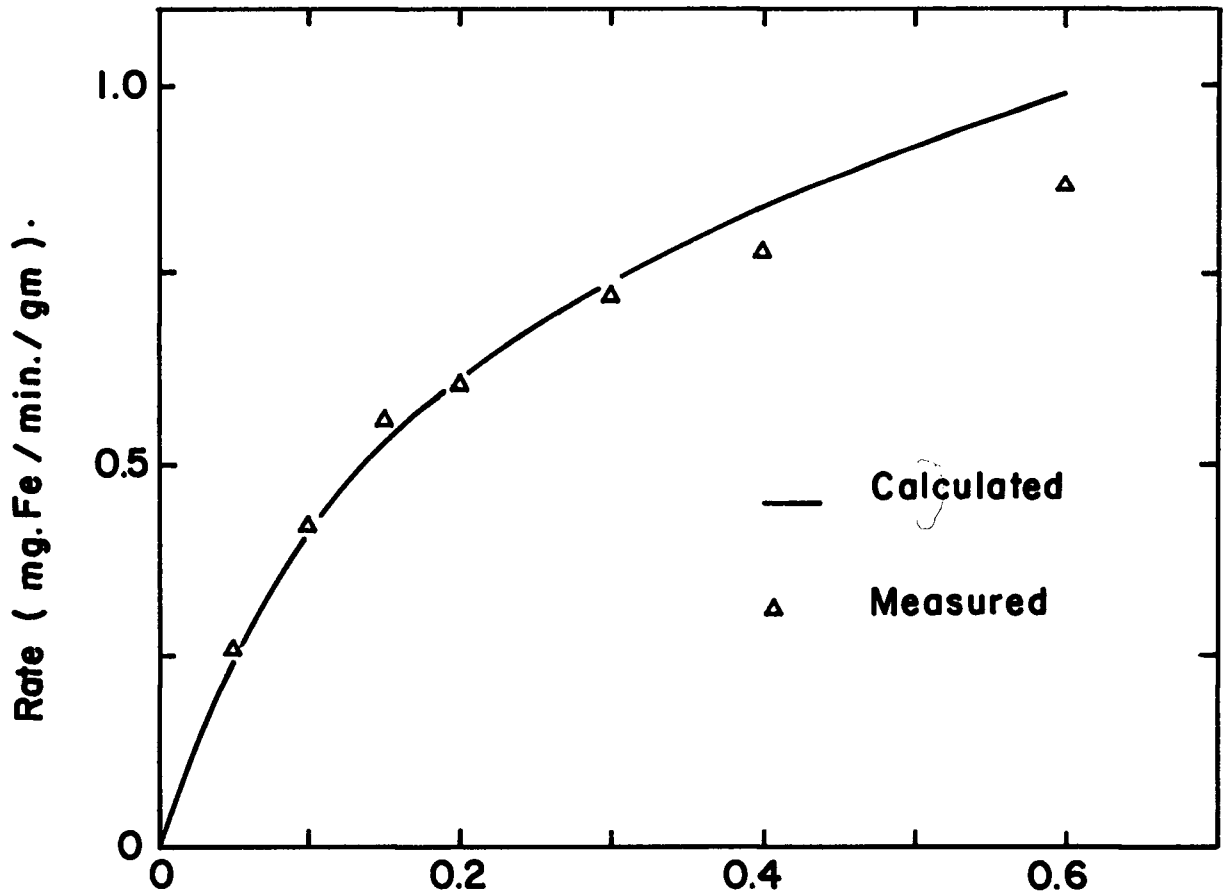


Figure 22. (H₂C₂O₄) (M / liter)

Rate of leaching of ferric oxide in oxalic acid versus the concentration of oxalic acid. (T = 80 ° C , pH = 2.8 , added ferrous = 6 mg / liter) (Table B.19 , Appendix B) .

are known to produce variations in the absolute rates of leaching of the oxide (44, 101). In order to eliminate the effect of unknown total surface area variations between the various Ti doped synthetic $\alpha\text{-Fe}_2\text{O}_3$ samples, relative rates were considered by taking the ratios of the absolute rates of leaching of each oxide in 0.2M oxalic acid at pH 2.80 and the absolute rates of dissolution of the oxides in 2.4M HCl, both at 80°C. These relative rates were indeed found to depend only on the Ti content of $\alpha\text{-Fe}_2\text{O}_3$ (Table B.13, Appendix B).

The relative rates of leaching of Ti doped $\alpha\text{-Fe}_2\text{O}_3$ versus the Ti content of the oxides are plotted in Figure 23. The points corresponding to the dissolution of $\alpha\text{-Fe}_2\text{O}_3$ containing 0.5 wt % Mg, and pure $\alpha\text{-Fe}_2\text{O}_3$ sintered under O_2 at 900°C, are added on this figure. The addition of Ti to $\alpha\text{-Fe}_2\text{O}_3$ can be seen to produce an enhancement of the relative rate of leaching of the oxides up to 0.8 wt % Ti, followed by a slight decrease between 0.8 and 3% Ti. The pure $\alpha\text{-Fe}_2\text{O}_3$ specimen sintered under O_2 exhibits only a slightly lower relative rate than the average relative rate obtained with pure specimens sintered under air, whilst the Mg doped $\alpha\text{-Fe}_2\text{O}_3$ sample shows a more pronounced decrease in relative rate of leaching.

4.5.8 The Effect of Temperature

Arrhenius plots were obtained between 50 and 90°C for two $\alpha\text{-Fe}_2\text{O}_3$ samples (samples D and E, Table 5), in 0.2M oxalic acid at pH 2.8 (Figure 24). The apparent activation energies of leaching of the oxides do not seem to be influenced by the Ti content of the oxides,

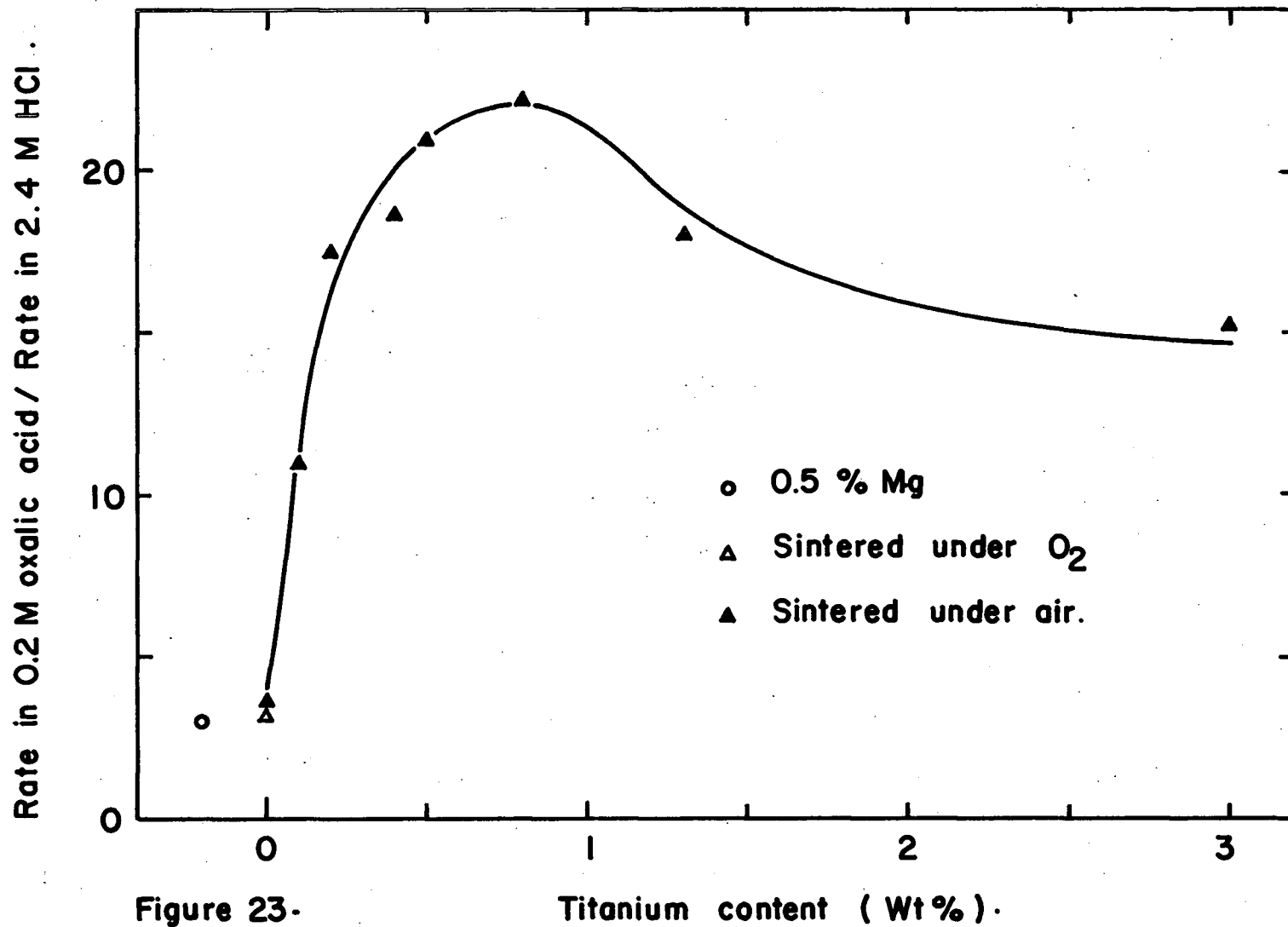


Figure 23-

Titanium content (Wt%).

Relative rate of leaching of ferric oxide in 0.2 M oxalic acid (pH=2.8, added ferrous = 6 mg / liter) and 2.4 M HCl at 80 °C versus the titanium content of the oxide . (Table B.13, Appendix B) .

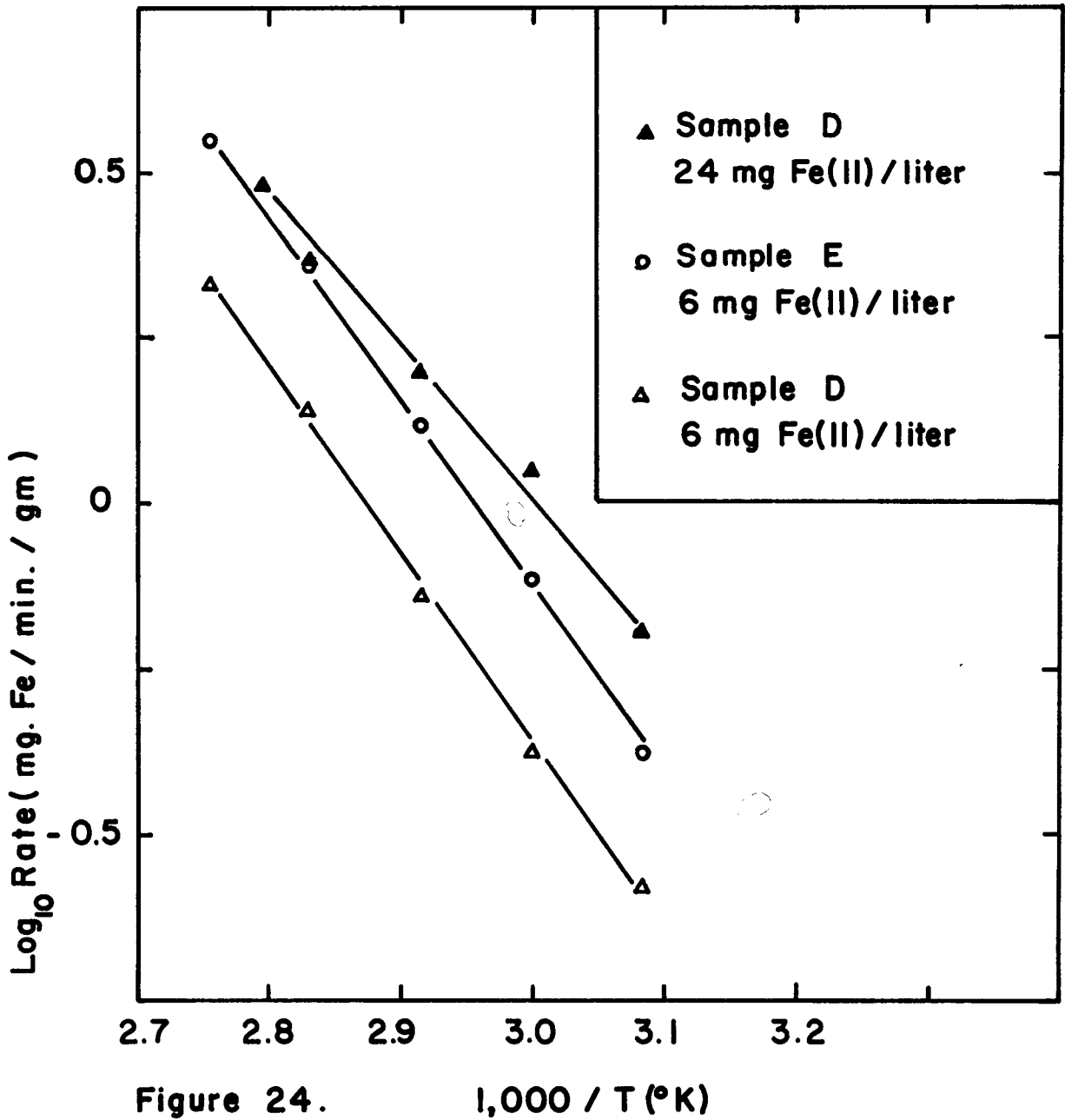


Figure 24. $1,000 / T (^{\circ}K)$

Arrhenius plots for the leaching of ferric oxides in 0.2 M oxalic acid. (pH = 2.8) (Table B.16 , Appendix B) .

but decrease with increasing additions of ferrous oxalate to the electrolyte, i.e. from 12.9 kcal/mole to 10.5 kcal/mole for additions from 20 mg/liter up to the limit of solubility of ferrous oxalate.

4.5.9 The Effect of pH

The rates of leaching of synthetic ferric oxide (sample 0, Table 5) at 80°C in 0.2M oxalic acid containing 6 mg/liter of added Fe^{++} were measured as a function of pH (Figure 25). The absolute rates of leaching of the oxide show a maximum around pH 2.8 and become small below pH 1 and above pH 4.5. The rates of leaching plotted in Figure 25 were normalized to 1 for the maximum rate of leaching. The decrease in rate of dissolution of $\alpha\text{-Fe}_2\text{O}_3$ above pH 2.8 was not due to the decrease in solubility of ferric species in solution, since at pH 4, for example, a constant rate of leaching was obtained up to 20 percent dissolution of $\alpha\text{-Fe}_2\text{O}_3$ and total dissolution of the 1 gm ore was eventually attained.

4.5.10 Distribution of Ferrous Species in 0.2M Oxalic Acid as a Function of pH

The experimental results suggest that there is a definite relation between the observed rates of leaching of ferric oxide and some ferrous species in the electrolyte. Hence, it is of considerable interest to estimate the distribution of ferrous species in 0.2M oxalic acid at 80°C versus the pH of the solution. Unfortunately the stability constants corresponding to the formation of the mono-, di- and tri-oxalato ferrous complexes are only known at 25°C and large

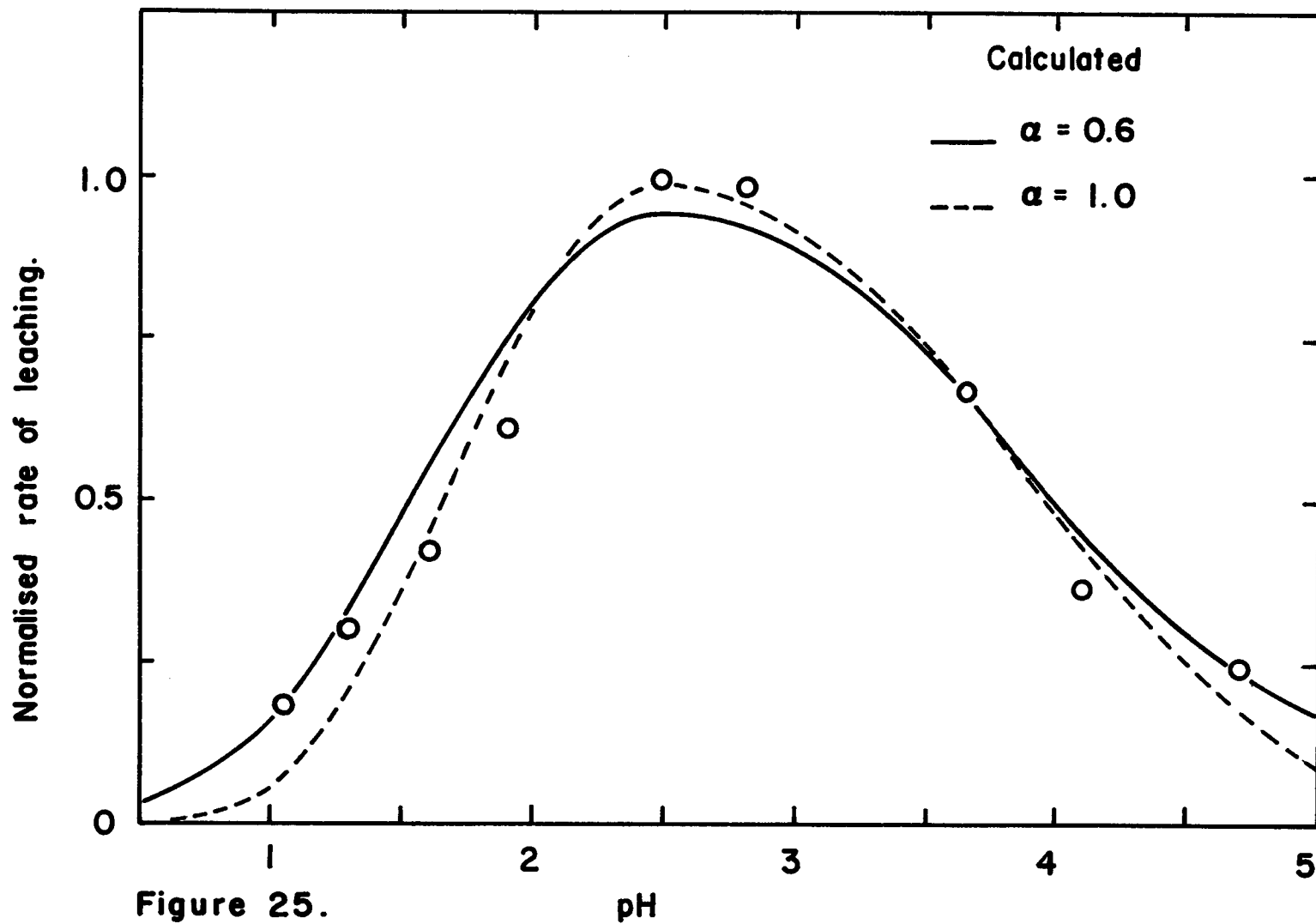
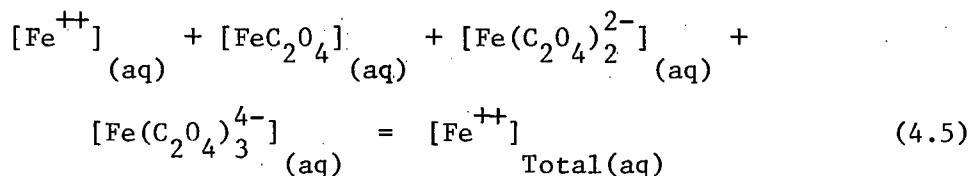
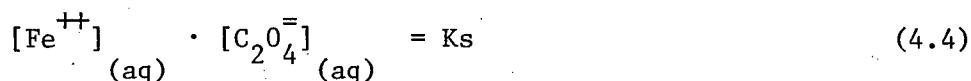
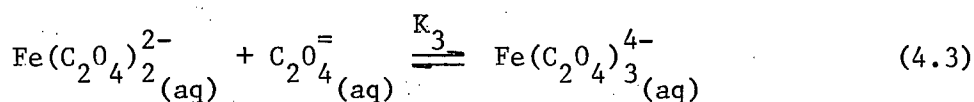
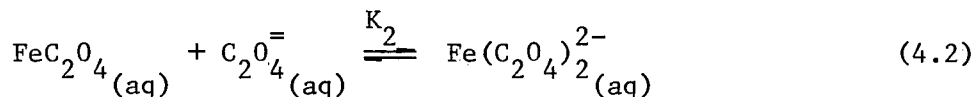
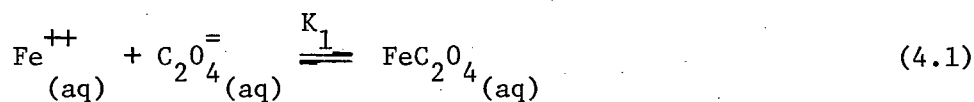


Figure 25. Normalised rate of leaching of ferric oxide in 0.2 M oxalic acid versus pH. (T = 80 ° C , Fe(II) = 6 mg / liter) (Table B.18 , Appendix B) .

differences are found between the pK's reported in the literature (104,105,106). These pK's can easily be estimated experimentally at 80°C by using the following relations:



where (4.1), (4.2), and (4.3) refer to the formation of the successive oxalato-ferrous complexes, K_s is the solubility constant for ferrous oxalate and (4.5) represents the balance of the ferrous content of the solution. From the combination of these five equations the total solubility of ferrous species, $[\text{Fe}^{++}]_{\text{Total}}$, can be calculated as a function of the concentration of $\text{C}_2\text{O}_4^{2-}$ and becomes:

$$[\text{Fe}^{++}]_{\text{Total}} = \frac{K_s}{[\text{C}_2\text{O}_4^{2-}(\text{aq})]} + \frac{K_1 K_s}{[\text{C}_2\text{O}_4^{2-}(\text{aq})]} + \frac{K_1 K_2 K_s}{[\text{C}_2\text{O}_4^{2-}(\text{aq})]^2} + \frac{K_1 K_2 K_3 K_s}{[\text{C}_2\text{O}_4^{2-}(\text{aq})]^3} \quad (4.6)$$

The concentration of $C_2O_4^{2-}$ in 0.2M oxalic acid at 80°C can be calculated as a function of pH (Table B.2, Appendix B) and $[Fe^{++}]_{Total}$ in these solutions can be obtained by adding an excess of ferrous oxalate to the solution at the pH of interest. The experimental curve of $\log[Fe^{++}]_{Total}$ versus $\log[C_2O_4^{2-}]$ in 0.2M oxalic acid is given in Figure 26. The values of K_s , K_1 , K_2 and K_3 can be reasonably well estimated by comparing expression (4.6) to the experimental results (Table B.3, Appendix B). The distribution of the various ferrous species in 0.2M oxalic acid at 80°C versus pH was then calculated by using relations (4.1), (4.2) and (4.3) and is represented in Figure 27 (Table B.17, Appendix B). The maximum concentrations of $FeC_2O_4(aq)$ and $Fe(C_2O_4)_2^{2-}(aq)$ occur at pH 2.1 and 3.8 respectively and $Fe(C_2O_4)_3^{4-}(aq)$ reaches a maximum of 55% above pH 5 as $[C_2O_4^{2-}]$ is limited to 0.2M/liter; the 45% remainder is then $Fe(C_2O_4)_2^{2-}(aq)$.

4.6 The Leaching of Ferric Oxide in Malonic Acid in the Presence of Added Ferrous Ion.

The rates of leaching of ferric oxide (Michigan) were investigated in 0.5M malonic acid at 80°C in the presence of 9 mg/liter of added ferrous ion versus the pH of the solution (Figure 28). The rate of leaching shows a maximum around pH 5.0 and becomes small below pH 2.7 and above pH 6.4. Unfortunately too little data are available to enable the concentration of malonato-ferrous complexes to be calculated as a function of pH.

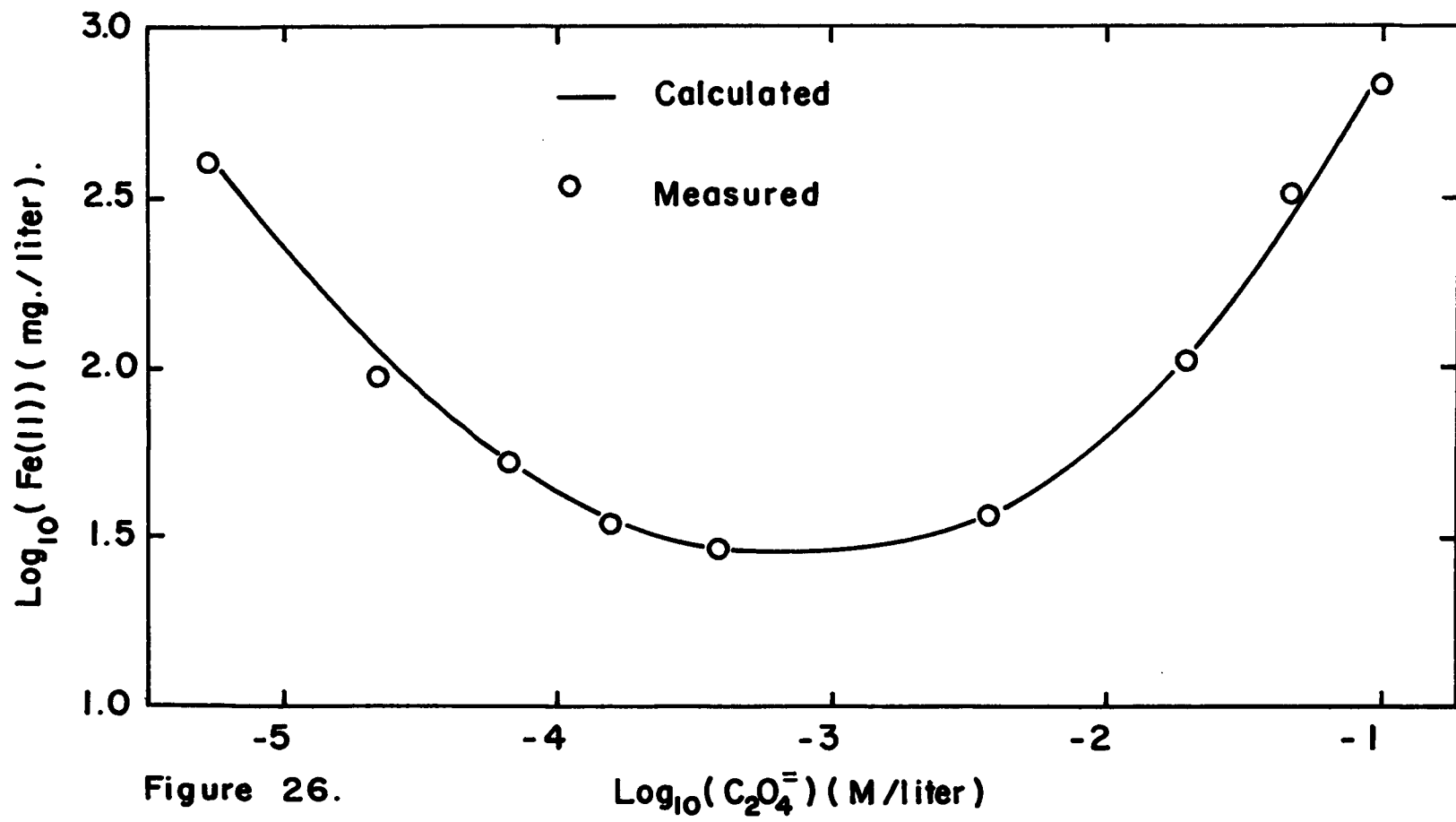
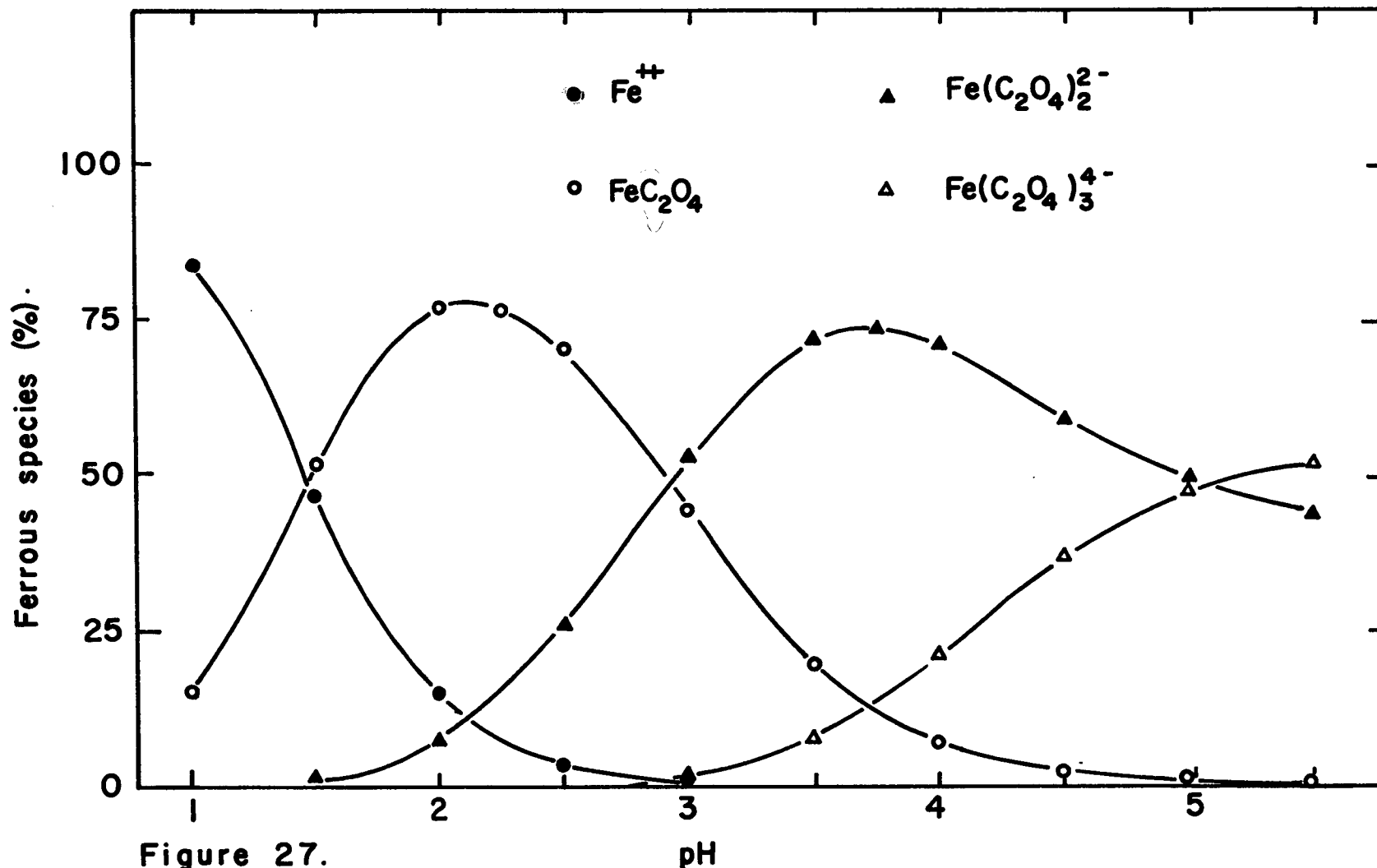


Figure 26.

Log-log plot of the total solubility of ferrous species in 0.2 M oxalic acid versus the concentration of oxalate ion at 80°C. (Table B.3, Appendix B).



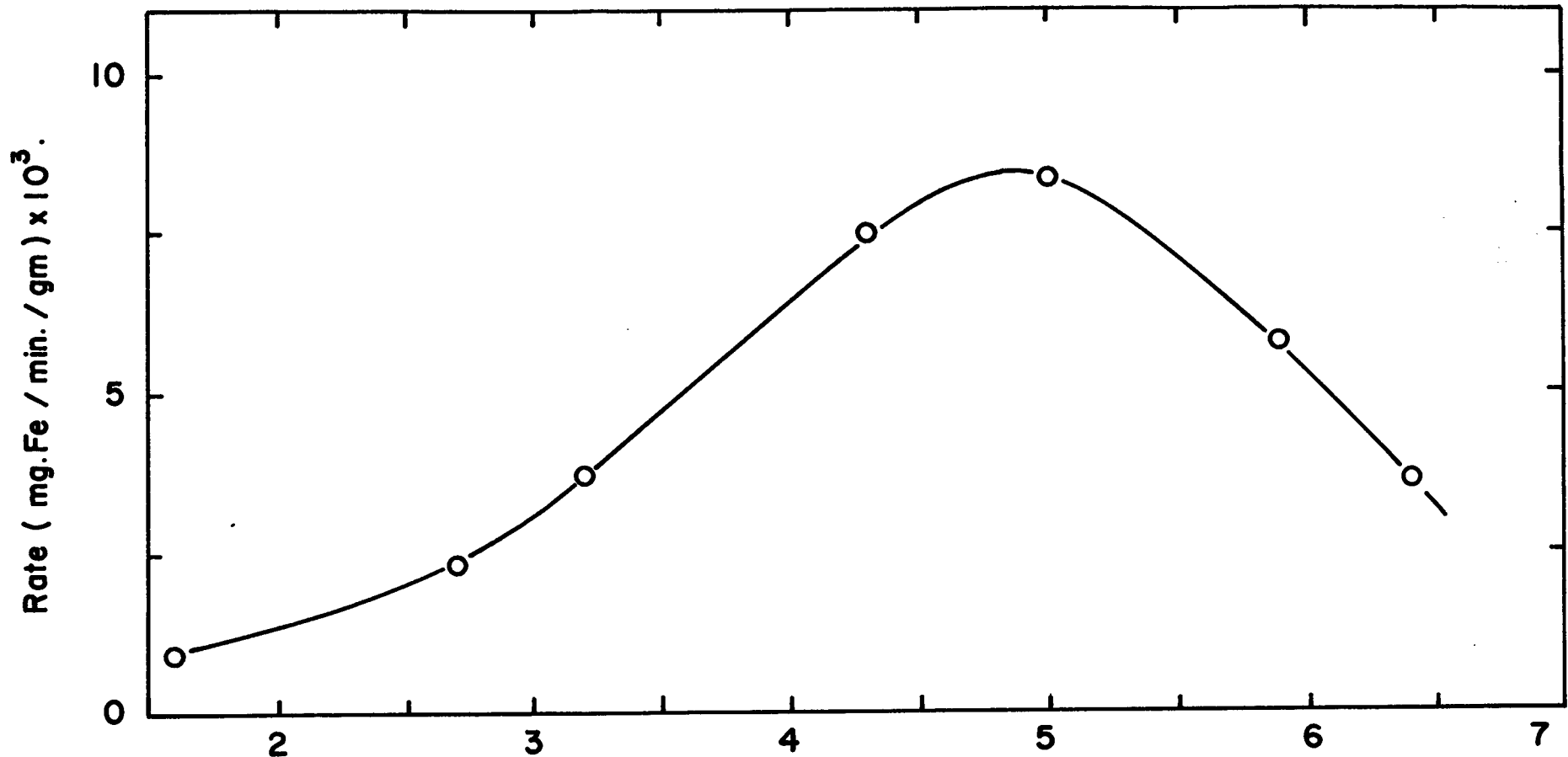


Figure 28.

pH

Rate of leaching of ferric oxide (Michigan) in 0.3 M malonic acid versus pH .
(T = 80 °C , Fe(II) = 9 mg / liter) (Table B. 20 , Appendix B) .

4.7 The Leaching of Ferric Oxide in Various Other Acids

4.7.1 In the Absence of Added Ferrous Salts in Solution

Leaching experiments with $\alpha\text{-Fe}_2\text{O}_3$ (Michigan) were carried out at 80°C in 0.2M solutions of maleic, tartaric, citric and sulphamic acids and with 4 gm/liter of ethylene-diamine tetraacetic acid (E.D.T.A.). None of these acids was found to provide high enough rates of leaching of $\alpha\text{-Fe}_2\text{O}_3$ to be of interest for detailed studies in relation to the present work.

4.7.2 In the Presence of Added Ferrous Salts in Solution

No effect of adding 10^{-4} M/liter of ferrous salts was observed on the rates of leaching of $\alpha\text{-Fe}_2\text{O}_3$ (Michigan) under the conditions of leaching mentioned above in 4.7.1.

Additional experiments were carried out on the leaching of $\alpha\text{-Fe}_2\text{O}_3$ in HCl solutions at 80°C in the presence of Fe(II) added as FeCl_2 (Figure 29). The addition of 12, 24 and 50 mg/liter of ferrous did not influence the rate of leaching of $\alpha\text{-Fe}_2\text{O}_3$ in 2.4N HCl solutions, but a pronounced increase in the rate in 6N HCl was observed. This increase in rate does not appear to show a first order dependence on the added ferrous concentration in solution.

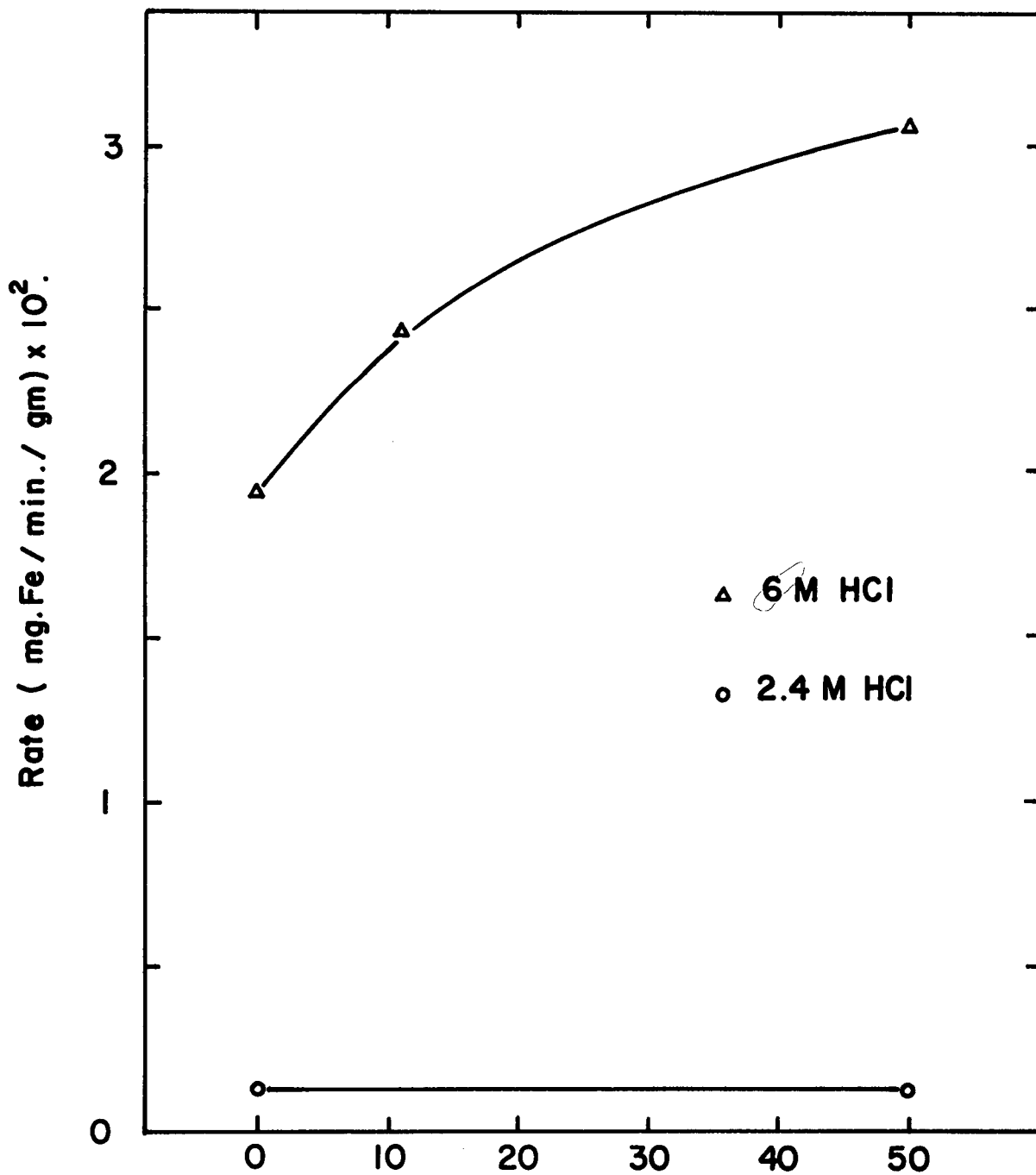


Figure 29- Fe(II) (mg./liter) .

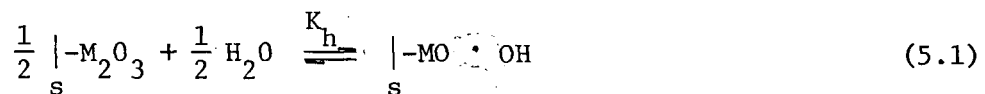
Rate of leaching of ferric oxide (Michigan) in HCl
versus the concentration of added ferrous ion. (T = 80 ° C)
(Table B.21 , Appendix B) .

5. DISCUSSION

5.1 The Direct Leaching of Metal Oxides in Acids5.1.1 Model for the Mechanism of Leaching

The results obtained on the leaching of aluminum oxides in hydrochloric acid solutions indicate that the absolute rates of leaching of $\gamma\text{-Al}_2\text{O}_3$ remain close to those of $\alpha\text{-Al(OH)}_3$ up to 1.2N HCl (Figure 12), but then rapidly diverge from the latter towards a constant rate of leaching at higher HCl concentrations. This may suggest that the rate of hydroxylation of $\gamma\text{-Al}_2\text{O}_3$ eventually becomes slower than that of the dissolution of the hydroxylated surface, causing the overall rate of leaching of the oxide to reach a constant value as the activity of water in the electrolytes is approximately constant. If, as it appears, the rate of hydroxylation of aluminum oxides decreases for oxides which have been heated to increasingly higher temperatures (16), this may explain the immeasurably low rates of leaching obtained with $\alpha\text{-Al}_2\text{O}_3$ calcined at 1200°C.

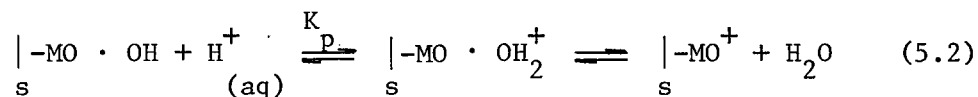
In general, however, it appears that the hydroxylation of oxide surfaces is rapid and the first step of the leaching of oxides can be represented in the case of a M_2O_3 oxide, for example, by the following equilibrium equation:



The oxide surface species which are formed upon hydroxylation are

not known, but infrared studies on oxide surfaces (11) suggest that at least one hydroxyl group per surface oxide cation is present. This is also supported by Onoda and De Bruyn (107) who, in studies on the hydroxylation of the hematite ($\alpha\text{-Fe}_2\text{O}_3$) surface identified the presence of a hydrated surface layer approximating the goethite ($\alpha\text{-FeO}\cdot\text{OH}$) composition.

The species present in an aqueous solution of an acid, HX, are in general H^+ and X^- ions, and to a lesser extent OH^- and HX. As discussed before, H^+ is at the origin of the positive charge which develops at oxide surfaces in acids of pH below the pH of Z.P.C. of the oxide. This can be represented either by the adsorption of H^+ ions or the dissociation of chemisorbed water at the surface of the oxide. If it may be assumed that charging of the oxide surface is a rapid reaction, the following equilibrium equation can be written:



where K_p is the protonation equilibrium constant for the adsorption of hydrogen ions at the oxide surface. As proposed in earlier work by Warren and coworkers (8,9), a mechanism of the leaching of ferric oxides in perchloric acid, involving the adsorption of H^+ ions followed by the rate controlling desorption in solution of the resulting surface species, was in good agreement with the observed first order kinetics of the leaching of these oxides in dilute solutions of the acid.

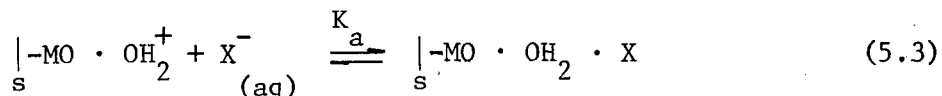
Whether undissociated acid will adsorb at the uncharged oxide

surfaces, as postulated by Wadsworth and Wadia (49) for the leaching of Cu_2O in H_2SO_4 solutions is considered to be doubtful for the following reasons:

- (a) The concentration of undissociated acid in solution is often very low compared to the concentration of ionized species (i.e. $\text{H}_2\text{SO}_4, \text{HCl}, \text{HClO}_4$).
- (b) If it is assumed that the leaching of ferric oxides in perchloric acid involves in a first step the adsorption of the undissociated acid, the overall rate of dissolution of these oxides would be expected to be at least proportional to the activity of undissociated HClO_4 . This in turn is proportional to the product of the activities of the species into which the acid dissociates, namely $a_{\text{H}^+} \cdot a_{\text{ClO}_4^-}$. This product, with the assumption that $a_{\text{H}^+} \cdot a_{\text{ClO}_4^-}$ is also proportional to $a_{\text{H}^+}^2$ or, in dilute solutions of the acid, to the square of the total concentration of perchloric acid. These findings do not correlate with the experimental results (Figure 6).
- (c) The adsorption of undissociated acid, HX , at the oxide surface cannot be distinguished in a rate expression from the adsorption of X^- ions at sites already protonated by H^+ ions as proposed in equation (5.2), simply because $a_{\text{HX}} = K_d \cdot a_{\text{H}^+} \cdot a_{\text{X}^-}$ where K_d is the dissociation constant for HX in water.

The three factors mentioned in (a), (b) and (c) above make it reasonable to assume that undissociated acid does not participate in the leaching of oxides.

Anions other than OH^- , i.e. X^- , may, under favorable conditions, adsorb at positively charged oxide surface sites produced in equilibrium reaction (5.2). If this adsorption process is a fast reaction, it can be conveniently written under the form of the following equilibrium equation:

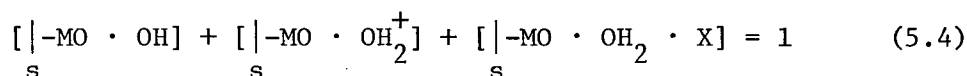


where K_a is the equilibrium constant for the adsorption of X^- at protonated oxide sites. An equilibrium of the form of equation (5.3) can be written for every anion present in solution, and thus also for multi-charged species which are obtained for example in the case of polyacids. The adsorption of OH^- ions does not need to be considered, as this reaction is already taken care of by the surface hydroxylation step (5.1).

A model for the leaching of metal oxides involving the steps (5.1), (5.2) and (5.3) proposed above is no different to the one proposed by Warren and coworkers (8,9) for the leaching of ferric oxides in dilute hydrochloric acid solutions (<2N HCl), and it is recalled that this model does not appear to provide an explanation for the leaching of ferric oxides in sulphuric acid and in concentrated perchloric and hydrochloric acids (Figure 8, curve A). However, examination of the present results on the direct leaching of metal oxides suggests that all oxides studied show a dependence of their rates of leaching on the concentration of the acids which decreases up to a maximum of one order with increasing acidity. This observation is thought to correspond to the progressive saturation of the oxide surfaces by a species whose concentration in solution is proportional to the concentration of the acid, i.e. H^+ or X^- . Since it was suggested that X^- species adsorb preferentially at sites protonated by H^+ ions, it is proposed that the oxides surfaces may become saturated by H^+ ions first, followed eventually by saturation by X^- ions (109).

Saturation of the oxides surfaces by H^+ and X^- ions can be

accounted for by writing a mass balance equation stating that the total surface area of the oxide, i.e. unity, is equal to the sum of the surface portions created in pre-equilibria equations (5.1, (5.2) and (5.3), namely:



Taking into account this surface balance restriction, the proposed model was tentatively compared with the results on the leaching of ferric oxides in HCl solutions (Figure 8, curve B). It was concluded that although this model could account for the rates of leaching up to somewhat higher acid concentrations, an increasingly poorer correlation with the results at high acidities was still obtained. It may thus be suggested that at least one more step is involved in the leaching of metal oxides in acids and that the contribution of this step to the overall rate of leaching becomes more apparent at high acidities. Hence, the further reaction of sites created at the oxide surface in preceding reactions, i.e. protonated and anion covered sites, is suggested to occur. The possible steps are:

(a) The adsorption of H^+ ions at positively protonated sites, i.e. $\left[\underset{s}{|-MO \cdot OH_2^+} \right]$.

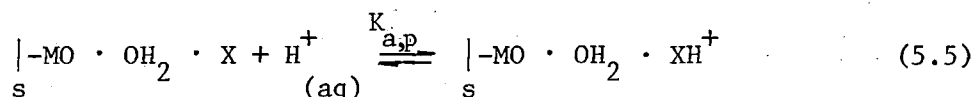
(b) The adsorption of X^- ions at anion containing sites, i.e. $\left[\underset{s}{|-MO \cdot OH_2 \cdot X} \right]$.

(c) The adsorption of H^+ ions at anion containing sites.

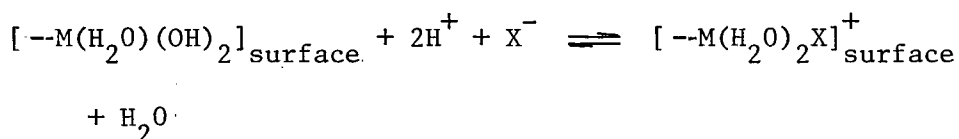
Steps (a) and (b) can probably be neglected as the former involves the interaction of two positively charged species and the latter

suggests that the oxide surface may become negatively charged.

If step (c), the adsorption of H^+ ions at anion containing sites, is assumed to be a quick reaction, the following equilibrium equation can be proposed:



where $K_{a,p}$ is the equilibrium constant for the protonation of anion covered oxide surface sites. The formation of positively charged anion containing sites has been proposed by other workers. Ahmed(58) suggested that an equilibrium of the form



is at the origin of the excess positive charge observed at oxide surfaces in the presence of anions which are known to adsorb at these surfaces. It can easily be seen that this equilibrium equation is the combination of equilibrium equations (5.1), (5.2), (5.3) and (5.5) proposed in the present model. Wadsworth and Wadia (49) postulated in their model for the leaching of Cu_2O in H_2SO_4 that one of the dissolution steps is the reaction of H^+ ions with the oxide surface portion which is covered with undissociated acid. This step is also consistent with equation (5.5) if the latter is written under the form of a rate equation, because, although the steps leading to the formation of $\left| \underset{s}{-MO \cdot OH_2} \cdot X \right.$ species are assumed to be different in the present

model, the same surface species are also produced by the adsorption of undissociated acid, HX, at the hydroxylated oxide surface.

With a few exceptions, which will be discussed later on, the model may now account for all the results on the direct leaching of metal oxides which were investigated in the present work, if it is assumed that the rate determining steps for the leaching of these oxides are the desorptions into solution of the metal surface species produced in pre-equilibria (5.2), (5.3) and (5.5). The basis for this assumption is that in order to correlate the proposed model to the experimental results, it was necessary to consider together the contribution of all three adsorption steps: (5.2), (5.3) and (5.5). However, it is clear from the discussion that these steps are successive and inter-related. As a result it is not possible to consider the case in which these steps are simultaneously rate controlling, since if it is assumed that one of the adsorption reactions is rate controlling it is automatically implied that the preceding steps are rapidly achieved equilibria and the succeeding steps are quick reactions. This is not the case for the desorption steps since these reactions are independent. The possibility remains that the formation of activated complexes at the oxide surfaces, which indeed also are independent reactions, are rate determining, but if this was the case it was expected that the energies of activation for the dissolution of oxides would depend on the nature of the acid and, as was discussed in the review of literature (Table 3), the energies of activation show little dependence on the type of acid used.

A general form of the rate expression for the direct leaching of metal oxides in acids can be derived using the pre-equilibria equations (5.1), (5.2), (5.3) and (5.5) and the surface balance equation (5.4) which has the form:

$$\text{Rate} = \frac{k_1 \cdot K_p \cdot a_{H^+} + k_2 \cdot K_p \cdot K_a \cdot a_{H^+} \cdot a_{X^-} + k_3 \cdot K_p \cdot K_a \cdot K_{a,p} \cdot a_{H^+}^2 \cdot a_{X^-}}{1 + K_p \cdot a_{H^+} + K_p \cdot K_a \cdot a_{H^+} \cdot a_{X^-}} \quad (5.6)$$

in which K_p , K_a and $K_{a,p}$ are the equilibrium constants defined above, and k_1 , k_2 and k_3 are rate constants respectively corresponding to the desorption reactions from protonated, anion containing, and protonated anion containing oxide surface sites. In rate expression (5.6) it was also assumed that the concentration of unhydroxylated oxide surface sites is zero, i.e. K_h is large, and that the concentration of protonated anion containing sites, i.e. $[|-MO \cdot OH_2XH^+|_s]$, is sufficiently small to be neglected in the surface balance equation (5.4).

In the following sections of the discussion an attempt is made to correlate the estimated values of the constants in rate expression (5.6) for each of the systems studied to thermodynamic equilibrium properties exhibited by the oxide-electrolyte interface and species in solution.

5.1.2 Leaching of Metal Oxides in HClO₄ Solutions

The results on the kinetics of leaching of ferric oxides, cuprous and cupric oxides (Figures 5 and 6) were compared with the proposed general rate expression (5.6) with $X^- \equiv ClO_4^-$. The conversion from concentrations

to the corresponding activities of H^+ and ClO_4^- in solution was made by using literature values of the mean activity coefficients of the acid at 25°C (108) and with the assumption that $a_{\pm} = a_{H^+} = a_{ClO_4^-}$, where a_{\pm} is the mean activity of perchloric acid (Table B.4, Appendix B). The calculated values of the constants in rate expression (5.6) obtained from the best fit with the experimental results for each oxide are given in Table 6, and the corresponding rate curves are plotted together with the results in Figures 5 and 6 (Table B.5, Appendix B). Rate expression (5.6) in the case of $HClO_4$ can be simplified and becomes:

$$\text{Rate} = \left[\frac{K_p \cdot a_{H^+}}{1 + K_p \cdot a_{H^+}} \right] \cdot (k_1 + k_2 \cdot K_a \cdot a_{ClO_4^-}) \quad (5.7)$$

with $a_{H^+} = a_{ClO_4^-} = a_{\pm}$

Although the calculated rates appear lie within 5% of the measured rates, the constants in Table 6 may only be considered as approximate because the activities a_{H^+} and $a_{ClO_4^-}$ were estimated for 25°C, whereas the experiments were sometimes conducted at quite different temperatures. The K_p values in Table 6 are the largest for the oxides exhibiting the higher pH's of Z.P.C. This observation agrees well with the expected behavior of oxide surfaces, because oxide surfaces showing a basic character are anticipated to become more completely protonated by hydrogen ions with increasing acidity of the leach solution than those of oxides exhibiting an acid character. In other words, it is calculated from rate equation (5.7) that 90% of the active

TABLE 6

Leaching of Metal Oxides in HClO_4
Calculated Constants in Rate Expression (5.6)

OXIDE	Z.P.C.	T° of leach	k_1	k_2	k_3	K_p	K_a	$K_{a,p}$	$k_2 \cdot K_a$	E Activation energy (Table 3) (kcal/mole)
	≤(pH)	(°C)	$\left(\frac{\text{mg Metal}}{\text{min} \cdot \text{gm}}\right)$	←	←	(molal ⁻¹)	←	←	$\left(\frac{\text{mgmgMetal}}{\text{min} \cdot \text{gm} \cdot \text{molal}}\right)$	
Cu_2O	>11.5	12	30.0	>200	N	19.0	$\leq 10^{-1}$	N	19.4	-
CuO	9.5	12	5.3	>10	N	5.0	$< 10^{-1}$	N	1.64	≈18.0
$\alpha\text{-FeO} \cdot \text{OH}^*$	8.5	110	5.97×10^{-2}	N	N	1.25	$< 10^{-3}$	N	$< 10^{-5}$	17.8-22.5
$\alpha\text{-Fe}_2\text{O}_3$	8.5	90	2.00×10^{-3}	N	N	1.25	$< 10^{-3}$	N	$< 10^{-6}$	19.2-22.9

* Hay (99)

N ≡ negligible

oxide surface portion becomes covered by hydrogen ions at an activity of H^+ of 0.5 in the case of cuprous oxide and of 8 in the case of ferric oxides. Equation (5.7) shows that whilst the value of the product $k_2 \cdot K_a$ can be calculated, the individual values of the constants k_2 and K_a cannot be obtained. However, limiting values of these constants can be estimated by modifying rate equation (5.7) by the following relation:

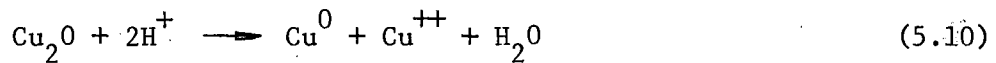
$$K_p \cdot K_a \cdot a_{H^+} \cdot a_{ClO_4^-} \ll K_p \cdot a_{H^+} + 1 \quad (5.8)$$

This equation states implicitly that the anion covered oxide surface portion is negligibly small, and with the assumption that the experimental measured rates may vary by a maximum of 10%, the inequality (5.8) becomes:

$$K_a < \frac{0.1 \cdot (K_p \cdot a_{H^+} + 1)}{K_p \cdot a_{H^+} \cdot a_{ClO_4^-}} \quad (5.9)$$

Expression (5.9) is valid up to the highest concentrations of acid which were used, i.e. $a_{H^+} = a_{ClO_4^-} = 1$ in the case of Cu_2O and CuO and $a_{H^+} = a_{ClO_4^-} = 100$ in the case of ferric oxides. This allows an estimate of the higher limits of K_a for these oxides, namely $K_a < 0.1$ for CuO and Cu_2O and $K_a < 10^{-3}$ for the ferric oxides. These rather small values of the equilibrium constants for perchlorate ion adsorption do agree with the thermodynamic properties of this ion.

It should be mentioned that Cu_2O dissolves only half its copper in $HClO_4$ solutions according to the overall reaction:



This is because the Cu^+ ion disproportionates in the presence of ClO_4^- , and suggests that the applicability of the model to the case of Cu_2O may only be fortuitous.

The proposed model appears to describe very well the variation of absolute rates of leaching of the oxides with the concentration of perchloric acid, but it fails to account for the wide differences observed between these rates from one oxide to the other (cf. results). It is suggested that whole or part of these differences may be associated with one or more of the following factors:

- (a) Differences in entropies and enthalpies of activation for leaching. However, with the exception of Cu_2O , the energies of activation of the oxides are not very different (Table 6).
- (b) Differences in the types and concentrations of defects present in the oxides, if it can be assumed that the active surface for dissolution is controlled by defects (110).
- (c) Differences in the total surface areas in relation to grain and particle sizes, and shapes and porosity of the particles.

5.1.3 Leaching of Metal Oxides in HCl Solutions

With the exception of γ - and α - Al_2O_3 , the results on the leaching of the metal oxides which were investigated correlate well with the proposed model leading to rate equation (5.6), with $\text{X}^- \equiv \text{Cl}^-$. The activities of the hydrogen and chloride ions as a function of acid concentration were calculated with the assumption that $a_{\pm} = a_{\text{H}^+} = a_{\text{Cl}^-}$.

where a_{\pm} is the mean activity of HCl, and with the help of literature values of the mean activity coefficients of HCl for temperatures up to 60°C (111,112) and by extrapolation of these coefficients up to 85°C (101) (Table B.6, Appendix B). The values of the constants in the general rate expression (5.6) were calculated for each oxide with the aim of obtaining the best fit with the experimental results and are reproduced in Table 7. The calculated rate curves and the experimental points are shown in Figures 7,8 and 9 (Tables B.7 and B.8, Appendix B). Rate expression (5.6) can be rewritten for the leaching of oxides in HCl solutions and becomes:

$$\text{Rate} = \left[\frac{K_p \cdot a_{H^+}}{1 + K_p \cdot a_{H^+} + K_p \cdot K_a \cdot a_{H^+} \cdot a_{Cl^-}} \right] \cdot (k_1 + k_2 \cdot K_a \cdot a_{Cl^-} + k_3 \cdot \dots \dots K_a \cdot K_{a,p} \cdot a_{H^+} \cdot a_{Cl^-}) \text{ with } a_{\pm} = a_{H^+} = a_{Cl^-} \quad (5.11)$$

As can be seen in Table 7, both K_p , the protonation equilibrium constant, and K_a , the equilibrium constant for chloride ion adsorption, are small for ferric oxide in comparison with the corresponding constants obtained for the other oxides, whilst the complexity constant for the formation of the mono-chloro-ferric complex, K_c , is relatively large in comparison with the complexity constants associated with the formation of the mono-chloro complexes of aluminum and cupric ions. This suggests that there is no direct correlation between the affinity of an anion to adsorb at an oxide surface and its tendency to complex the oxide metal cation. Indeed, it appears that K_p and K_a vary in the same way from one oxide to the other and that these cons-

TABLE 7

Leaching of Metal Oxides in HCl
Calculated Constants in Rate Expression (5.6)

OXIDE	Z.P.C. (pH)	T° of leach (°C)	k ₁ $\left(\frac{\text{mg Metal}}{\text{min} \cdot \text{gm}}\right)$	k ₂ ←	k ₃ ←	K _p (molal ⁻¹)	K _a ←	K _{a,p} ←	k ₃ · K _{a,p} $\left(\frac{\text{mg Metal}}{\text{min} \cdot \text{gm} \cdot \text{molal}}\right)$	K _c [*] (ref. 50) (molal ⁻¹)	E (Table 3) $\left(\frac{\text{kcal}}{\text{mole}}\right)$
Cu ₂ O	>11.5	12	N	55.8	-	19.0	3.16	-	118	10 ^{4.73}	-
CuO	9.5	12	6.10	52.5	>10	5.0	0.6	<10 ⁻¹	1.26	10	≈18.0
Al(OH) ₃	9.1	80	0.525	7.3	>20	3.0	0.333	<4x10 ⁻³	0.110	small	15-22
α-Fe ₂ O ₃	8.5	80	3x10 ⁻⁴	4.39x10 ⁻²²	>10	1.2	0.142	<10 ⁻³	0.016 ⁻²	300	19-23

* K_c: stability constant for the equilibrium:



For Cu₂O, K_c corresponds to $Cu^{+} + 2Cl^{-} \rightleftharpoons CuCl_2^{-}$

N ≡ negligible

tants thus depend on the acid-base properties of the oxide surface, i.e. the electrostatic field exerted by this surface. Apart from cuprous oxide, the magnitude of the complexity constants, K_c , seems to correlate fairly well with those of the rates of desorption of the metals from chloride containing oxide sites relative to the rates of desorption of the metals from protonated oxide sites. Indeed, the estimated ratio of the rate constants, k_2/k_1 , in Table 7, is large for ferric oxide and small for gibbsite and cupric oxide. Although the product $k_3 \cdot K_{a,p}$ can be calculated, only limiting values of the individual constants k_3 and $K_{a,p}$ can be estimated, by assuming that the experimental results may be affected by a maximum error 10% (Table 7).

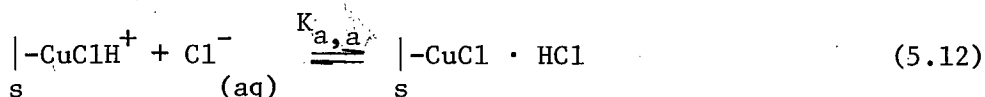
Additional evidence for the validity of the general rate expression (5.11) is given by the fact that the calculated rates of leaching of ferric oxide for the experiments in which the activities of H^+ and Cl^- ions were controlled by using $LiCl-HCl-H_2O$, $NaOH-HCl-H_2O$ and $HClO_4-HCl-H_2O$ electrolytes are very close to the measured rates of leaching (Figures 10 and 11) (Table B.9, Appendix B). These calculations were carried out with the following assumptions:

(a) At constant total ionic strength, the mean activity coefficients are the same for the $HCl-H_2O$ and the $HCl-LiCl-H_2O$ systems (113)

(b) At constant total ionic strength, the mean activity coefficients for the $HClO_4-HCl-H_2O$ and $NaOH-HCl-H_2O$ systems are the average values of the mean activity coefficients of the individual $HClO_4-H_2O$ and $HCl-H_2O$ systems in the former case, and of the

individual NaOH-H₂O and HCl-H₂O systems in the latter.

The kinetics of the leaching of cuprous oxide in HCl merits special attention. Indeed, the values of rate constants k_1 , k_2 and $k_3 \cdot K_{a,p}$ for the leaching of this oxide do not seem to show any correlation with the known behavior of cuprous species in chloride solutions. For example, the value of rate constant k_2 for the desorption of the mono-chloro-cuprous complex in solution is large (Table 7), but it is known that CuCl is almost insoluble in water (114) (1.1×10^{-3} M/liter at 25°C). Contrary to its behavior in HClO₄ solutions, in which Cu₂O produces cupric ions in solution with half the copper becoming elemental, in HCl solutions this oxide apparently dissolves only in the form of cuprous species. It was also experimentally observed that, in contrast to the behavior of ferric oxide, cuprous oxide dissolves more quickly in dilute HClO₄ than in dilute HCl at equal acidity (Figures 5 and 13). Eventually, the rate of leaching of Cu₂O becomes greater in HCl than in HClO₄ with increasing acidity ($a_{H^+} > 1$). Moreover, the addition of 0.09M of NaCl to a 0.09M HClO₄ leach solution resulted in the same rate of dissolution of Cu₂O as in 0.09M HCl. It is therefore proposed that due to the relative insolubility of CuCl, the Cu₂O surface already becomes covered with CuCl in very dilute HCl solutions, and that this surface then protonates as proposed in the last step of the general model and eventually even becomes di-chlorinated by Cl⁻ ion adsorption at these protonated sites, according to the following equilibrium:



Equation (5.12) thus represents an additional step in the proposed general model in 5.1.1. By adding a term for di-anion adsorption to rate expression (5.6), and with the assumption that the concentration of $[-MO \cdot OH_2 \cdot X \cdot H^+]$ sites is not negligible, equation (5.6) for the HCl-Cu₂O system becomes:

$$\begin{aligned} \text{Rate} = & \frac{k_1 \cdot K_p \cdot a_{H^+} + k_2 \cdot K_p K_a \cdot a_{H^+} \cdot a_{Cl^-} + k_3 \cdot K_p K_a K_a \cdot a_{H^+}^2 \cdot a_{Cl^-} \dots}{1 + K_p \cdot a_{H^+} + K_p \cdot K_a \cdot a_{H^+} \cdot a_{Cl^-}} \\ & \dots \frac{k_4 \cdot K_p \cdot K_a \cdot K_a \cdot K_a \cdot a_{H^+}^2 \cdot a_{Cl^-}^2}{+ K_p \cdot K_a \cdot K_a \cdot a_{H^+}^2 \cdot a_{Cl^-}} \end{aligned} \quad (5.13)$$

By dividing the numerator and denominator of rate expression (5.13) by $K_p \cdot K_a \cdot a_{H^+} \cdot a_{Cl^-}$, the following equation is obtained:

$$\text{Rate} = \frac{\left(\frac{k_1}{K_a \cdot a_{Cl^-}} \right) + k_2 + k_3 \cdot K_a \cdot a_{H^+} + k_4 \cdot K_a \cdot a_{H^+} \cdot a_{Cl^-}}{\left(\frac{(1 + K_p \cdot a_{H^+})}{K_p \cdot K_a \cdot a_{H^+} \cdot a_{Cl^-}} \right) + 1 + K_a \cdot a_{H^+}} \quad (5.14)$$

If it can be assumed that the surface of Cu₂O becomes rapidly saturated by Cl⁻ ions in dilute HCl, then $(1 + K_p \cdot a_{H^+}) \ll K_p \cdot K_a \cdot a_{H^+} \cdot a_{Cl^-}$ and $(k_1/K_a \cdot a_{Cl^-} + k_2) \approx 0$. Rate expression (5.14) can thus be simplified to:

$$\text{Rate} = \left[\frac{K_a \cdot a_{H^+}}{1 + K_a \cdot a_{H^+}} \right] \cdot (k_3 + k_4 \cdot K_a \cdot a_{Cl^-}) \quad (5.15)$$

with $a_{\pm} = a_{H^+} = a_{Cl^-}$

The numerical values of the constants in rate expression (5.15) were calculated by comparing this equation with the experimental results (Figure 13) (Table B.7, Appendix B). Limiting values of the individual constants k_4 , K_a and $K_{a,a}$ were obtained by allowing a 10% error in the experimental results (Table 8). These new values of the constants are in agreement with the surface properties of Cu_2O in HCl. Furthermore, the chloride covered cuprous oxide surface is expected to exhibit a more acid pH of Z.P.C. than the hydroxylated surface, i.e. $K_{a,p} < K_p$ in Table 8. The limiting values of k_4 and $K_{a,a}$ suggest that chloride ions show little affinity for adsorption at protonated chlorinated cuprous oxide sites, but that the desorption of cuprous species from dichlorinated oxide sites is rapid in comparison with the desorption of species from the other oxide sites. This observation seems to agree with the fact that the complexity constant for the formation of CuCl_2^- is large (Table 7).

As discussed in 5.1.1, the results on the leaching of $\gamma\text{-Al}_2\text{O}_3$ and $\alpha\text{-Al}_2\text{O}_3$ (Figure 12) are consistent with the proposed model if it is assumed that the rate of leaching of these oxides in solutions of acidity greater than 1N HCl is controlled by the slow hydroxylation reaction at the oxide surfaces. It is to be noted that the energy of activation of 13.1 kcal/mole obtained for the dissolution of $\gamma\text{-Al}_2\text{O}_3$ in 3 N HCl between 50 and 90°C is close to the reported energy of activation of 15.8 kcal/mole for the hydroxylation of the surface of $\gamma\text{-Al}_2\text{O}_3$ (19).

The wide differences observed between the rates of leaching of the oxides from one to the other have been discussed in 5.1.2.

TABLE 8

Leaching of Cu_2O in HCl
 Constants in Rate Expressions (5.14) and (5.15)

k_1	k_2	k_3	k_4	K_p	$K_{a,p}$	$K_{a,p}$	$K_{a,a}$	$k_4 \cdot K_{a,a}$
$\left(\frac{\text{mg Cu}}{\text{min} \cdot \text{gm}} \right)$	(molal^{-1})	(molal^{-1})	(molal^{-1})	(molal^{-1})	$\left(\frac{\text{mg Cu}}{\text{min} \cdot \text{gm} \cdot \text{molal}} \right)$			
N	N	38.6	$>10^3$	19	$>2 \times 10^4$	3.0	$<10^{-1}$	150

N \equiv negligible

5.1.4 The Leaching of Metal Oxides in H₂SO₄ Solutions

The general model for the leaching of oxides given in 5.1.1 was applied to the leaching of ferric, cuprous, cupric and manganous oxides in H₂SO₄ solutions, with $X^- \equiv \text{HSO}_4^-$ and $X^- \equiv \text{SO}_4^{2-}$, since H₂SO₄ produces two types of anions in solution upon its dissociation. The mean activity coefficients of H₂SO₄ have been estimated from literature data up to 60°C (115,116) and by extrapolation up to 80°C, with the assumption that $a_{\pm} = a_{\text{H}^+} = a_{\text{HSO}_4^-}$ where a_{\pm} is the mean activity of H₂SO₄ (Table B.10, Appendix B). The following expression for the rate of leaching of oxides in H₂SO₄ in terms of the general model was sufficient to describe the experimental results:

$$\text{Rate} = \frac{k_1 \cdot K_p \cdot a_{\text{H}^+} + k_2 \cdot K_p \cdot K_a \cdot a_{\text{H}^+} \cdot a_{\text{SO}_4^{2-}} + k_3 \cdot K_p \cdot K_a \cdot K_{a,p} \cdot a_{\text{H}^+}^2 \dots}{1 + K_p \cdot a_{\text{H}^+} + \dots} \quad (5.16)$$

$$\dots \frac{k_4 \cdot K_p \cdot K'_a \cdot a_{\text{H}^+} \cdot a_{\text{HSO}_4^-}}{K_p \cdot K_a \cdot a_{\text{H}^+} \cdot a_{\text{SO}_4^{2-}}}$$

This expression for the rate of leaching contains terms for the protonation of the oxide surface, SO₄⁼ and HSO₄⁻ adsorption at protonated sites, and protonation of sulphated sites. It is also suggested that the oxide surface may become saturated successively by adsorbed H⁺, and SO₄⁼ ions. Since it is assumed that $a_{\text{H}^+} = a_{\text{HSO}_4^-}$ and having $a_{\text{H}^+} \cdot a_{\text{SO}_4^{2-}} = K_{d,2} \cdot a_{\text{HSO}_4^-}$ where K_{d,2} is the second dissociation constant of H₂SO₄ in water (117), it is deduced that $a_{\text{SO}_4^{2-}} \approx K_{d,2}$. The above rate equation can be simplified to yield:

$$\text{Rate} = \frac{k_{(1)} \cdot a_{\text{H}^+} + k_{(2)} \cdot a_{\text{H}^+}^2}{1 + K_{(1)} \cdot a_{\text{H}^+}} \quad (5.17)$$

where the constants in equation (5.16) have been grouped in single constants $k_{(i)}$ and $K_{(i)}$ for the terms in a_{H^+} and $a_{\text{H}^+}^2$. The numerical values of the constants in rate expression (5.17) were calculated by comparing this equation with the experimental results (Figures 15 and 16) (Tables B.11, Appendix B) and are reported in Table 9. The numerical values of the individual constants k_1 , k_2 , and K_p and K_a , and of the combination of constants ($k_3 \cdot K_p \cdot K_a \cdot K_{a,p} \cdot K_{d,2} + k_4 \cdot K_p \cdot K'_a$) and ($K_a \cdot K_{a,p} \cdot K_{d,2} + K'_a$) in rate equation (5.16) can be estimated when the same values as obtained for the leaching of the oxides in HClO_4 are assigned to k_1 and K_p . However, the limited range of acidities which could be used for the leaching of some of the oxides makes this estimation only reasonable in the case of $\alpha\text{-Fe}_2\text{O}_3$ (Table 9). The large value of K_a suggests that $\text{SO}_4^{=}$ ions are strongly adsorbed at the ferric oxide surface and the much smaller limiting values of $K_{a,p}$ and K'_a suggest that the adsorption of H^+ ions at $\text{SO}_4^{=}$ containing sites and of HSO_4^- ions at protonated ferric oxide sites is not as spontaneous. The desorption of ferric species from protonated sulphated sites cannot be distinguished from that of the species from bisulphate containing sites and therefore $k_3 = k_4$. The large value of rate constant k_3 compared with k_2 suggests that the desorption of ferric species from a HSO_4^- containing surface site is more rapid than from a $\text{SO}_4^{=}$ containing site. This might be due to the double coordinating ability exhibited by $\text{SO}_4^{=}$ ions, which is lacking

TABLE 9

Leaching of Metal Oxides in H₂SO₄
 Calculated Constants in Rate Expression (5.17)

OXIDE	Z.P.C. (pH)	T ^o of leach (°C)	k(1) $\left(\frac{\text{mg-Metal}}{\text{min}\cdot\text{gm}\cdot\text{molal}}\right)$	k(2) $\left(\frac{\text{mg Metal}}{\text{min}\cdot\text{gm}\cdot\text{molal}^2}\right)$	K(1) (molal ⁻¹)	K _c * (ref 50) (molal ⁻¹)	E Activation energy (Table 3) $\left(\frac{\text{kcal}}{\text{mole}}\right)$
Cu ₂ O	>11.5	12	2.87 x 10 ³	2.31 x 10 ⁴	123	10 ^{2.15}	14.0 (ref
CuO	9.5	12	3.91 x 10 ²	3.14 x 10 ³	123	10 ^{2.15}	≈18.0
MnO	>9	12	1.85 x 10 ³	1.80 x 10 ⁴	20.7	10 ^{2.26}	-
α-Fe ₂ O ₃	8.5		6.27 x 10 ⁻²	1.8 x 10 ⁻²	1.89	10 ^{4.04}	19.0 - 23.0

*K_c stability constant for the equilibrium



Calculated Constants in Rate Expression (5.16)

OXIDE	k ₁ $\left(\frac{\text{mg Metal}}{\text{min}\cdot\text{gm}}\right)$	k ₂ ←	K _{d,2} (ref 117) (molal ⁻¹)	K _p (molal ⁻¹)	K _a (molal ⁻¹)	K' _a (molal ⁻¹)	K _{a,p} (molal ⁻¹)	k ₃ =k ₄ $\left(\frac{\text{mg Metal}}{\text{min}\cdot\text{gm}}\right)$
α-Fe ₂ O ₃	3 x 10 ⁻⁴	0.09	1.86 x 10 ⁻³	1.2	3.06 x 10 ²	<3 x 10 ⁻²	<16	>0.5

with HSO_4^- .

5.1.5 The Leaching of Ferric Oxide in $\text{H}_2\text{C}_2\text{O}_4$ Solutions

The general rate expression (5.6) was applied to the leaching of ferric oxide in oxalic acid solutions, with $\text{X}^- \equiv \text{C}_2\text{O}_4^{2-}$ and $\text{X}^- \equiv \text{HC}_2\text{O}_4^-$, and becomes:

$$\begin{aligned} \text{Rate} = & k_1 \cdot K_p \cdot a_{\text{H}^+} + k_2 \cdot K_p \cdot K_a \cdot a_{\text{H}^+} \cdot a_{\text{C}_2\text{O}_4^{2-}} + k_3 \cdot K_p \cdot K_a \cdot K_{a,p} \dots \\ & \dots \cdot a_{\text{H}^+}^2 \cdot a_{\text{C}_2\text{O}_4^{2-}} + k_4 \cdot K_p \cdot K'_a \cdot a_{\text{H}^+} \cdot a_{\text{HC}_2\text{O}_4^-} + k_5 \cdot K_p \dots \\ & \dots \cdot K'_a \cdot K'_a \cdot a_{\text{H}^+}^2 \cdot a_{\text{HC}_2\text{O}_4^-} \end{aligned} \quad (5.18)$$

In writing equation (5.18) it was assumed that the concentration of the oxide surface species produced in the corresponding pre-equilibrium reactions is negligibly small, i.e. that the ferric oxide surface did not become saturated by species from solution. As no distinction can be made between the desorption of ferric species from protonated oxalate containing sites and HC_2O_4^- containing sites, k_3 is equal to k_4 . Moreover, $a_{\text{H}^+}^2 \cdot a_{\text{C}_2\text{O}_4^{2-}} = K_{d,1} \cdot a_{\text{H}^+} \cdot a_{\text{HC}_2\text{O}_4^-}$ and $a_{\text{H}^+}^2 \cdot a_{\text{C}_2\text{O}_4^{2-}} = K_{d,1} \cdot a_{\text{H}^+} \cdot a_{\text{H}_2\text{C}_2\text{O}_4}$, where $K_{d,1}$ and $K_{d,2}$ are respectively the first and second dissociation constants of $\text{H}_2\text{C}_2\text{O}_4$ in water. Thus, rate expression (5.18) can be simplified and becomes:

$$\begin{aligned} \text{Rate} = & k(1) \cdot a_{\text{H}^+} + k(2) \cdot a_{\text{H}^+} \cdot a_{\text{C}_2\text{O}_4^{2-}} + k(3) \cdot a_{\text{H}^+} \cdot a_{\text{HC}_2\text{O}_4^-} + \dots \\ & \dots k(4) \cdot a_{\text{H}^+} \cdot a_{\text{H}_2\text{C}_2\text{O}_4} \end{aligned} \quad (5.19)$$

where the constants in (5.18) have been grouped in single rate constants $k_{(i)}$. As the experiments were carried out in dilute solutions of oxalic acid (0.3 M/liter), the concentration and activities of species in solution were assumed to be equal. The numerical values of the constants, $k_{(i)}$, were obtained by comparing rate expression (5.19) with the experimental results (Figure 19) (Table 10) and limiting values of the individual rate and equilibrium constants in (5.18) were estimated by allowing a 10% error in the experimental results (Table B.12, Appendix B).

It is concluded that the model for the leaching of oxides given in 5.1.1 is applicable to the leaching of ferric oxide in oxalate solutions. The large values of the rate constants k_2 , k_3 and k_5 suggest that the desorption of ferric species from oxalate containing sites is rapid and is in agreement with the large complexing affinity of the $C_2O_4^{=}$ ion for Fe^{+++} ions in solution (50).

5.1.6 The Leaching of Ferric Oxide in Various Other Acids

According to the previous discussions, a rapid leach rate should be obtained if an acid is selected producing anions in solution which are strong metal ion complexers and show affinity for adsorption at oxide surfaces. A typical acid which was chosen is ethylene-diamine-tetra-acetic acid, i.e. E.D.T.A., or H_4X . Although the pK for the formation of FeX^- species in this acid is 25.1 (118), E.D.T.A. solutions did not leach ferric oxide at an appreciable dissolution rate. At least three factors may be suggested for this observation:

TABLE 10

Leaching of $\alpha\text{-Fe}_2\text{O}_3$ (Michigan) in Oxalic Acid.
 Calculated Constants in Rate Expressions (5.18) and (5.19)

$k_{(1)}$ $\left(\frac{\text{mg Fe}}{\text{min}\cdot\text{gm}\cdot\text{molal}}\right)$	$k_{(2)}$ $\left(\frac{\text{mg Fe}}{\text{min}\cdot\text{gm}\cdot\text{molal}^2}\right)$	$k_{(3)}$ $\left(\frac{\text{mg Fe}}{\text{min}\cdot\text{gm}\cdot\text{molal}^2}\right)$	$k_{(4)}$ $\left(\frac{\text{mg Fe}}{\text{min}\cdot\text{gm}\cdot\text{molal}^2}\right)$	
$\approx 10^{-3}$	4.6×10^2	5.8×10^{-1}	1.1×10^{-1}	
k_1 $\left(\frac{\text{mg Fe}}{\text{min}\cdot\text{gm}}\right)$	k_2 $\left(\frac{\text{mg Fe}}{\text{min}\cdot\text{gm}}\right)$	$k_3 = k_4$ $\left(\frac{\text{mg Fe}}{\text{min}\cdot\text{gm}}\right)$	k_5 $\left(\frac{\text{mg Fe}}{\text{min}\cdot\text{gm}}\right)$	
$\approx 3 \times 10^{-4}$	$> 4.0 \times 10^{-2}$	$> 5.0 \times 10^{-2}$	$> 5 \times 10^{-2}$	
K_p (molal^{-1})	K_a (molal^{-1})	K'_a (molal^{-1})	$K_{a,p}$ (molal^{-1})	$K'_{a,p}$ (molal^{-1})
1.2	10^4	< 10	< 10	< 1

- (a) The solubility of E.D.T.A. at pH 2.7 is only around 0.01 M/liter.
- (b) At this pH, the complexing species, X^{4-} are only present at a concentration of approximately 5×10^{-14} M/liter.
- (c) The anionic species present in solution at pH 2.7 are H_3X^- and H_2X^{2-} and these anions not only are weak ferric ion complexers, but also may compete for the adsorption sites at the oxide surface.

These factors are also suggested to be the cause of the very low rates of leaching of ferric oxide in maleic, malonic, tartaric, citric and sulphamic acids.

5.2 The Acid Leaching of Ferric Oxides in the Presence of Added Ferrous Salts in Solution

5.2.1 The Leaching of Ferric Oxide in $H_2C_2O_4$ Solutions

At least two different mechanisms can be suggested for the leaching of ferric oxide in oxalic acid in the presence of added ferrous oxalate (119). In one mechanism, adsorbed ferrous oxalate species may lose whole or part of their oxalate groups to neighboring ferric sites of the oxide surface. The desorption of the resulting ferric oxalate complexes and the now oxalate-depleted ferrous species will result in the dissolution of the oxide whilst the ferrous content in solution is kept constant. In another mechanism adsorbed ferrous oxalate species may lose electrons to the oxide lattice, probably at defects. The desorption of the resulting

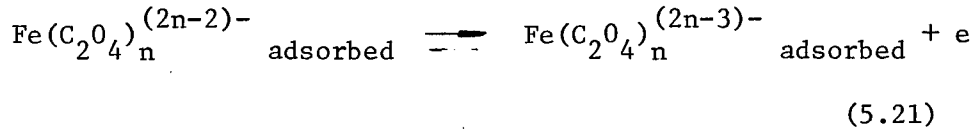
ferric oxalate complexes and the ferrous ions from the substrate will again lead to the leaching of the oxide and restoration of the ferrous content of the solution.

As the leaching of $\alpha\text{-Fe}_2\text{O}_3$ was not affected by the presence of Mn^{2+} , Cu^{2+} , Co^{2+} , Ni^{2+} and Zn^{2+} oxalate complexes in 0.2 M oxalate solution, it is concluded that a mechanism by group transfer in the ferrous oxalate catalyzed dissolution of $\alpha\text{-Fe}_2\text{O}_3$ is not likely to be operative.

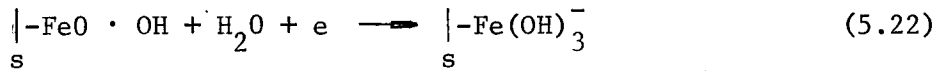
Hence, a mechanism involving leaching by electron transfer at the oxide-electrolyte interface is proposed. The increasing relative rates of leaching of $\alpha\text{-Fe}_2\text{O}_3$ with increasing Ti content of the oxide can either be attributed to the corresponding rise of the electronic bulk conductivity of the oxide or to the increasing ferrous content of the oxide, if ferrous sites are active dissolution centres. Although the bulk conductivity of $\alpha\text{-Fe}_2\text{O}_3$ increases by more than ten orders of magnitude for Ti contents from 0 to 0.8 wt % (92), the corresponding relative rates of leaching of $\alpha\text{-Fe}_2\text{O}_3$ only increase by a factor of six (Figure 23), indicating that there is very little correlation between rate of leaching and bulk conductivity of $\alpha\text{-Fe}_2\text{O}_3$. However, the possibility remains that the surface conductivity of $\alpha\text{-Fe}_2\text{O}_3$ in the oxalate electrolyte does not vary much (120), due to the adsorption of the oxalato-ferrous complexes at the oxide surface. This may also be the reason why the addition of 0.5% Mg to $\alpha\text{-Fe}_2\text{O}_3$ reduces the relative rate of leaching of the oxide by only 25%, despite the fact that the bulk conductivity of the oxide becomes p-type (Figure 23).

If, as it is assumed, the overall leaching reaction involves electron-transfer, an anodic and a cathodic reaction can be included in the model of the leaching. It is suggested that these reactions are:

(a) anodic



(b) cathodic



It is further suggested that the electron-transfer reaction is also the rate determining step in the overall dissolution reaction of $\alpha\text{-Fe}_2\text{O}_3$. The Butler-Volmer equation can be written for the above anodic and cathodic reactions using the high-field approximation (121), if η_a and η_c , the anodic and cathodic overpotentials, are assumed to be sufficiently large. Hence, the anodic current per unit area at the oxide surface can be expressed as:

$$i_a = i_{a,o} \cdot \exp \left[(1-\alpha_a) \frac{F}{RT} \cdot \eta_a \right] \quad (5.23)$$

where $i_{a,o}$ is the exchange-current density, and α_a , the transfer coefficient, is defined as the fraction of the overpotential contributing to the increase in the rate of the reaction.

The cathodic current per unit area becomes:

$$i_c = -i_{c,o} \cdot \exp \left[-\alpha_c \cdot \frac{F}{RT} \cdot \eta_c \right] \quad (5.24)$$

At a potential E_M , i.e. the mixed potential, $|i_c| = |i_a|$. Using the equilibrium potentials E_a and E_c corresponding to the anodic and cathodic reactions, and by rearrangement of equations (5.23) and (5.24), the expression of E_M is given by:

$$E_M = \left[\frac{1-\alpha_a}{1-\alpha_a + \alpha_c} \right] \cdot E_a + \left[\frac{\alpha_c}{1-\alpha_a + \alpha_c} \right] \cdot E_c \quad (5.25)$$

Delahay and Berzins (122) introduced an equation which correlates the exchange-current density, i_o , to the potential independent rate-constant of the reaction at the surface, k_o , and to the activities of the oxidized and reduced species of the couples, with the assumption that the potential in the outer plane of closest approach of the redox species is constant:

$$i_o = k_o \cdot F \cdot a^{1-\alpha} \cdot a_R^\alpha \quad (5.26)$$

The difference, $E_c - E_a$, can be expressed in terms of the equilibrium constant K of the overall reaction by use of the Nernst equation as follows:

$$\frac{F}{RT} \cdot [E_c - E_a] = \ln K + \ln \left[\frac{a_s[-FeO \cdot OH] \cdot a[Fe(C_2O_4)_n^{(2n-2)-}]_{ads.}}{a_s[-Fe(OH)_3] \cdot a[Fe(C_2O_4)_n^{(2n-3)-}]_{ads.}} \right] \quad (5.27)$$

The suitable combination of equations (5.23), (5.25), (5.26) and (5.27) leads to the general expression for the current density involved in the electrochemical reaction at the oxide surface, namely:

$$\begin{aligned}
 i = & F \cdot (k_{o,a}) \left(\frac{\alpha_c}{1-\alpha_a + \alpha_c} \right) \cdot (k_{o,c}) \left(\frac{1-\alpha_c}{1-\alpha_a + \alpha_c} \right) \cdot K \left(\frac{\alpha_c \cdot (1-\alpha_a)}{1-\alpha_a + \alpha_c} \right) \dots \\
 & \dots \left(a_{[\text{Fe}(\text{C}_2\text{O}_4)_n]_{\text{ads}}^{(2n-2)-}} \right) \left(\frac{\alpha_c}{1-\alpha_a + \alpha_c} \right) \cdot \left(a_{\text{S}}[-\text{FeO}\cdot\text{OH}] \right) \left(\frac{1-\alpha_a}{1-\alpha_a + \alpha_c} \right)
 \end{aligned} \tag{5.28}$$

Thus, if the overall rate of leaching of $\alpha\text{-Fe}_2\text{O}_3$ is controlled by the electron transfer step, and if only negatively charged ferrous oxalate species are involved in the dissolution, i.e. $\text{Fe}(\text{C}_2\text{O}_4)_2^{2-}$ and $\text{Fe}(\text{C}_2\text{O}_4)_3^{4-}$, the rate of dissolution of $\alpha\text{-Fe}_2\text{O}_3$ can be expressed by:

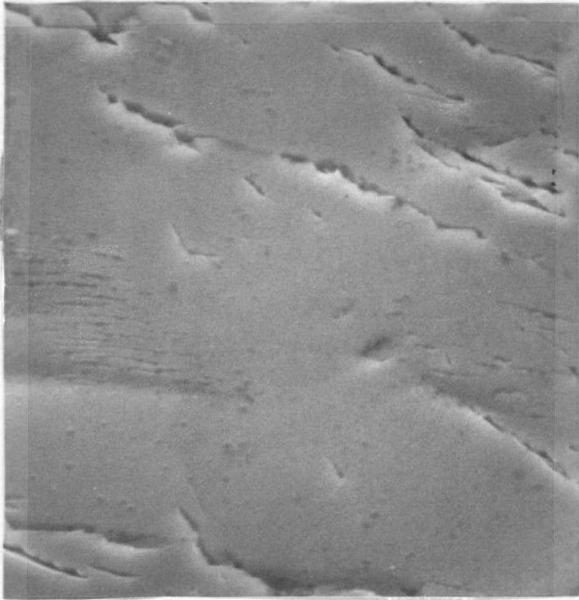
$$\text{Rate} = k_1 \cdot \left(a_{[\text{Fe}(\text{C}_2\text{O}_4)_2]_{\text{ads}}^{2-}} \right) \left(\frac{\alpha_c}{1-\alpha_a + \alpha_c} \right) + k_2 \cdot \left(a_{[\text{Fe}(\text{C}_2\text{O}_4)_3]_{\text{ads}}^{4-}} \right) \left(\frac{\alpha'_c}{1-\alpha'_a + \alpha'_c} \right) \tag{5.29}$$

where k_1 and k_2 contain the constant terms in expression (5.28) and the conversion factors and the activity of $[-\text{FeO}\cdot\text{OH}]_{\text{S}}$ in (5.28) is assumed to be unity. The activities of the adsorbed oxalato-ferrous complexes depend in turn on the activities of H^+ and the corresponding oxalato-ferrous complexes in solution, if the same model as for the direct dissolution of ferric oxide in the presence of adsorbing anions can be applied. The rate expression in its complete form, i.e. including the dependence on H^+ and ferrous species in solution, becomes:

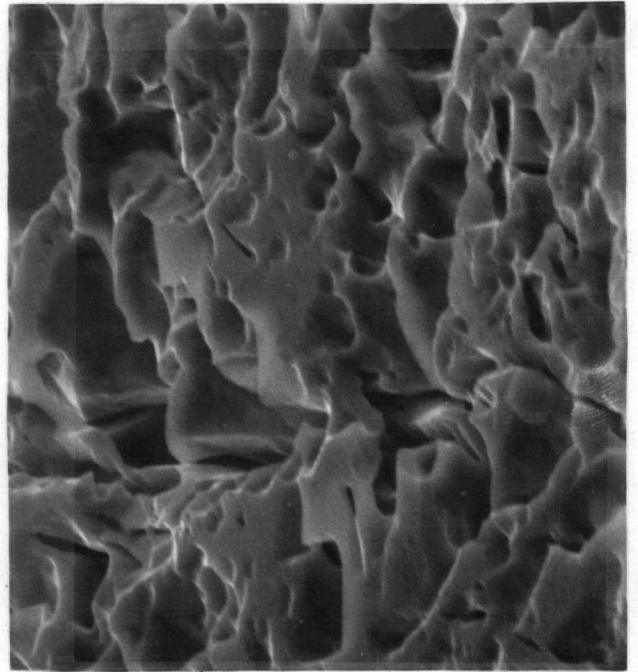
$$\text{Rate} = k_{(1)} \cdot (a_{\text{H}^+} \cdot a_{\text{Fe}(\text{C}_2\text{O}_4)_2^{2-}}) \left(\frac{\alpha_c}{1-\alpha_a + \alpha_c} \right) + k_{(2)} \cdot (a_{\text{H}^+} \cdot a_{\text{Fe}(\text{C}_2\text{O}_4)_3^{4-}}) \left(\frac{\alpha'_c}{1-\alpha'_a + \alpha'_c} \right) \tag{5.30}$$

The rates of leaching of $\alpha\text{-Fe}_2\text{O}_3$ (0% Ti) and $\alpha\text{-Fe}_2\text{O}_3$ (1.3% Ti) in 0.2 M oxalic acid at a constant pH of 2.80 show respectively a 0.66 and 0.60 power dependence on the concentration of added ferrous oxalate (Figure 21). It thus appears that the effect of the Ti content of $\alpha\text{-Fe}_2\text{O}_3$ is to modify the values of the transfer coefficients α_a , α_c , α'_a and α'_c in rate expression (5.30). For simplicity, it is assumed that $\alpha_a = \alpha_c = \alpha'_a = \alpha'_c$ (Table B.18, Appendix B). The numerical values of $k_{(1)}$ and $k_{(2)}$ in (5.30) were calculated using the experimental results on the variation of leaching of $\alpha\text{-Fe}_2\text{O}_3$ versus pH (Figure 25) (Table B.18, Appendix B). Rate expression (5.30) is found to correlate very well with these results. Finally, the experimental rates of leaching of $\alpha\text{-Fe}_2\text{O}_3$ as a function of the concentration of oxalic acid at a constant pH of 2.80 and in the presence of 6 mg/liter of added ferrous ion compare well with the calculated rates using rate equation (5.30) (Figure 22) (Table B.19, Appendix B).

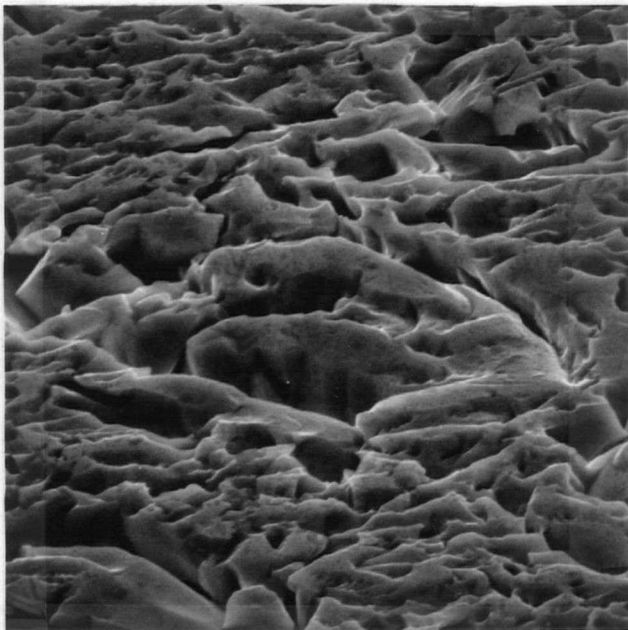
It should be noted that the morphology of the acid attack of the basal plane of a $\alpha\text{-Fe}_2\text{O}_3$ single crystal is significantly different in ferrous species containing oxalic acid than in HCl, H_2SO_4 and HClO_4 solutions (Figure 30a to 30d). In the latter acids, uniform attack (HClO_4) or evenly distributed pitting attack (HCl, H_2SO_4) of the basal plane of $\alpha\text{-Fe}_2\text{O}_3$ is observed, whilst in oxalic acid in the presence of ferrous species localized etching can be seen (Figure 30d). The etch pits appear to be aligned along three crystallographic directions with their edges, which are parallel to these directions, forming pseudo hexagons in the basal plane. These directions may correspond



(a)



(b)



(c)



(d)

Figure 30. Morphology of the acid attack on the basal plane of a $\alpha\text{-Fe}_2\text{O}_3$ single crystal.

(a) 9 M HClO_4 , 80°C , 10 days, x 2,000; (b) 6 M HCl , 60°C , 10 min, x 2,000
 (c) 6 M H_2SO_4 , 60°C , 20 min, x 2,000; (d) 0.2 M oxalic acid, 6 mg/liter Fe(II) , 80°C , 20 min, x 1,000

to the intersection of rhombohedral planes and the basal plane of $\alpha\text{-Fe}_2\text{O}_3$. It is suggested that the cathodic reaction, i.e. (5.22), takes place at defects associated with the observed crystallographic directions and that the anodic reaction, i.e. (5.21), proceeds at evenly distributed protonated sites of the oxide surface. The cathodic reaction will cause pitting of the oxide surface, since it is proposed that ferrous ions which are formed during the reduction of ferric ions in the oxide lattice desorb from cathodic sites. Conversely, the anodic reaction will not modify the morphology of the oxide surface, since only species from solution are involved in this reaction, i.e. the oxidation of oxalato-ferrous to oxalato-ferric species.

5.2.2 The Leaching of Ferric Oxide in Malonic Acid

Due to the lack of data on the stability constants of equilibria reactions associated with the formation of malonato-ferrous species, the results on the leaching of ferric oxide in malonic acid (Figure 28) can only be interpreted qualitatively. The similar variation of the rate of leaching of $\alpha\text{-Fe}_2\text{O}_3$ in malonic and oxalic acids as a function of pH (Figures 25 and 28) suggests that the oxide dissolves by the same mechanism in both acids. It is proposed that malonato-ferrous species adsorb at protonated $\alpha\text{-Fe}_2\text{O}_3$ sites, followed by the rate determining electron transfer between these adsorbed species and the oxide lattice. The desorptions of the resulting malonato-ferric species and ferrous ions from the oxide surface will result in the leaching of the oxide. The results (Figures 25 and 28) show that the pH corresponding to the

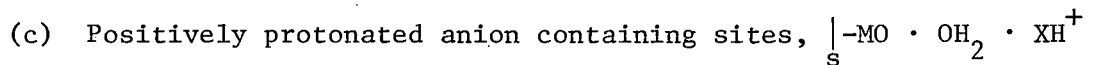
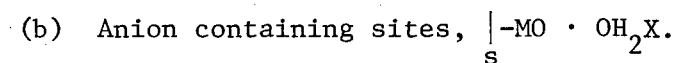
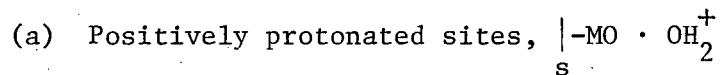
maximum rate of leaching of $\alpha\text{-Fe}_2\text{O}_3$ in oxalic acid is shifted towards a more basic pH in the case of malonic acid, i.e. from pH 2.8 to about 5. It is suggested that this difference can be associated with the distribution of the complexing ions in the two acids, i.e. malonic acid becomes completely dissociated in water at a higher pH than oxalic acid (123).

5.2.3 The Leaching of Ferric Oxide in HCl

The results presented in Figure 29 (Table B.21, Appendix B) indicate that the rate of leaching of $\alpha\text{-Fe}_2\text{O}_3$ in HCl in the presence of ferrous species in solution is only enhanced in strong HCl solutions. This suggests that only highly complexed ferrous species, i.e. FeCl_3^- and FeCl_4^{2-} , are active in producing an increase in the rate of leaching of the oxide. Due to the possible similarities between the ferrous catalyzed leaching of ferric oxide in both oxalic, malonic and hydrochloric acids, it is proposed that ferrous chloride complexes act as redox couples at the oxide surface. The necessity of having highly complexed ferrous species in solution may be due to either the increased adsorption affinity of negatively charged complexes at positively charged oxide sites and/or to the enhanced rate of electron-transfer between these adsorbed ferrous species and the oxide lattice (Table 4).

6. CONCLUSIONS

1. The direct leaching in acids of most of the oxides which were investigated can be described quantitatively by a general model written in terms of the rate controlling desorptions into solution of surface metal complexes formed in rapid adsorption pre-equilibria. These surface metal complexes are essentially created at three kinds of oxide sites:



2. The order of complexing power of the anions of the acids for the oxide metal ions in solution is in the order of the calculated rate constants for the desorption of metal complexes from oxide sites containing these anions and does not correlate with the adsorption affinity of the anions.

3. The affinity for adsorption of the anions of the acids at a given oxide surface appears to depend essentially on the negative charge and the relative water structure promoting effect of the anions, whereas the tendency for adsorption of a given anion at different oxide surfaces can be related to the pH's of Z.P.C. of the oxides.

4. The rates of leaching of the dehydrated forms of aluminum oxides

appear to become controlled by the rates of hydroxylation of the oxide surfaces with increasing acidity of the electrolyte. This suggests that the hydroxylation of the oxide surface is a prerequisite for enhanced speed of dissolution by species in solution.

5. The leaching of ferric oxides in acids may be considerably enhanced by the presence of small quantities of ferrous species in solution.

It seems that at least two conditions have to be fulfilled to observe this catalytic effect with ferric oxides:

(a) The electrolyte should form highly complexed ferrous species which are susceptible to fast electron transfer with ferric ions at the oxide surface.

(b) These ferrous complexes should exhibit affinity for adsorption at the oxide surface.

The experimental results suggest that oxalato-, chloro- and malonato-ferrous complexes may fall in this category of complexes.

The mechanism of the ferrous catalyzed leaching of ferric oxides is thought to involve electrochemical reactions at the oxide surface.

It appears that the electron-transfer steps between the adsorbed ferrous complexes and the $\alpha\text{-Fe}_2\text{O}_3$ surface are rate controlling.

7. SUGGESTIONS FOR FUTURE WORK

Although the proposed general mechanism for the leaching of metal oxides in acids can account for the rates of leaching on a relative basis, it does not provide an explanation for the observed large differences in the absolute rates of leaching.

Future studies on pure polycrystalline and single crystals of a variety of metal oxides should be made to elucidate this problem. At the same time this might provide more information on the following aspects of the leaching:

- (a) anisotropy, i.e. preferential attack on characteristic crystal faces of the oxides.
- (b) the effect of crystal defects.
- (c) the effect of impurities; this could be substantiated through controlled oxide doping.

The fundamental studies should be extended to applied problems of oxide leaching and should include some of the current problems, for example the separation of mixed nickel and copper oxides and aluminum and iron oxides. The extraction of metals from pyrometallurgical fumes such as lead-zinc-iron oxides which are produced in the iron blast furnace, and iron-manganese oxides which are obtained in the ferro-manganese production should also be considered.

The possible positive or negative catalytic effects of small quantities of complexed cations in solution on the rates of leaching of metal oxides also warrants further research.

8. APPENDIX A

Chemical Analysis and X-Ray Diffraction Patterns

TABLE A.1

Analysis of Goethite (Minnesota) and Hematite (Michigan).

Element	Hematite		Goethite	
	Weight %	Weight as Oxide M_mO_n	Weight %	Weight as Oxide M_mO_n
H ₂ O	0.84	0.13	7.20	0.11
Al	5.00	9.55	-	-
Ca	1.00	1.40	-	-
Fe	57.94	76.00 Fe ₂ O ₃ 7.10 FeO·OH	52.21	69.93 FeO·OH 11.81 Fe ₂ O ₃
Na	0.50	0.85	-	-
Mn	0.10	0.14	0.30	0.44
Si	3.00	5.88	8.95	17.52
Ti	0.50	0.85	-	-
Others	0.05	-	0.01	-
	Total	101.90	Total	99.81

TABLE A.2

X-Ray Diffraction Patterns of Synthetic Hematite (Table 5)
 (Using the k_{α} Fe Radiation)

dÅ	Reported		Sample B		Sample O		Sample P		Sample E	
	2θ	I/I ₁								
3.66	30.66	25	30.6	20	30.7	10	30.5	43	30.6	30
2.69	42.18	100	42.2	100	42.3	100	42.0	100	42.1	100
2.51	45.36	50	45.5	50	45.5	60	45.2	75	45.3	75
2.201	53.18	30	52.3	40	52.3	20	52.1	33	52.1	40
1.838	63.56	40	63.6	40	63.5	50	63.5	47	63.5	50
1.690	69.90	60	69.9	60	69.9	60	68.8	56	69.8	50
1.596	74.68	16	74.8	10	74.6	-	74.5	21	74.6	10
1.484	81.42	35	81.4	30	81.3	20	81.3	37	81.4	40
1.452	83.62	35	83.5	30	83.5	20	83.5	33	83.6	40

TABLE A.3

X-Ray Diffraction Pattern for Synthetic Cu_2O and CuO
 (Using the k_α Cu Radiation)

Cu_2O					CuO				
dÅ	Reported	I/I_0	This Study		dÅ	Reported	I/I_0	This Study	
	2θ		2θ	I/I_0		2θ		2θ	I/I_0
3.020	29.50	9	29.70	15	2.751	32.52	12	32.70	15
2.365	36.40	100	36.50	100	2.530	35.44	49	35.40	50
2.135	42.30	37	42.40	45	2.523	35.54	100	35.60	100
1.510	61.30	27	61.30	30	2.323	38.72	96	38.80	90
1.287	73.50	17	73.60	20	2.312	38.92	30	38.90	50
1.233	77.40	4	77.30	14	1.959	46.30	3	46.30	5
					1.866	48.76	25	48.90	30
					1.714	53.41	8	53.60	10
					1.581	58.31	14	58.35	15
					1.505	61.56	20	61.50	25
					1.418	65.80	12	65.90	10
					1.410	66.22	15	66.25	12
					1.375	68.14	19	68.15	20
					1.304	72.42	7	72.50	5
					1.265	75.02	6	75.10	55
					1.262	75.22	7	75.25	5

TABLE A.4

Chemical Analysis of Pyrolusite, β -MnO₂

Element or Compound	Weight %
MnO ₂	75.20
SiO ₂	5.89
Fe	0.02
CuO	3.84
P	0.045
Others	15.0

TABLE A.5

X-Ray Diffraction Patterns of $\text{Al}(\text{OH})_3$, $\gamma\text{-Al}_2\text{O}_3$ and $\alpha\text{-Al}_2\text{O}_3$,
(Using the k_α Cu Radiation)

$\text{Al}(\text{OH})_3$					$\gamma\text{-Al}_2\text{O}_3$					$\alpha\text{-Al}_2\text{O}_3$				
dÅ	Reported		This Work		dÅ	Reported		This Work		dÅ	Reported		This Work	
	2θ	I/I ₀	2θ	I/I ₀		2θ	I/I ₀	2θ	I/I ₀		2θ	I/I ₀	2θ	I/I ₀
4.85	18.28	320	18.3	200	4.56	19.44	40	-	-	3.49	25.50	75	25.7	55
4.37	20.30	50	20.4	55	2.80	31.92	20	-	-	2.554	35.10	100	35.2	100
4.32	20.54	23	20.6	30	2.39	37.60	80	37.5	80	2.383	37.72	45	37.9	33
3.306	26.94	15	26.95	15	2.28	39.50	50	39.4	10	2.088	43.30	100	43.4	100
3.187	27.97	12	28.1	13	1.977	45.84	100	45.8	50	1.741	52.52	50	52.7	36
3.112	28.66	7	28.8	7	1.520	60.90	30	-	-	1.603	57.44	90	57.6	85
2.454	36.58	23	36.8	17	1.395	67.13	100	67.2	100	1.512	61.25	11	61.2	8
2.420	27.12	20	37.2	6						1.4055	66.46	38	66.6	30
2.388	37.64	27	37.9	26						1.3746	68.16	50	68.2	40
2.285	39.40	5	39.4	6						1.2396	76.84	18	76.9	12
2.244	40.15	10	40.2	11						1.2347	77.20	5	77.2	6
2.168	41.62	7	41.8	13										
2.043	44.30	17	44.2	20										
1.993	45.50	11	45.5	12										
1.921	47.28	11	47.4	9										
1.799	50.70	13	50.7	15										
1.750	52.22	16	52.2	14										
1.689	54.26	13	54.6	10										

9. APPENDIX B

Calculated and Experimental Results

TABLE B.1

pH of a 0.2 M Oxalic Acid Aqueous Solution at 80°C
as a Function of Added HClO_4 and NaOH.

HClO_4 (M/liter)	NaOH (M/liter)	pH Measured	pH Calculated*
0.9	0	-	0.04
0.45	0	-	0.35
0.18	0	-	0.75
0	0	1.05	1.05
0	0.05	1.3	1.30
0	0.10	1.6	1.59
0	0.15	1.9	2.00
0	0.20	2.8	2.85
0	0.25	3.55	3.68
0	0.30	4.0	4.20
0	0.35	4.5	4.65

TABLE B.2

Calculated Distribution of Oxalate Species in
0.2 M Oxalic Acid at 80°C

pH	$[C_2O_4^{=}]$ (%) 100%=1	$[HC_2O_4^-]$ (%) 100%=1	$[H_2C_2O_4]$ (%) 100%=1
0.0	1.21×10^{-6}	3.82×10^{-2}	9.60×10^{-1}
0.5	1.14×10^{-5}	1.14×10^{-1}	8.85×10^{-1}
1.0	9.00×10^{-5}	2.84×10^{-1}	7.15×10^{-1}
1.5	5.55×10^{-4}	5.55×10^{-1}	4.41×10^{-1}
2.0	2.53×10^{-3}	7.95×10^{-1}	2.00×10^{-1}
2.5	9.25×10^{-3}	9.25×10^{-1}	7.35×10^{-2}
3.0	2.99×10^{-2}	9.45×10^{-1}	2.38×10^{-2}
3.5	9.00×10^{-2}	9.00×10^{-1}	7.15×10^{-3}
4.0	2.40×10^{-1}	7.60×10^{-1}	1.91×10^{-3}
4.5	5.00×10^{-1}	5.00×10^{-1}	3.98×10^{-4}
5.0	7.60×10^{-1}	2.41×10^{-1}	6.05×10^{-5}

$$\text{where } [H_2C_2O_4] = \frac{[H^+]^2 \cdot K_{d,1} \cdot K_{d,2}}{1 + K_{d,2}[H^+] + K_{d,1}K_{d,2}[H^+]^2} \quad (\text{b.1})$$

$$[HC_2O_4^-] = \frac{K_{d,2}[H^+]}{1 + K_{d,2}[H^+] + K_{d,1}K_{d,2}[H^+]^2} \quad (\text{b.2})$$

$$[C_2O_4^{=}] = \frac{1}{1 + K_{d,2}[H^+] + K_{d,1} \cdot K_{d,2}[H^+]^2} \quad (\text{b.3})$$

and $K_{d,1} = 10^{1.4}$ (102), $K_{d,2} = 10^{4.5}$ (103) are respectively the first and second dissociation constants of oxalic acid at 80°C.

TABLE B.3

Total Solubility of Ferrous Species in 0.2 M Oxalic Acid
as a Function of pH at 80°C (Figure 18).

pH	$[C_2O_4^{=}]$ (M/liter)	$\log_{10}[C_2O_4^{=}]$	Measured		Calculated (Equation (4.6))*	
			$[Fe^{++}]_{Total}$ (mgFe/liter)	$\log_{10}[Fe^{++}]_{Total}$	$[Fe^{++}]_{Total}$ (mgFe/liter)	$\log_{10}[Fe^{++}]_{Total}$
0.70	5.28×10^{-6}	-5.280	390-406	2.590-2.610	420	2.622
1.05	2.19×10^{-5}	-4.660	90-100	1.950-2.000	117	2.068
1.35	6.66×10^{-5}	-4.177	51-55	1.706-1.741	52.6	1.722
1.60	1.54×10^{-4}	-3.813	33-36	1.518-1.556	34.7	1.540
1.90	3.80×10^{-4}	-3.420	28-30	1.447-1.477	30.5	1.484
2.80	3.78×10^{-3}	-2.423	35-40	1.544-1.600	37.0	1.568
3.55	2.0×10^{-2}	-1.700	102-110	2.008-2.041	116.0	2.062
4.00	4.8×10^{-2}	-1.320	320-336	2.505-2.526	283.0	2.451
4.50	1.0×10^{-1}	-1.000	665-680	2.823-2.833	705.0	2.847

*Stability Constants	Ref (104) (25°C)	Ref (105) (25°C)	Ref (106) (25°C)	This Work (80°C)
$\log_{10} K(i)$				
$\log_{10} K_1$	-	-	-	4.0
$\log_{10} (K_2 \cdot K_1)$	5.1	4.52	9.57	6.3
$\log_{10} (K_3 \cdot K_2 \cdot K_1)$	6.21	5.22	-	7.1
K_s	-	-	-	3.76×10^{-8}

TABLE B.4

Calculated Mean Activities of HClO_4 Solutions, at 25°C

HClO_4 Molarity (M/liter)	HClO_4 Molality (Molal)	γ_{\pm} (25°C) Mean Activity Coefficient (ref.108)	$a_{\pm} = a_{\text{H}^+} = a_{\text{ClO}_4^-}$ Mean Activity* (Molal)
0.045	0.045	0.850	0.38
0.09	0.09	0.805	0.0725
0.15	0.15	0.790	0.12
0.18	0.18	0.780	0.14
0.36	0.36	0.773	0.28
0.45	0.45	0.770	0.346
0.50	0.50	0.769	0.38
0.75	0.76	0.790	0.60
0.90	0.94	0.820	0.77
1.00	1.05	0.823	0.86
1.50	1.58	0.925	1.46
1.80	1.92	1.05	2.02
3.00	3.34	1.65	5.50
4.50	5.30	3.60	19.0
6.00	7.56	9.50	72.0

*The mean activity is calculated as

$a_{\pm} = m \cdot \gamma_{\pm}$ where m is the molality and γ_{\pm} the mean activity coefficient of HClO_4 .

TABLE B.5

Experimental and Calculated Rates of Leaching of Metal Oxides
in HClO_4 Solutions (Table 6, Figures 5 and 6).

Oxide (origin, temperature of leach)	HClO_4 Molarity (M/liter)	a_{\pm} Mean Activity (Molal)	Rates of Leaching			
			Measured		Calculated [Equation (5.6), Table 6]	
			Absolute ($\frac{\text{mg Metal}}{\text{min} \cdot \text{gm}}$)	Relative	Absolute ($\frac{\text{mg Metal}}{\text{min} \cdot \text{gm}}$)	Relative
Cu_2O Synthetic 12°C	0.045	0.038	12.8	0.296	13.1	0.304
	0.09	0.0725	17.5	0.405	18.5	0.430
	0.18	0.141	24.4	0.565	24.3	0.563
	0.36	0.278	29.5	0.683	30.4	0.705
	0.90	0.770	43.2	1.000	42.2	0.980
CuO Synthetic 12°C	0.045	0.038	0.90	1.180	0.985	0.197
	0.09	0.0725	1.42	0.282	1.475	0.295
	0.45	0.346	3.91	0.782	3.80	0.760
	0.90	0.770	5.00	1.000	5.20	1.040
$\alpha\text{-Fe}_2\text{O}_3$ Michigan 90°C	0.45	0.346	0.65×10^{-3}	0.65	0.603×10^{-3}	0.603
	0.90	0.770	1.00×10^{-3}	1.00	0.975×10^{-3}	0.975
	1.80	2.02	1.40×10^{-3}	1.40	1.435×10^{-3}	1.435
	3.00	2.02	1.70×10^{-3}	1.70	1.77×10^{-3}	1.77
	4.50	19.0	1.80×10^{-3}	1.80	1.91×10^{-3}	1.91

continued

TABLE B.5 continued

Oxide	HClO ₄	a _±	Measured		Calculated	
			Absolute	Relative	Absolute	Relative
α-FeO·OH	0.75	0.60	2.60x10 ⁻²	0.865	2.55x10 ⁻²	0.850
Minnesota	1.50	1.46	4.16x10 ⁻²	1.39	3.96x10 ⁻²	1.32
110°C	3.00	5.50	5.27x10 ⁻²	1.76	5.20x10 ⁻²	1.73
(after Hay)	4.50	19.00	5.61x10 ⁻²	1.87	5.74x10 ⁻²	1.91
	6.00	72.00	6.15x10 ⁻²	2.05	5.97x10 ⁻²	1.99
α-FeO·OH	0.15	0.12	4.50x10 ⁻³	0.214		0.261
Natural	0.50	0.38	1.07x10 ⁻²	0.560		0.643
1100°C	0.75	0.60	1.92x10 ⁻²	0.915		0.850
(after	1.00	0.86	2.22x10 ⁻²	1.06		1.04
Surana))	1.50	1.46	3.30x10 ⁻²	1.57		1.32

TABLE B.6

Calculated Mean Activities of HCl Solutions

HCl Molarity (M/liter)	HCl Molality (Molal)	γ_{\pm} (12°C) Mean Activity Coefficient	a_{\pm} (12°C) $a_{\text{H}^+} = a_{\text{Cl}^-}$ Mean Activity (Molal)	γ_{\pm} (80°C) Mean Activity Coefficient	a_{\pm} (80°C) Mean Activity (Molal)	γ_{\pm} (85°C) Mean Activity Coefficient	a_{\pm} (85°C) Mean Activity (Molal)
0.06	0.06	0.82	0.0493				
0.12	0.12	0.79	0.095				
0.20	0.20					0.73	0.15
0.24	0.24	0.765	0.183				
0.36	0.36	0.761	0.274				
0.48	0.48	0.757	0.364				
0.50	0.51						
0.60	0.61	0.755	0.453	0.69	0.42	0.69	0.35
0.72	0.73	0.752	0.541				
1.00	1.02						
1.20	1.22	0.845	1.03	0.75	0.91	0.71	0.72
1.50	1.54						
1.80	1.85			0.83	1.54	0.78	1.21
2.00	2.09						
2.40	2.50	0.970	2.42	0.94	2.36	0.85	1.78
3.00	3.20						
3.60	3.89			1.24	4.83	1.06	3.39
4.00	4.36						
4.80	5.35	2.35	12.0	1.70	9.10	1.35	5.89
5.00	5.57						
5.40	6.08			2.07	12.6	1.80	10.0
6.00	6.84	4.10	28.0	2.49	17.0	2.48	16.9
7.00	8.18					3.30	27.0
7.20	8.42			3.54	29.80		

TABLE B.7

Experimental and Calculated Rates of Leaching of Metal Oxides
in HCl Solutions (Table 7, Figures 7,8,9,12,13 and 14).

Oxide (origin, temperature of leach)	HCl Molarity (M/liter)	a_{\pm} Mean Activity (Molal)	Rates of Leaching			
			Measured		Calculated [Equation (5.6), Table 7]	
			Absolute ($\frac{\text{mg Metal}}{\text{min}\cdot\text{gm}}$)	Relative	Absolute ($\frac{\text{mg Metal}}{\text{min}\cdot\text{gm}}$)	Relative
Cu ₂ O Synthetic 12°C	0.06	0.0493	5.7	0.0425	4.31	0.332
	0.12	0.095	11.3	0.0843	10.9	0.0815
	0.24	0.183	21.4	0.16	24.1	0.180
	0.48	0.364	53.5	0.40	49.3	0.368
	0.60	0.453	63.0	0.47	61.7	0.460
	1.20	1.03	134.0	1.00	134.0	1.00
Cu ₂ O* Synthetic 12°C	0.06	0.0493	5.7	0.0425	5.7	0.0425
	0.12	0.095	11.3	0.0843	11.3	0.0843
	0.24	0.183	21.4	0.16	22.7	0.169
	0.48	0.364	53.5	0.40	47.6	0.356
	0.60	0.453	63.0	0.47	60.5	0.451
	1.20	1.03	134.0	1.00	144.0	1.07
CuO Synthetic 12°C	0.12	0.095	2.14	0.110	2.85	0.146
	0.36	0.274	6.50	0.334	7.75	0.397
	0.72	0.541	12.0	0.615	13.8	0.707
	1.2	1.03	19.5	1.00	21.6	1.11
	2.4	2.42	35.5	1.82	34.4	1.76
	4.8	12.0	55.0	2.82	59.2	3.04
6.0	28.0	83.5	4.28	82.6	4.24	

*Calculated [Equation (5.15) Table 8].

continued

TABLE B.7 continued

Oxide	HCl	a_{\pm}	Measured		Calculated	
			Absolute Rate	Relative Rate	Absolute Rate	Relative Rate
CuO Synthetic 12°C	0.12	0.095	2.14	0.110	2.85	0.146
	0.36	0.274	6.50	0.334	7.75	0.397
	0.72	0.541	12.0	0.615	13.8	0.707
	1.2	1.03	19.5	1.00	21.6	1.11
	2.4	2.42	35.5	1.82	34.4	1.76
	4.8	12.0	55.0	2.82	59.2	3.04
	6.0	28.0	83.5	4.28	82.6	4.24
Al(OH) ₃ Synthetic 80°C	1.2	0.91	1.46	1.00	1.65	1.13
	2.4	2.36	3.34	2.28	3.36	2.30
	3.6	4.83	4.75	3.25	4.89	3.35
	4.8	9.10	6.60	4.51	6.31	4.33
	6.0	17.0	7.80	5.34	7.86	5.38
γ -Al ₂ O ₃ Synthetic 80°C	0.6	0.42	0.957	0.81		
	1.2	0.91	1.19	1.00		
	2.4	2.36	1.87	1.57		
	3.6	4.83	2.05	1.73		
	4.8	9.10	2.33	1.96		
	6.0	17.0	2.46	2.06		

continued

TABLE B.7 continued

Oxide	HCl	a_{\pm}	Measured		Calculated	
			Absolute	Relative	Absolute	Relative
α -Fe ₂ O ₃ Michigan 80°C	0.6	0.42	1.00x10 ⁻³	0.265	1.09x10 ⁻³	0.279
	1.2	0.91	3.77x10 ⁻³	1.00	3.75x10 ⁻³	0.995
	1.8	1.54	7.75x10 ⁻³	2.05	8.53x10 ⁻³	2.26
	2.4	2.36	1.58x10 ⁻²	4.20	1.64x10 ⁻²	4.35
	3.6	4.83	4.12x10 ⁻²	10.9	4.49x10 ⁻²	11.9
	4.8	9.1	9.25x10 ⁻²	24.5	1.03x10 ⁻¹	27.3
	5.4	12.6	1.69x10 ⁻¹	44.8	1.55x10 ⁻¹	41.1
	6.0	17.0	2.15x10 ⁻¹	57.0	2.20x10 ⁻¹	58.4
	7.2	29.8	4.50x10 ⁻¹	119.0	4.22x10 ⁻¹	112.0
α -Fe ₂ O ₃ Synthetic 85°C (After Bath)	0.2	0.15	1.1x10 ⁻³	0.013		0.0476
	0.5	0.35	1.1x10 ⁻²	0.130		0.215
	1.0	0.72	5.5x10 ⁻²	0.645		0.65
	2.0	1.78	3.3x10 ⁻¹	3.88		2.78
	3.0	3.39	9.6x10 ⁻¹	11.3		7.08
	4.0	5.89	1.85	21.8		15.3
	5.0	10.0	3.12	36.7		30.8
	6.0	16.9	5.36	63.0		58.4
	7.0	27.0	7.83	92.0		99.5
α -Fe ₂ O ₃ Single Crystal 85°C (After Bath)	3.0	3.39		6.5		7.08
	4.0	5.89		16.2		15.3
	5.0	10.0		29.6		30.8
	6.0	16.9		55.3		58.4

continued

TABLE B.7 continued

Oxide	HCl	a_{\pm}	Measured		Calculated	
			Absolute	Relative	Absolute	Relative
α -Fe ₂ O ₃ Single crystal 85°C (After Bath)	3.0	3.39		6.5		7.08
	4.0	5.89		16.2		15.3
	5.0	10.0		29.6		30.8
	6.0	16.9		55.3		58.4
α -FeO·OH Natural 85°C (After Surana)	1.0	0.72	1.57×10^{-1}	0.654		0.65
	1.2	0.91	2.40×10^{-1}	1.00		0.995
	1.5	1.21	3.415×10^{-1}	1.42		1.50
	2.0	1.78	6.645×10^{-1}	2.76		2.78
	3.0	3.39	1.63	6.80		7.08
	4.0	5.89	3.56	15.25		15.25
Ferric Oxides Natural 80°C (After Roach, average results)	1.2	0.91		1.0		0.995
	2.4	2.36		4.3		4.35
	3.6	4.83		10.74		11.9
	4.8	9.10		19.38		27.3

TABLE B.7.a

Calculated Relative Rates of Leaching of Ferric Oxide
Using Simplified Rate Expressions

(1) After Surana and Warren (Curve A, Figure 7):

$$\text{Rate} = k_1 \cdot a_{\text{H}^+} \cdot a_{\text{Cl}^-} = k_1 \cdot (a_{\pm})^2 \quad k_1 = 1.2$$

a_{\pm} (Molal)	Relative Rate of Leaching	Relative Rate $\frac{\text{Rate}}{a_{\pm}}$ (Molal ⁻¹)
0.91	1.0	1.1
1.00	1.2	1.2
2.00	4.8	2.4
3.00	10.8	3.6
4.00	19.2	4.8
5.00	30.0	6.0

(2) After the following rate expression (Curve B, Figure 7):

$$\text{Rate} = \frac{k_1 \cdot a_{\text{H}^+} \cdot a_{\text{Cl}^-}}{1 + K \cdot a_{\text{H}^+}} = \frac{k_1 \cdot (a_{\pm})^2}{1 + K \cdot a_{\pm}}$$

with $k_1 = 2.85$ $K = 1.5$

a_{\pm} (Molal)	Relative Rate of Leaching	Relative Rate $\frac{\text{Rate}}{a_{\pm}}$ (Molal ⁻¹)
0.91	1.00	1.10
1.00	1.14	1.14
2.00	2.85	1.46
3.00	4.66	1.55
4.00	6.50	1.62
5.00	8.40	1.68
6.00	10.3	1.72

TABLE B.8

Ratios of the Relative Rates of Leaching of Ferric Oxides and
 a_{\pm} as a Function of a_{\pm}

HCl Molarity (M/liter)	a_{\pm} Mean Activity (Molal)	<u>Relative Rate</u> a_{\pm} Measured (if Table B.7) (Molal ⁻¹)					Calculated (Molal ⁻¹)
		α -Fe ₂ O ₃ Michigan	α -Fe ₂ O ₃ Bath	α -Fe ₂ O ₃ Single Crystal Bath	α -FeO·OH Surana	Ferric Oxides Roach	
0.2	0.15		0.087				0.318
0.5	0.35		0.372				0.615
0.6	0.42	0.631					0.663
1.0	0.72		0.896		0.906		0.902
1.2	0.91	1.10			1.10	1.10	1.09
1.5	1.21				1.17		1.24
1.8	1.54	1.33					1.47
2.0	1.78		2.18		1.55		1.56
2.4	2.36	1.78				1.82	1.84
3.0	3.39		3.32	1.92	2.00		2.08
3.6	4.83	2.26				2.22	2.46
4.0	5.89		3.70	2.75	2.59		2.59
4.8	9.10	2.69				2.13	3.00
5.0	10.0		3.67	2.96			3.08
5.4	12.6	3.56					3.26
6.0	16.9	3.35	3.73	3.27			3.43
7.0	27.0		3.41				3.68
7.2	29.8	4.00					3.76

TABLE B.9

Experimental and Calculated Rates of Leaching of Ferric Oxide (Michigan) in
HCl-LiCl, HCl-NaOH and HCl-HClO₄ Solutions (Table 7, Figures 10 and 11).

HCl Molarity (M/liter)	LiCl ← ←	γ_{\pm} (80°C) Mean Activity Coefficient	m_{H^+} Molality (Molal)	m_{Cl^-} ← ←	a_{H^+} ← ←	a_{Cl^-} ← ←	Relative Rate	
							Measured	Calculated Equation(5.6)
2.4	0	0.94	2.5	2.50	2.36	2.36	4.17	4.44
2.4	0.6	1.06	2.5	3.20	2.66	3.40	5.97	6.18
2.4	1.2	1.28	2.5	3.89	3.16	4.83	8.63	8.80
2.4	2.4	1.70	2.5	5.35	4.25	9.10	17.0	15.50

HCl Molarity (M/liter)	HClO ₄ ← ←	NaOH ← ←	γ_{\pm} (80°C) Mean Activity Coefficient	m_{H^+} Molality (Molal)	m_{Cl^-} ← ←	a_{H^+} ← ←	a_{Cl^-} ← ←	Relative Rate	
								Measured	Calculated Equation(5.6)
2.4	0	1.8	0.70	0.6	2.5	0.42	1.75	1.14	1.03
2.4	0	1.2	0.74	1.2	2.5	0.89	1.85	1.93	1.85
2.4	0	0	0.94	2.5	2.5	2.36	2.36	4.17	4.44
2.4	0.9	0	1.24	3.3	2.5	4.10	3.10	7.55	7.80
2.4	1.2	0	1.44	3.9	2.5	5.61	3.60	9.30	11.0
2.4	1.8	0	1.90	4.6	2.5	8.75	4.75	18.5	18.6

TABLE B.10

Calculated Mean Activities of H_2SO_4 Solutions

The mean activity of H_2SO_4 was calculated as $a_{\pm} = \gamma_{\pm} \cdot m_{\pm}$ where γ_{\pm} and m_{\pm} respectively the mean activity coefficient and molality of H_2SO_4 . It is assumed that

$$a_{\pm} = a_{\text{HSO}_4^-} = a_{\text{H}^+} \text{ and } m_{\text{H}^+} = m_{\text{HSO}_4^-} = m_{\pm}$$

H_2SO_4 Molarity (M/liter)	H_2SO_4 Molality (Molal)	γ_{\pm} (12°C) Mean Activity Coefficient	γ_{\pm} (85°C) Mean Activity Coefficient	a_{\pm} (12°C) Mean Activity (Molal)	a_{\pm} (85°C) Mean Activity (Molal)
0.036	0.036	0.735	0.452	0.0264	0.0163
0.09	0.09	0.515	0.307	0.0463	0.0276
0.18	0.18	0.403	0.248	0.0726	0.0446
0.27	0.27	0.366		0.099	
0.36	0.36	0.326	0.191	0.117	0.0690
0.54	0.55	0.274	0.152	0.151	0.0836
0.72	0.74	0.259	0.151	0.192	0.112
0.90	0.93	0.245	0.146	0.228	0.136
1.00	1.03		0.142		0.146
1.08	1.12	0.242		0.271	
1.8	1.93		0.132		0.255
2.0	2.17		0.131		0.284
3.0	3.42		0.148		0.506
3.8	4.45		0.164		0.730
4.0	4.80		0.169		0.810
5.0	6.25		0.197		1.23
7.4	10.7		0.296		3.17
9.0	15.0		0.435		6.55

TABLE B.11

Experimental and Calculated Rates of Leaching of Metal Oxides in
 H_2SO_4 Solutions (Table 9, Figures 15 and 16).

Oxide (origin, temperature of leach)	H_2SO_4 Molarity (M/liter)	a_{\pm} Mean Activity (Molal)	Rates of Leaching			
			Measured		Calculated (Equation 5.17, Table 9)	
			Absolute ($\frac{mg\ Metal}{min \cdot gm}$)	Relative	Absolute ($\frac{mg\ Metal}{min \cdot gm}$)	Relative
Cu ₂ O Synthetic 12°C	0.036	0.0264	21.6	0.288	21.6	0.288
	0.09	0.0463	25.0	0.333	27.3	0.364
	0.18	0.0726	33.2	0.442	33.2	0.442
	0.54	0.151	49.0	0.653	49.0	0.653
	1.08	0.271	75.0	1.000	72.3	0.965
CuO Synthetic 12°C	0.036	0.0264	2.50	0.245	2.94	0.288
	0.09	0.0463	3.80	0.372	3.71	0.364
	0.36	0.117	5.46	0.535	5.76	0.565
	0.54	0.151	6.70	0.653	6.70	0.653
	0.72	0.192	7.60	0.745	7.88	0.772
1.08	0.271	10.2	1.000	9.85	0.965	
MnO Synthetic 12°C	0.036	0.0264	38.2	0.151	38.0	0.150
	0.09	0.0463	56.0	0.221	63.5	0.250
	0.18	0.0726	89.5	0.353	90.0	0.355
	0.27	0.099	115.0	0.455	118.0	0.466
	0.36	0.117	143.0	0.565	135.0	0.533
α -Fe ₂ O ₃ Michigan 85°C	0.09	0.0276	1.93×10^{-3}	0.305	1.64×10^{-3}	0.259
	0.18	0.0446	2.58×10^{-3}	0.407	2.58×10^{-3}	0.407
	0.36	0.069	3.44×10^{-3}	0.543	3.84×10^{-3}	0.605

continued

TABLE B.11 continued

Oxide	H ₂ SO ₄	a _±	Rates of Leaching			
			Absolute	Relative	Absolute	Relative
α-Fe ₂ O ₃ Michigan 85°C	0.90	0.0276	1.93x10 ⁻³	0.305	1.64x10 ⁻³	0.259
	1.80	0.255	1.08x10 ⁻²	1.70	1.09x10 ⁻³	1.72
	3.80	0.73	1.88x10 ⁻²	2.96	1.93x10 ⁻³	3.05
	7.40	3.17	2.84x10 ⁻²	4.48	3.10x10 ⁻³	4.89
	9.00	6.55	3.64x10 ⁻²	5.74	3.64x10 ⁻³	5.74
α-FeO·OH Natural 80°C (After Surana)	1.0	0.146		1.08		1.08
	2.0	0.284		1.88		1.85
	3.0	0.506		2.40		2.00
	4.0	0.810		3.44		3.25
	5.0	1.23		4.15		3.80
Ferric Oxides Natural 80°C (After Roach) Average Results	1.0	0.146		1.08		1.08
	2.0	0.284		2.05		1.85
	4.0	0.810		3.66		3.25
	5.0	1.23		4.60		3.80

TABLE B.12

Calculated and Experimental Rates of Leaching of $\alpha\text{-Fe}_2\text{O}_3$ (Michigan)
in 0.3 M Oxalic Acid at 90°C versus pH (Figure 18).

pH	$[\text{C}_2\text{O}_4^{2-}]$ (M/liter)	$[\text{HC}_2\text{O}_4^-]$ (M/liter)	$[\text{H}_2\text{C}_2\text{O}_4]$ (M/liter)	Rate of Leaching	
				Measured $\left(\frac{\text{mg Fe}}{\text{min}\cdot\text{gm}}\right)$	Calculated (Equation (5.19), Table 10) $\left(\frac{\text{mg Fe}}{\text{min}\cdot\text{gm}}\right)$
0.35	1.75×10^{-6}	2.46×10^{-2}	2.76×10^{-1}	21.6×10^{-3}	20.25×10^{-3}
0.75	9.77×10^{-6}	5.50×10^{-2}	2.45×10^{-1}	11.05×10^{-3}	11.28×10^{-3}
1.05	3.28×10^{-5}	9.24×10^{-2}	2.07×10^{-1}	7.50×10^{-3}	8.14×10^{-3}
1.30	8.36×10^{-5}	1.33×10^{-1}	1.67×10^{-1}	6.80×10^{-3}	6.71×10^{-3}
2.80	5.64×10^{-3}	2.82×10^{-1}	1.12×10^{-2}	4.40×10^{-3}	4.35×10^{-3}
4.00	7.20×10^{-2}	2.28×10^{-1}	5.73×10^{-4}	3.40×10^{-3}	3.32×10^{-3}
4.50	1.50×10^{-1}	1.50×10^{-1}	1.89×10^{-4}	2.16×10^{-3}	2.20×10^{-3}

TABLE B.13

Experimental Relative Rates of Leaching of α -Fe₂O₃
in 0.2 M Oxalic Acid at 80°C versus the Ti Content (Figure 23)

Sample (cf Table 5)	Ti (wt %)	Rate of Leaching in 2.4 N HCl at 80°C (mg Fe/min.gm.)	Rate of Leaching in 0.2 M Oxalic Acid at 80°C (mg Fe/min.gm.)	Relative Rate
A	0	1.64×10^{-1}	6.55×10^{-1}	4.00
D	0	1.96×10^{-1}	6.76×10^{-1}	3.46
G	0	1.83×10^{-1}	7.12×10^{-1}	3.90
H	0	1.71×10^{-1}	6.46×10^{-1}	3.77
P	0	1.35×10^{-1}	4.94×10^{-1}	3.66
B	0	3.31×10^{-1}	1.08	3.26
I	0.1	1.37×10^{-1}	1.51	11.0
J	0.2	1.36×10^{-1}	2.38	17.5
K	0.4	3.0×10^{-2}	5.62×10^{-1}	18.7
F	0.5	4.3×10^{-2}	9.00×10^{-1}	21.0
L	0.8	2.0×10^{-2}	4.44×10^{-1}	22.2
C	1.3	6.6×10^{-2}	1.20	18.0
E	3.0	7.8×10^{-2}	1.15	15.4
X	0.5	2.37×10^{-1}	7.96×10^{-1}	3.00

Average
3.76

TABLE B.14

The Effect of Added Ferrous Oxalate on the Leaching of $\alpha\text{-Fe}_2\text{O}_3$ in 0.2 M Oxalic Acid at 80°C and pH 2.8 (Figures 20 and 21)

$[\text{Fe}^{++}]_{\text{added}}$ ($\frac{\text{mg Fe}}{\text{liter}}$)	$\log_{10}[\text{Fe}^{++}]$	Rate of Leaching ($\frac{\text{mg Fe}}{\text{min}\cdot\text{gm}}$)			
		Sample Q (Table 5)		Sample C (Table 5)	
		Rate	\log_{10} Rate	Rate	\log_{10} Rate
3.0	0.477	0.330	-0.482	0.772	-0.142
6.0	0.778	0.596	-0.225	1.19	0.076
12.0	1.079	0.950	-0.022	1.19	0.278
18.0	1.255	1.20	0.079	2.16	0.334
24.0	1.380	1.29	0.110	2.45	0.389
36.0	1.556	1.30	0.114	2.50	0.398

In Figure $\text{Rate} = k \cdot [\text{Fe}^{++}]^n$

$$\text{with: Sample Q: } n = \frac{-0.022 + 0.482}{1.079 - 0.477} = \frac{0.460}{0.698} = 0.66$$

$$\text{Sample C: } n = \frac{0.278 + 0.142}{1.079 - 0.477} = \frac{0.420}{0.698} = 0.60$$

TABLE B.15

Effect of Sample Weight (Sample Q, Table 5).
 Leaching of $\alpha\text{-Fe}_2\text{O}_3$ in 0.2 M Oxalic Acid at 80°C and pH 2.8,
 with 6 mg Fe^{++} /liter.

Time (min)	$\left(\frac{\text{mg Fe}}{\text{liter}}\right)$		Rate $\left(\frac{\text{mg Fe}}{\text{min}\cdot\text{gm}}\right)$	
	1 gm sample	2 gm sample	1 gm sample	2 gm sample
10	5.7	10.1		
20	11.6	19.9	0.590	0.530
30	17.8	28.9		
40	23.6	42.4		

TABLE B.16

Effect of Temperature on the Rate of Leaching of $\alpha\text{-Fe}_2\text{O}_3$
in 0.2 M Oxalic Acid at pH 2.8 (Figure 27).

Temperature		$\frac{1000}{T}$	Rate of Leaching (mg Fe/min.gm.)					
(°C)	(°K)	(°K) ⁻¹	Sample D (Table 5)			Sample E (Table 5)		
			Rate $\left(\frac{6\text{mg Fe}^{++}}{\text{liter}}\right)$	log ₁₀ Rate	Rate (50-65 mesh) $\left(\frac{24\text{mg Fe}^{++}}{\text{liter}}\right)$	log ₁₀ Rate	Rate $\left(\frac{6\text{mg Fe}^{++}}{\text{liter}}\right)$	log ₁₀ Rate
50	323	3.085	0.150	-0.824	0.360	-0.444	0.237	-0.626
60	333	3.000	0.238	-0.624	0.630	-0.200	0.433	-0.364
70	343	2.915	0.409	-0.389	0.891	-0.050	0.736	-0.133
80	353	2.830	0.775	-0.111	1.31	0.117	1.275	0.106
85	358	2.795	-	-	1.72	0.236	-	-
90	363	2.755	1.200	0.079	-	-	2.000	0.300

Activation energies: Sample D (6mg Fe⁺⁺/liter) 12.2 kcal/mole \pm 0.5
 Sample D (24mg Fe⁺⁺/liter) 10.5 kcal/mole \pm 0.5
 Sample E (6mg Fe⁺⁺/liter) 12.9 kcal/mole \pm 0.5

TABLE B.17

Calculated Distribution of Ferrous Oxalate Species in 0.2 M Oxalic Acid versus pH, at 80°C (Figure 27) (using the stability constants K_1 , K_2 , K_3 in Table B.3).

pH	Fe ⁺⁺ (%)	Fe(C ₂ O ₄) (%)	Fe(C ₂ O ₄) ₂ ²⁻ (%)	Fe(C ₂ O ₄) ₃ ⁴⁻ (%)
1.00	8.47x10 ⁻¹	1.53x10 ⁻¹	5.50x10 ⁻⁴	6.23x10 ⁻⁸
1.25	6.82x10 ⁻¹	3.19x10 ⁻¹	2.97x10 ⁻³	8.73x10 ⁻⁷
1.50	4.70x10 ⁻¹	5.22x10 ⁻¹	1.16x10 ⁻²	8.10x10 ⁻⁵
1.75	2.81x10 ⁻¹	6.86x10 ⁻¹	3.35x10 ⁻²	5.15x10 ⁻⁵
2.00	1.53x10 ⁻¹	7.72x10 ⁻¹	7.80x10 ⁻²	2.48x10 ⁻⁴
2.25	7.80x10 ⁻¹	7.70x10 ⁻¹	1.51x10 ⁻¹	9.43x10 ⁻⁴
2.50x	3.80x10 ⁻¹	7.03x10 ⁻¹	2.60x10 ⁻¹	3.03x10 ⁻³
2.75	1.76x10 ⁻²	5.90x10 ⁻¹	3.95x10 ⁻¹	8.35x10 ⁻³
3.00	7.46x10 ⁻³	4.47x10 ⁻¹	5.36x10 ⁻¹	2.02x10 ⁻²
3.25	-	3.09x10 ⁻¹	6.50x10 ⁻¹	4.30x10 ⁻²
3.50	-	2.00x10 ⁻¹	7.20x10 ⁻¹	8.17x10 ⁻²
3.75	-	1.22x10 ⁻¹	7.37x10 ⁻¹	1.40x10 ⁻¹
4.00	-	7.45x10 ⁻²	7.15x10 ⁻¹	2.16x10 ⁻¹
4.25	-	4.57x10 ⁻²	6.58x10 ⁻¹	2.98x10 ⁻¹
4.50	-	2.97x10 ⁻²	5.95x10 ⁻¹	3.75x10 ⁻¹
4.75	-	2.10x10 ⁻²	5.40x10 ⁻¹	4.36x10 ⁻¹
5.00	-	1.66x10 ⁻²	5.03x10 ⁻¹	4.82x10 ⁻¹
5.50	-	1.35x10 ⁻²	4.50x10 ⁻¹	5.25x10 ⁻¹
6.00	-	1.16x10 ⁻²	4.40x10 ⁻¹	5.48x10 ⁻¹

Note: 100% = 1

TABLE B.18

Experimental and Calculated Rates of Leaching of α -Fe₂O₃ (Sample 0, Table 5)
at 80°C versus pH (Figure 25).

pH	[Fe(C ₂ O ₄) ₂ ²⁻] (M/liter)	[Fe(C ₂ O ₄) ₃ ⁴⁻] (M/liter)	Measured		Calculation [Equation (5.30)]	
			Absolute ($\frac{\text{mg Fe}}{\text{min} \cdot \text{gm}}$)	Normalized	Normalized $\alpha_a = \alpha_c = \alpha'_a = \alpha'_c = 0.6$ $k_{(1)} = 1.31 \times 10^4$ $k_{(2)} = 5.00 \times 10^4$	Normalized $\alpha_a = \alpha_c = \alpha'_a = \alpha'_c = 1$ $k_{(1)} = 9.84 \times 10^6$ $k_{(2)} = 1.97 \times 10^8$
0.50	9.80x10 ⁻¹⁰	1.38x10 ⁻¹⁴	-	-	0.026	0.003
1.05	7.82x10 ⁻⁸	1.08x10 ⁻¹¹	0.113	0.185	0.170	0.069
1.30	4.00x10 ⁻⁷	1.40x10 ⁻¹⁰	0.182	0.298	0.330	0.196
1.60	1.85x10 ⁻⁶	1.80x10 ⁻⁹	0.256	0.420	0.563	0.465
1.90	5.70x10 ⁻⁶	1.36x10 ⁻⁸	0.370	0.606	0.760	0.740
2.50	2.60x10 ⁻⁵	3.03x10 ⁻⁷	0.610	1.000	0.942	1.000
2.80	4.18x10 ⁻⁵	9.94x10 ⁻⁷	0.603	0.988	0.920	0.960
3.65	7.37x10 ⁻⁵	1.14x10 ⁻⁵	0.400	0.655	0.676	0.664
4.10	6.91x10 ⁻⁵	2.48x10 ⁻⁵	0.220	0.360	0.445	0.440
4.70	5.50x10 ⁻⁵	4.25x10 ⁻⁵	0.146	0.239	0.236	0.182
5.00	5.03x10 ⁻⁵	4.82x10 ⁻⁵	-	-	0.163	0.100

TABLE B.19

Effect of Oxalic Acid Concentration on the Rate of Leaching of α -Fe₂O₃ (Sample Q, Table 5) at 80°C and at pH 2.8 (Figure 22).

[H ₂ CO ₄] Molarity (M/liter)	[Fe(C ₂ O ₄) ₂ ²⁻] Molarity (M/liter)	[Fe(C ₂ O ₄) ₃ ⁴⁻] Molarity (M/liter)	Rates of Leaching	
			Measured ($\frac{\text{mg Fe}}{\text{min. gm}}$)	Calculated [Equation (5.30)]* ($\frac{\text{mg Fe}}{\text{min. gm}}$)
0.05	1.46x10 ⁻⁵	8.65x10 ⁻⁸	0.263	0.268
0.10	2.62x10 ⁻⁵	3.31x10 ⁻⁷	0.421	0.415
0.15	3.50x10 ⁻⁵	6.25x10 ⁻⁷	0.560	0.519
0.20	4.18x10 ⁻⁵	9.94x10 ⁻⁷	0.605	0.605
0.30	5.18x10 ⁻⁵	1.85x10 ⁻⁶	0.723	0.740
0.40	5.85x10 ⁻⁵	2.78x10 ⁻⁶	0.780	0.845
0.60	6.61x10 ⁻⁵	4.70x10 ⁻⁶	0.870	1.000

* $\alpha_a = \alpha_c = \alpha'_a = \alpha'_c = 0.6$

TABLE B.20

Rate of Leaching of $\alpha\text{-Fe}_2\text{O}_3$ (Sample H, Table 5) in 0.5 M Malonic Acid at 80°C versus pH in the presence of 9mg/liter of added Ferrous Ion (Figure 28).

pH	Rate of Leaching ($\frac{\text{mg Fe}}{\text{min}\cdot\text{gm}}$)
1.6	9.90×10^{-3}
2.7	2.33×10^{-2}
3.2	3.75×10^{-2}
4.3	7.50×10^{-2}
5.0	8.35×10^{-2}
5.9	5.78×10^{-2}
6.4	3.67×10^{-2}

TABLE B.21

Effect of Adding Ferrous Ion on the Leaching of
 $\alpha\text{-Fe}_2\text{O}_3$ (Michigan) in HCl Solutions at 80°C (Figure 29).

[HCl] Molarity (M/liter)	[Fe ⁺⁺] added (mg/liter)	Rates of Leaching ($\frac{\text{mg Fe}}{\text{min. gm}}$)
2.4	0.0	1.30×10^{-3}
2.4	50.0	1.31×10^{-3}
6.0	0.0	1.95×10^{-2}
6.0	12.5	2.44×10^{-2}
6.0	50.0	3.32×10^{-2}

10. REFERENCES

1. Pearson, T.G., "The Chemical Background of the Aluminum Industry", Royal Institute of Chemistry, Monograph No.3, 1955.
2. Steintveit, G., "Treatment of Zinc Plant Residues by the Jarosite Process": Paper No.29, at Symposium on Advances in Extractive Metallurgy and Refining, London, October 1971.
3. Uranium Ore Processing, edited by J.W. Clegg and D.D. Foley, Addison-Wesley, Reading, Penn., 1958.
4. Sully, A.H., Manganese, Butterworths Scientific Publications, London, 1955.
5. Pourbaix, M., Atlas of Electrochemical Equilibria in Aqueous Solutions, Pergamon Press, London, 1966.
6. Burkin, A.R., The Chemistry of Hydrometallurgical Processes, Spon, London, 1966.
7. Habashi, F., Principles of Extractive Metallurgy, Vol.2: Hydro-metallurgy, Gordon and Breach, New York, 1970.
8. Warren, I.H. and Monhemius, A.J., Paper No.5, The Conference of Metallurgists, Toronto, 1966.
9. Surana, V.S. and Warren, I.H., Trans. Inst. Min. Metall. (Sect. C: Mineral Process Extr. Metall.), Vol.78, 1969,
10. Mackay, T.L. and Wadsworth, M.E., Trans. A.I.M.E., Vol.212, 1958, pp. 597-603.
11. Hair, M.L., Infra-Red Spectroscopy in Surface Chemistry, Marcel Dekker Inc., New York, 1967.
12. Peri, J.B., and Hannan, R.B., J. Phys. Chem., Vol.64, 1960, pp. 1526-1530.
13. Peri, J.B., J. Phys. Chem., Vol.69, 1965, pp.220-230.
14. Young, G.J., J. Colloid Sci., Vol.13, 1958, pp.67-85.

15. Fripiat, J.J.; Gastuche, M.C. and Brichard, R., *J. Phys. Chem.*, Vol.66, 1962, pp. 805-812.
16. Bielanski, A.; and Sedzimir, A., *Proc. Fourth Inter. Symp. on Reactivity of Solids*, Amsterdam, 1960, pp. 301-309.
17. Wade, N.H. and Hackerman, N., *J. Phys. Chem.*, Vol.64, 1960, p. 1196.
18. Hendriksen, B.A., Pearce, D.R. and Rudham, R., *J. of Cat.*, Vol.24, 1972, pp. 82-87.
19. Morimoto, T., Shiomi, J. and Tanaka, H., *Bull. Chem. Soc. Jap.*, Vol.37; 1964, p. 392.
20. Baker, F.S., Phillips, C. and Sing, K.S.W., *Proc. Symp. on Oxide-Electrolyte Interfaces*, Electrochem. Soc., Ed. Alwitt, R.S.
21. Wade, W.H. and Hackerman, N., *J. Phys. Chem.*, Vol.65, 1961, p.1681.
22. Primet, M., Pichat, P. and Mathieu, M., *J. Phys. Chem.*, Vol.75, 1971, pp. 1216-1226.
23. Munuera, G. and Stone, F.S., *Discuss. Far. Soc.*, Vol.52, 1971, pp. 205-214.
24. Blyholder, G. and Richardson, E.A., *J. Phys. Chem.*, Vol.66, 1962, pp. 2597-2602.
25. McCafferty, E. and Zettlemyer, A.C., *Discuss. Far. Soc.*, Vol.52, pp. 239-257.
26. Anderson, P.J., Horlock, R.F. and Oliver, J.F., *Trans. Farad. Soc.*, Vol.61, 1965, pp. 2754-2762.
27. Stuart, W.I. and Whateley, T.L., *Trans. Farad. Soc.*, Vol.61, 1965, pp. 2763-2771.
28. Amphlet, C.B., *Inorganic Ion Exchangers*, Elsevier Pub. Co., Amsterdam, 1964.
29. Parks, G., *Chem. Rev.*, Vol.65, 1965, pp. 177-198.
30. Healey, T.W., Herring, A.P. and Fuerstenau, D.W., *J. Colloid Sci.*, Vol.21, 1966, pp. 435-444.
31. O'Connor, D.J., Johansen, P.G. and Buchanan, A.S., *Trans. Farad. Soc.*, Vol.19, 1954, pp. 229-236.

32. Robinson, McD., Park, J.A. and Fuerstenau, D.W., J. Am. Ceram. Soc., Vol.47, 1964, pp. 516-520.
33. Graham, P. and Crawford, D.J., J. Colloid, Sci., Vol.18, 1947, pp. 509-519.
34. Adamson, A.W., Physical Chemistry of Surfaces, Interscience, New York, 1960, p. 593.
35. Brockman, H., Discuss. Farad. Soc., Vol.7, 1949, p. 58.
36. Berube, J.G. and De Bruyn, P.L., J. Colloid Sci., Vol.28, pp. 92-105.
37. DuMont, F. and Watillon, A., Discuss. Farad. Soc., Vol.52, 1971, pp. 352-360.
38. Robinson, R.A. and Stokes, R.H., "Electrolyte Solutions", Butterworths, London, 1959.
39. Nightingale, E.R., "Chemical Physics of Ionic Solutions", B.E. Conway and R.G. Banadas ed., Wiley, New York, 1964, p. 87.
40. Hingston, F.J., Posner, A.M. and Quirk, J.P., Discuss. Farad. Soc., Vol.52, 1971, pp. 334-351.
41. Azuma, K. and Kametani, H., Trans. A.I.M.E., Vol.230, 1964, pp. 853-862.
42. Roach, G.I.D., "A Study of the Leaching of Goethite and Hematite", M.A.Sc. Thesis, University of British Columbia, 1970.
43. Warren, I.H. et al, Trans. Inst. Min. Metall. (Sect. C: Mineral Process. Extr. Metall.), Vol.78, 1969, pp. C21-27.
44. Warren, I.H., and Roach, G.I.D., Trans. Inst. Min. Metall. (Sect. C: Mineral Process Extr. Metall.), Vol.80, 1971, pp. C152-155.
45. Clay, J.P. and Thomas, A.W., J. Amer. Chem. Soc., Vol.60, 1938, pp. 2384-2389.
46. Graham, R.P. and Thomas, A.W., J. Amer. Chem. Soc., Vol.69, 1947, pp. 816-821.
47. Packter, A. and Dhillon, H.S., Z. Phys. Chemie, Leipzig, Vol.250, 1972, pp. 217-229.
48. Azuma, K. and Kametani, H., Trans. A.I.M.E., Vol.242, 1968, pp. 1025-1034.

49. Wadsworth, M.E. and Wadia, D.R., *Trans. A.I.M.E.*, Vol.203, 1955, pp. 755-759.
50. Sillen, L.G. and Martell, A.E., *Stability Constants of Metal-Ion Complexes*, The Chem. Soc., London, Special Publication No.17, 1964.
51. Koch, G., *Z. Electrochem.*, Vol.69, 1965, pp. 141-145.
52. Vishnyakov, I.A., Pogorelyi, A.D. and Tsarenko, V.Ya, *Izv. Vyssh. Ucheb. Zaved., Tsvet. Met.*, Vol.15, 1972, pp. 22-27.
53. Kabai, J., *Kem. Kozlem.*, Vol.38, 1972, pp. 57-92.
54. Nernst, W., *Z. Physik. Chem.*, Vol.47, 1904, pp. 52-55.
55. Pearson, R.L. and Wadsworth, M.E., *Trans. A.I.M.E.*, Vol.212, 1958, pp. 597-603.
56. Takeuchi, T., Hanson, K.C. and Wadsworth, M.E., *J. Inorg. Nucl. Chem.*, Vol.33, 1971, pp. 1089-98.
57. Judge, J.S., *J. Electrochem. Soc.*, Vol.118, 1971, pp. 1772-1775.
58. Ahmed, S.M. and Maksimov, D., *Studies of the Double Layer at the Oxide-Solution Interface*, Department of Energy, Mines, and Resources, Mines Branch, Ottawa, 1968.
59. Biermann, W.J. and Heinrichs, M., *Can. J. Chem.*, Vol.38, 1960, pp. 1449-1454.
60. Libby, W.F., *J. Phys. Chem.*, Vol.56, 1952, p. 863.
61. Weiss, J., *Proc. Roy. Soc., London*, A222, 1954, p. 128.
62. Halpern, J. and Orgel, L.E., *Discus. Farad. Soc.*, No.29, 1960, p. 32
63. Hush, N.S., *Trans. Farad. Soc.*, Vol.57, 1961, p.557-
64. Sacher, E. and Laidler, K.J., *Trans. Farad. Soc.*, Vol.59, 1963, p. 396
65. Marcus, R.A., *Ann. Rev. Phys. Chem.*, Vol.15, 1964, p. 155
66. Ruff, I., *Chem. Soc. Q. Rev.*, Vol.22, 1968, pp. 199-221.
67. Taube, H., *J. Amer. Chem. Soc.*, Vol.77, 1955, pp. 4481

68. Taube, H., and Myers, H., J. Amer. Chem. Soc., Vol.76, 1954, p. 2103.
69. Sutin, N., Chemistry in Brit., No.27, 1972, p. 148.
70. Silverman, J. and Dodson, R.W., J. Phys. Chem., Vol.56, 1952, p. 846.
71. Eichler, E. and Wahl, A.C., J. Am. Chem. Soc., Vol.80, 1958, p. 4145.
72. Hudis, J. and Wahl, A.C., J. Am. Chem. Soc., Vol.75, 1953, p. 4153.
73. Horne, R.A., J. Phys. Chem., Vol.64, 1960, pp. 1512-1517.
74. Reynolds, W.L. and Fukushima, S., Inorg. Chem., Vol.2, 1963, p. 176.
75. Reynolds, W.L., Liu, N. and Mickus, J., J. Am. Chem. Soc., Vol.83, 1961, p. 1078.
76. Sutin, N. and Gordon, B.M., J. Am. Chem. Soc., Vol.83, 1961, p. 70.
77. Gordon, B.M., Williams, L.L. and Sutin, N., J. Am. Chem. Soc., Vol.83, 1961, p.2061.
78. Wahl, A.C. and Deck, C.F., J. Am. Chem. Soc., Vol.76, 1954, p.4054.
79. Weiss, J., J. Chem. Phys., Vol.19, 1951, p. 1066.
80. Ogard, A.E. and Taube, H., J. Am. Chem. Soc., Vol.80, 1958, p. 1084.
81. Horne, R.A., Ph.D. Thesis, Columbia University, 1955.
82. Sheppard, J.C. and Brown, L.C., J. Phys. Chem., Vol.67, 1963, pp. 1025-1028.
83. Laxen, P.A., Proc. Symp. Sao Paulo, 1970; Int. Atomic En. Agency, Vienna, 1971, pp. 321-330.
84. Neeles, C.R. and Finkelstein, N.P. Private Communication to Laxen, P.A. (ref.83).
85. Hunt, J.B. and Taube, H., U.S.-O.N.R. Proj. N.R. 052-415, Final Report - Part II (Jan. 1963).
86. Neeles, C.R.S. and Nicol, M.J., Nat. Inst. Metall., Project C.81/70, Report No.1380, Johannesburg, South Africa, (Jan. 1972).

87. Koch, D.F.A., *Austr. J. Chem.*, Vol.10, 1957, pp. 150-159.
88. Warren, I.H. and Devuyt, E., *Trans. A.I.M.E.*, Vol.252, 1972, pp. 388-391.
89. Herring, A.P. and Ravitz, S.F., *Trans. A.I.M.E.*, Vol.232, 1965, pp. 191-196.
90. Habashi, F. and Thurston, G., *Energia Nucl.*, Milan, Vol.14, 1967, pp. 238-244.
91. Garrels, R.M. and Christ, C.L., *Solution, Minerals and Equilibria*, Harper and Row Pub., New York, 1965.
92. Morin, F.J., *Phys. Rev.*, Vol.83, 1951, pp. 1005-1010.
93. Geiger, G.H. and Wagner, Jr. J.B., *Trans. A.I.M.E.* Vol.233, 1965, pp. 2092-2100.
94. Gardner, R.F.G., Moss, R.L. and Tanner, D.W., *Brit. J. Appl. Phys.*, Vol.17, 1966, pp. 55-61.
95. Fortune, W.B. and Mellon, M.G., *Ind. Eng. Chem.*, Vol.10, 1938, pp. 60-64.
96. Wilson, A.D. and Sergeant, G.A., *Analyst*, Vol.88, 1963, pp. 109-112.
97. Crumpler, T.B., *Anal. Chem.*, Vol.19, 1947, pp. 325-326.
98. Charlot, G., *Nouveau Traité de Chimie Analytique*; Masson and C^{ie}, Paris, 1961, p. 786.
99. Hay, M.G., M.Sc. Thesis, Department of Metallurgy, University of British Columbia, 1973.
100. Surana, V.S., M.A.Sc. Thesis, Department of Metallurgy, University of British Columbia, 1969.
101. Bath, M.D., M.A.Sc. Thesis, Department of Metallurgy, University of British Columbia, 1968.
102. Kurz, J.L. and Farrar, J.M., *J. Am. Chem. Soc.*, Vol.91, 1969, pp. 6057-62.
103. Pinching, G.D. and Bates, R.G., *J. Res. Nat. Bur. Standards*, Vol.40, 1948, pp. 405-416.

104. Lingane, J.J., *J. Am. Chem. Soc.*, Vol.68, 1946, pp. 2448-2453.
105. Schaap, W.B., Laitinen, H.A. and Bailar, J.C., *J. Amer. Chem. Soc.*, Vol.76, 1954, pp. 5868-5872.
106. Toropova, V.F., *J. Gen. Chem. U.S.S.R.*, Vol.11, 1941, p. 1211.
107. Onoda, G.Y. and De Bruyn, P.L., *Surf. Science*, Vol.4, 1966, pp. 48-63.
108. Robinson, R.A. and Baker, O.J., *Trans. Roy. Soc., N.Z.*, Vol.76, 1946, p.76.
109. Warren, I.H. and Devuyt, E., *Int. Symp. of Hydrometallurgy*, Chicago, Illinois, U.S.A, ed. Evans, D.J.I. and Shoemaker, R.S., New York, 1973, pp. 229-264.
110. Thomas, J.M., *Chem. in Brit.*, Vol.6, 1970, pp. 60-64.
111. Harned, H.S. and Ehlers, R.W., *J. Am. Chem. Soc.*, Vol.55, 1933, p. 2179.
112. Akerlöf, G. and Teare, J.W., *J. Am. Chem. Soc.*, Vol.59, 1937, p. 1855.
113. G \ddot{u} ntelberg, E., *Z. Physik. Chem.*, Vol.123, 1926, p. 199.
114. *Handbook of Chemistry and Physics*, C.R.C. 49th Ed., 1968-1969.
115. Harned, H.S. and Hamer, W.J., *J. Am. Chem. Soc.*, Vol.57, 1935, pp. 27-33.
116. Young, T.F. and Blatz, L.A., *Chem. Rev.*, Vol.44, 1949, pp. 102-115.
117. Klotz, I.M. and Singleterry, C.R., *Theses*, University of Chicago, 1940.
118. Schwarzenbach, G. and Heller, J., *Helv. Chim. Acta*, Vol.34, 1951, p. 576.
119. Devuyt, E. and Warren, I.H. *Oxide-Electrolyte Interface*, *The Electrochem. Soc.*, ed. Alwitt R.S., 1973, pp. 112-121.
120. O'Connor, D.J., Street, N. and Buchanan, A.S., *Austr. J. Chem.*, 1954, pp. 245-255.

121. Bockris, J. O'M. and Reddy, A.K.N., Modern Electrochemistry, Vol.2, Phenum Press, New York, 1970, p. 862.
122. Delahay, P. and Berzins, T., J. Am. Chem. Soc., Vol.77, 1955, pp. 6448-6453.